
Bridging Domains with Approximately Shared Features

Ziliang Samuel Zhong^{*1,2} Xiang Pan^{*2} Qi Lei²

Abstract

Multi-source domain adaptation aims to reduce performance degradation when applying machine learning models to unseen domains. A fundamental challenge is devising the optimal strategy for feature selection. Existing literature is somewhat paradoxical: some advocate for learning invariant features from source domains, while others favor more diverse features. To address the challenge, we propose a statistical framework that distinguishes the utilities of features based on the variance of their correlation to label y across domains. Under our framework, we design and analyze a learning procedure consisting of learning approximately shared feature representation from source tasks and fine-tuning it on the target task. Our theoretical analysis necessitates the importance of learning approximately shared features instead of only the strictly invariant features and yields an improved population risk compared to previous results on both source and target tasks, thus partly resolving the paradox mentioned above. Inspired by our theory, we proposed a more practical way to isolate the content (invariant+approximately shared) from environmental features and further consolidate our theoretical findings.

1. Introduction

Machine learning models suffer from performance degradation when adapting to new domains (Koh et al., 2021). To mitigate this issue, (multi-source) domain adaptation has become a pivotal strategy, enabling the rapid transfer of knowledge from source domains to the target domain (Quinonero-Candela et al., 2008; Saenko et al., 2010). Despite its empirical success (Wang & Deng, 2018; Daumé III, 2007), a systematic theoretical understanding is still lacking.

A fundamental problem is devising the optimal strategy for feature selection in source domains. Most previous theoretical works pivot around specific domain adaptation algorithms and select features based on causality, which requires strong assumptions on the statistical relationship between source and target distributions. These assumptions include but are not limited to (1) the source domain covering the target domain (Shimodaira, 2000; Heckman, 1979; Cortes et al., 2010; Zadrozny, 2004); (2) the source and target domain having overlapping subgroups (Wei et al., 2020; Cai et al., 2021); (3) content features being exactly shared across domains (Arjovsky et al., 2019; Ben-David et al., 2010; Ahuja et al., 2020). Besides the limitation of learning causal features, existing literature also has paradoxical opinions on selecting non-causal features. For instance, some works suggest that we should learn invariant features, (Ahuja et al., 2020; Ben-David et al., 2010; Ajakan et al., 2014) while others suggest that we should learn diverse (even possibly spurious) features (Shen et al., 2022b; Wortsman et al., 2022) to get a more distributionally robust model. A more detailed discussion is deferred to the related work section.

To resolve the limitations and paradoxes in previous works, we will answer the following questions: *What features are robust to the natural distributional shifts in (multi-source) domain adaptation, and how can we learn them from purely observational data?*

Our contribution. In this work, we propose a novel theoretical framework that distinguishes **content (approximately shared + invariant)** vs. **environmental features** solely from observational data (based on how differently the features are utilized across tasks); see illustration diagram in Figure 1. Under our framework, we design and analyze a learning procedure

^{*}Equal contribution ¹Shanghai Frontiers Science Center of Artificial Intelligence and Deep Learning, New York University Shanghai ²Center for Data Science, New York University. Correspondence to: Ziliang Samuel Zhong <zz1706@nyu.edu>, Xiang Pan <xp2030@nyu.edu>, Qi Lei <q1518@nyu.edu>.

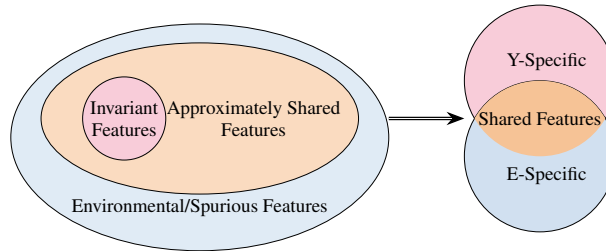


Figure 1. Diagram for different feature types, mathematically defined in Equation 4. Our work indicates that in addition to invariant features, we should utilize approximately shared features to fully transfer the knowledge from the source to the target domain. The practical way to learn the **approximately shared features** is learning features are correlated to both y and the environment e , which is the **y - e shared features**

consisting of (1) learning the content features via meta-representation learning on source domains and (2) fine-tuning the learned representation on the target domain. Our theoretical analysis yields a smaller and more interpretable population risk bound by removing the irreducible term in the previous works such as Tripuraneni et al. (2021); Du et al. (2021). It necessitates learning **invariant** and **approximately shared** features instead of only **invariant features** for a quick adaption to the target domain. Inspired by our theory, we proposed ProjectionNet, a more practical way to isolate the content (invariant+approximately shared) from environmental features. As illustrated in Figure 2, the feature space of ProjectionNet is more semantically meaningful than existing methods. Our findings effectively bridge the gap between different opinions in previous works mentioned above.

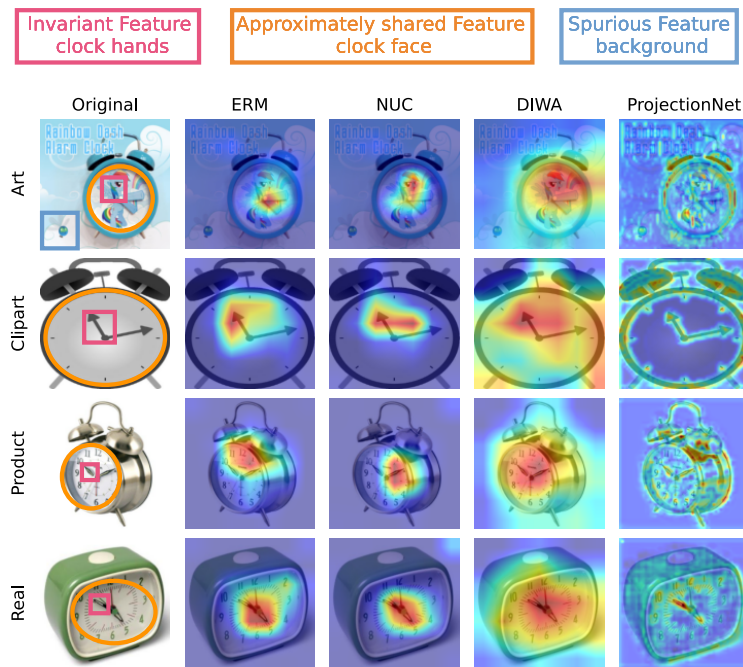


Figure 2. Feature Space Visualization: We show the GradCAM++ of the OfficeHome dataset with source pre-trained models feature space. We can see that ERM and NUC focus more locally; The DiWA feature is more globally distributed, while the feature space of ProjectionNet (ours) is more semantically meaningful.

1.1. Related Works

We discuss relevant work in (multi-source) domain adaptation categorized by the types of distributional shifts that cause performance degradation.

Selection bias describes the phenomenon of data collected in separate routines to present as if drawn from different distributions. It can be introduced by selecting individuals, groups, or data for analysis so that proper randomization is not achieved. For selection bias on individual samples, it can represent general covariate shift, and prior works accordingly proposed relevant methods including importance or hard-sample reweighting (Shimodaira, 2000; Heckman, 1979; Cortes et al., 2010; Zadrozny, 2004; Sun et al., 2011; Liu et al., 2021a; Nam et al., 2020), distribution matching/discrepancy minimization (Cortes et al., 2015; Ben-David et al., 2010; Berthelot et al., 2021), and domain-adversarial algorithms (Ajakan et al., 2014; Ganin et al., 2016; Long et al., 2018) between source and target domains in their feature representation space.

Subpopulation shift or dataset imbalance comes from selection bias on groups or subpopulations. People have investigated label propagation (Cai et al., 2021; Berthelot et al., 2021) or other consistency regularization (Miyato et al., 2018; Xie et al., 2020a; Yang et al., 2023) that migrate the predictions from source to target. Some more studies go beyond semi-supervised learning settings to contrastive representation learning (HaoChen et al., 2022; Shen et al., 2022a; Liu et al., 2021b) or self-training (Wei et al., 2020; Kumar et al., 2020). Under small covariate shift, learning algorithms have been investigated to achieve near minimax risks (Lei et al., 2021; Pathak et al., 2022).

Spurious correlation corresponds to the dependence between features and labels that is not fundamental or not consistent across domains. It poses a significant challenge in deploying machine learning models, as they can lead to reliance on irrelevant or environmental features and poor generalization. Specifically, with spurious or environmental features accompanying the invariant/content features, studies show fine-tuning can distort pretraining features (Kumar et al., 2022b), hurting out-of-distribution generalization. The existence of spurious features also brings about a trade-off between in-distribution and out-of-distribution performances.

Model ensemble (Kumar et al., 2022a) or model soups (Wortsman et al., 2022) are introduced to learn diverse features to compensate for the effect of spurious features. More approaches include introducing auxiliary information through human annotation (Srivastava et al., 2020) or from multiple sources (Xie et al., 2020b), through invariant feature representation learning (Arjovsky et al., 2019; Chen et al., 2022; Ahuja et al., 2020), through self-training (Chen et al., 2020) or overparametrization (Sagawa et al., 2020), feature manipulation (Shen et al., 2022b), adding regularizations (Park & Lee, 2021; Shi et al., 2023), or through causal approaches (Lu et al., 2021).

Finally, we discuss relevant results in representation learning that bear some resemblances but are fundamentally distinct in the presenting purposes.

Theoretical understanding on meta representation learning. Prior work on meta-representation learning (Du et al., 2021; Chua et al., 2021; Tripuraneni et al., 2020; 2021) focused on when and how one can identify the ground-truth representation from multiple training tasks. All their results (as well as (Chen & Marchand, 2023) that is more closely to our work) suffer from an irreducible term stemming from source representation error. Besides that, we are more interested in handling the spurious correlation and adapting to the new task sample efficiently.

1.2. Notations

Let $[n] = \{1, \dots, n\}$. We use $\|\cdot\|$ to denote the ℓ_2 norm of a vector or the spectral norm of a matrix. We denote the Frobenius norm of a matrix as $\|\cdot\|_F$. Let $\langle \cdot, \cdot \rangle$ be the Euclidean inner product between two vectors or matrices. The $d \times d$ identity matrix is denoted as I_d .

For a vector $\mathbf{v} \in \mathbb{R}^m$ v_k is the k -th entry and $\mathbf{v}_{[k:\ell]}$ is the vector formed by \mathbf{v} 's k -th to ℓ -th entries, $1 \leq k < \ell \leq m$. For a matrix $A \in \mathbb{R}^{m \times n}$, $m \geq n$, A_k is the k -th column and $A_{[k:\ell]}$ is the matrix formed by A 's k -th to ℓ -th columns, $1 \leq k < \ell \leq n$. Denote $\mathcal{P}_A = A(A^\top A)^\dagger A^\top \in \mathbb{R}^{m \times m}$, which is the projection matrix onto $\text{span}(A) = \{A\mathbf{v} \mid \mathbf{v} \in \mathbb{R}^n\}$. Here \dagger stands for the Moore-Penrose pseudo-inverse. We define $\mathcal{P}_A^\perp = I_m - \mathcal{P}_A$ which is the projection matrix onto the orthogonal complement of $\text{span}(A)$. The k -th smallest eigenvalue and k -th smallest singular value of A are denoted by $\lambda_k(A)$ and $\sigma_k(A)$ respectively. We denote $\mathcal{O}(n)$ as the n -dimensional orthogonal group.

We use $\gtrsim, \lesssim, \asymp$ to denote greater than, less than, equal to up to some constant. Our use of O, Ω, Θ is standard.

2. Methodology

This paper focuses on multi-source domain adaptation. Suppose we have E source environments indexed by $1, \dots, E$ and a target environment indexed by $E + 1$. For $e \in [E]$, each source environment provides a dataset with n_1 samples

denoted by $\{(\mathbf{x}_i^e, y_i^e)\}_{i=1}^{n_1}$. Similarly, for $e = E + 1$, the target environment provides a dataset with n_2 samples denoted by $\{(\mathbf{x}_i^e, y_i^e)\}_{i=1}^{n_2}$. For $e \in [E + 1]$, each tuple (\mathbf{x}_i^e, y_i^e) is an i.i.d. sample drawn from an environment-specific data distribution μ_e over the joint data space $\mathcal{X} \times \mathcal{Y}$ where $\mathcal{X} \subseteq \mathbb{R}^d$ is the input space and $\mathcal{Y} \subseteq \mathbb{R}$ is the output space. We are interested in the few-shot setting where the number of training samples from the target environment is much smaller than that from the source environments, *i.e.*, $n_2 \ll n_1$.

2.1. Data Generation Process

As illustrated in Figure 1, there are two types of features: **content (approximately shared + invariant)** and **environmental (spurious) features**, which are distinguished based on how differently they are utilized across environments, *i.e.*, the variance of their correlation to y . To theoretically model the features of these two types, we introduce the following data generation process.

Let $\phi_D : \mathcal{X} \rightarrow \mathcal{Z}$ be a representation function from the input space $\mathcal{X} \subseteq \mathbb{R}^d$ to some latent space $\mathcal{Z} \subseteq \mathbb{R}^D$. Let Φ_D denote the function class to which ϕ_D belongs. Here d is the ambient input dimension and D is the representation dimension.

For $k < D$, we define the following low-dimensional representation function classes induced by some fixed Φ_D

$$\begin{aligned}\Phi_k &:= \{f : f(\mathbf{x}) = \phi_{D[1:k]}(\mathbf{x}), \phi_D \in \Phi_D\}, \\ \Phi_{D-k} &:= \{f : f(\mathbf{x}) = \phi_{D[k+1:D]}(\mathbf{x}), \phi_D \in \Phi_D\},\end{aligned}\tag{1}$$

where $\phi_{D[1:k]}(\mathbf{x})$ and $\phi_{D[k+1:D]}(\mathbf{x})$ are defined as $\phi_D(\mathbf{x}) = [\phi_{D[1:k]}(\mathbf{x})^\top, \phi_{D[k+1:D]}(\mathbf{x})^\top]^\top$, the splitting of $\phi_D \in \Phi_D$.

We use different linear predictors on top of a common representation function ϕ_D^* to model the input-output relations in each environment. For $e \in [E + 1]$, let $\phi_D^* \in \Phi_D$ be some ground-truth representation shared by every environment and $\theta^{*1}, \dots, \theta^{*E+1} \in \mathbb{R}^D$ the environment-specific parameters characterizing the correlation of the features to the response y . The data generation process $(\mathbf{x}, y) \sim \mu_e$ can be described as

$$y = \langle \phi_D^*(\mathbf{x}), \theta^{*e} \rangle + z, \quad \mathbf{x} \sim p_e, \quad z \sim \mathcal{N}(0, \sigma^2),\tag{2}$$

where \mathbf{x} and z are statistically independent, and p_e is some environment-specific input distribution. Furthermore, the environment-specific parameters follow the multivariate Gaussian meta-distribution¹:

$$\theta^{*e} \stackrel{\text{i.i.d.}}{\sim} \mathcal{N}\left(\begin{bmatrix} \theta^* \\ \mathbf{0} \end{bmatrix}, \begin{bmatrix} \Lambda_{11} & 0 \\ 0 & \Lambda_{22} \end{bmatrix}\right),\tag{3}$$

where $\theta^* \in \mathbb{R}^k$, and $\Lambda_{11} \in \mathbb{R}^{k \times k}$, $\Lambda_{22} \in \mathbb{R}^{(D-k) \times (D-k)}$ are diagonal matrices with ascending entries, and $\|\Lambda_{11}\| < \|\Lambda_{22}\|$. Then equation 2 can be naturally split into

$$y = \langle \phi_{D[1:k]}^*(\mathbf{x}), \theta_{[1:k]}^{*e} \rangle + \langle \phi_{D[k+1:D]}^*(\mathbf{x}), \theta_{[k+1:D]}^{*e} \rangle + z.\tag{4}$$

In this setting, the first k entries of $\phi_D^*(\mathbf{x})$ are the low-dimensional content features that are (approximately) shared by all environments. The correlation of these features to y is relatively stable across environments because $\theta_{[1:k]}^{*e}$ distributes around θ^* with a small variance Λ_{11} . In particular, the **approximately shared features** are those corresponding to larger entries in Λ_{11} . On the other hand, the remaining $D - k$ entries are the **environmental features** that are uncorrelated with y on average but their correlation to y varies largely as the environment changes, characterized by $\|\Lambda_{22}\| > \|\Lambda_{11}\|$.

Remark 2.1 (Importance of approximately shared features). The inclusion of approximately shared features in the low-dimensional representation solves some prior paradoxes. On one hand, intuitively one would like to prioritize learning invariant features as shown in Arjovsky et al. (2019); on the other hand, the reason model soups (Wortsman et al., 2022) and model ensembles learn richer features but also are more robust to domain shifts is because the effect of environmental features is evened out during the model average (modeled by the zero-mean part in equation 3).

Remark 2.2 (Distinction to prior work). Compared with the state-of-the-art works on meta-learning theory, our data generation process is more reasonable and closer to real data. First, some existing works (Arjovsky et al., 2019; Ahuja et al.,

¹The assumption of Gaussian distribution is for simplicity. The fundamental requirement is for the meta distribution to be light-tail.

2020) consider that y is generated only from the strictly invariant features and ignore the effect of environmental features, *i.e.*, for $e \in [E + 1]$,

$$y = \langle \phi_k^*(\mathbf{x}), \boldsymbol{\theta}^{*e} \rangle + z, \quad \mathbf{x} \sim p_e, \quad \text{where } \phi_k^* \in \Phi_k, k < d.$$

However, for real data, the distinction between invariant and environmental features is not a clear-cut binary division. Second, the representation learning works (Du et al., 2021; Tripuraneni et al., 2020) make no distinction to the utilities of features (variance of correlation); they learn all features correlated to y and have a different focus from us. Their risk bound also has an irreducible term from source tasks without investigating how the representation error can be eliminated through fine-tuning.

2.2. The Meta-Representation Learning Algorithm

Given the data generation process above, a natural question to ask is how we can learn the content features from the source environments, *i.e.*, a low-dimensional representation $\phi_k \in \Phi_k$ and use the learned features on the target environment as a fine-tuning phase so that the performance is better than directly learning the target environment.

Before delving into the details of the algorithm, we introduce some auxiliary notations for clarity. For $e \in [E]$, we concatenate n_1 i.i.d. samples $\{(\mathbf{x}_i^e, y_i^e)\}_{i=1}^{n_1}$ into a data matrix $X^e \in \mathbb{R}^{n_1 \times d}$ and a response vector $\mathbf{y}^e \in \mathbb{R}^{n_1}$, *i.e.*, $X^e = [\mathbf{x}_1^e, \dots, \mathbf{x}_{n_1}^e]^\top$, and $\mathbf{y}^e = [y_1^e, \dots, y_{n_1}^e]^\top$. Similarly, for the target environment, we have $X^{E+1} \in \mathbb{R}^{n_2 \times d}$ and $\mathbf{y}^{E+1} \in \mathbb{R}^{n_2}$.

Given some representation function $\phi_D \in \Phi_D$ and data matrix X^e , $e \in [E]$, we overload the notation to allow ϕ_D to apply to all the samples in a data matrix simultaneously, *i.e.*, $\phi_D(X^e) = [\phi_D(\mathbf{x}_1^e), \dots, \phi_D(\mathbf{x}_{n_1}^e)]^\top \in \mathbb{R}^{n_1 \times D}$. Similarly, for the target environment, we have $\phi_D(X^{E+1}) \in \mathbb{R}^{n_2 \times D}$.

Then our meta-representation learning algorithm can be described as follows.

Source Pretraining: For each source environment $e \in [E]$, we set the prediction function to be $\mathbf{x} \mapsto \langle \phi_k(\mathbf{x}), \boldsymbol{\theta}^e \rangle$ ($\boldsymbol{\theta}^e \in \mathbb{R}^k$). Therefore, using the training data from E environments we can learn the content features represented by $\hat{\phi}_k^E \in \Phi_k$ via the following optimization:

$$\begin{aligned} & (\hat{\phi}_k^E, \hat{\boldsymbol{\theta}}^1, \dots, \hat{\boldsymbol{\theta}}^E) \\ &= \underset{\phi_k \in \Phi_k, \boldsymbol{\theta}^e \in \mathbb{R}^k}{\operatorname{argmin}} \frac{1}{2n_1 E} \sum_{e=1}^E \|\mathbf{y}^e - \phi_k(X^e)\boldsymbol{\theta}^e\|^2. \end{aligned} \quad (5)$$

Target Finetuning: For the target environment, we solve the following optimization to learn the final predictor $\mathbf{x} \mapsto \langle \phi_D(\mathbf{x}), \boldsymbol{\theta}^{E+1} \rangle$ ($\boldsymbol{\theta}^{E+1} \in \mathbb{R}^D$) that uses $\hat{\phi}_k^E$ obtained from Equation 5:

$$\begin{aligned} & (\hat{\phi}_D^{E+1}, \hat{\boldsymbol{\theta}}^{E+1}) \\ &= \underset{\phi_D \in \Phi_D, \boldsymbol{\theta}^{E+1} \in \mathbb{R}^D}{\operatorname{argmin}} \frac{1}{2n_2} \|\mathbf{y}^{E+1} - \phi_D(X^{E+1})\boldsymbol{\theta}^{E+1}\|^2 \\ & \quad + \frac{\lambda_1}{2n_2} \left\| \mathcal{P}_{\hat{\phi}_k^E(X^{E+1})}^\perp \phi_D(X^{E+1})\boldsymbol{\theta}^{E+1} \right\|^2 + \frac{\lambda_2}{2} \|\boldsymbol{\theta}^{E+1}\|^2. \end{aligned} \quad (6)$$

Equation 6 is the empirical risk minimization on the target environment with two regularizing terms. The first one penalizes the prediction on the directions *perpendicular* to the content features learned from source environments, which discourages the learning dynamics from capturing the environmental (spurious) features since we assume they are uncorrelated to y on average. The second one is the standard ℓ_2 regularization.

Remark 2.3. The above learning procedure enables us to learn and utilize the content features purely from the observational data even without any causal information on the features.

For $e \in [E + 1]$, to evaluate whether a predictor $\mathbf{x} \mapsto \langle \phi(\mathbf{x}), \boldsymbol{\theta} \rangle$ works well on some unseen data $(\mathbf{x}, y) \sim \mu^e$ sampled from that environment, we are interested in the excess risk $\operatorname{ER}_e(\phi, \boldsymbol{\theta}) = \frac{1}{2} \mathbb{E}_{\mathbf{x} \sim p^e} \left([\langle \phi_D^*(\mathbf{x}), \boldsymbol{\theta}^{*e} \rangle - \langle \phi(\mathbf{x}), \boldsymbol{\theta} \rangle]^2 \right)$ and its expectation over the meta distribution $\mathbb{E}_{\boldsymbol{\theta}^{*e}} [\operatorname{ER}_e(\phi, \boldsymbol{\theta})]$. For the target environment, we abbreviate ER_{E+1} as ER.

Bridging Domains with Approximately Shared Features

	OfficeHome					PACS					TerrainCognita					VLCS				
	A	C	P	R	Mean	A	C	P	S	Mean	L100	L38	L43	L46	Mean	C	L	S	V	Mean
DANN	0.6091	0.0297	0.6599	0.7408	0.5099	0.1463	0.1026	0.6707	0.2112	0.2827	0.0890	0.0770	0.2040	0.2806	0.1627	0.9437	0.3636	0.4006	0.4438	0.5379
DIWA	0.6914	0.5767	0.7838	0.7982	0.7125	0.9034	0.8154	0.9880	0.8244	0.8828	0.5776	0.4517	0.5995	0.4354	0.5161	0.9718	0.6014	0.7350	0.8047	0.7782
ERM	0.6914	0.5240	0.7793	0.8211	0.7039	0.8244	0.7906	0.9641	0.8270	0.8515	0.5190	0.4415	0.5693	0.3861	0.4789	0.9718	0.6503	0.7098	0.8136	0.7864
NUC-0.01	0.6996	0.5446	0.8018	0.8119	0.7145	0.8244	0.7521	0.9820	0.7888	0.8368	0.2025	0.4138	0.5516	0.2177	0.3464	0.3169	0.6692	0.7652	0.1391	0.4726
NUC-0.1	0.7284	0.5423	0.7995	0.8188	0.7223	0.8195	0.8120	0.9880	0.7990	0.8546	0.6181	0.4969	0.6121	0.2177	0.4862	0.9789	0.6842	0.7287	0.8077	0.7999
PN-Y	0.7243	0.4920	0.8063	0.8417	0.7161	0.7707	0.8128	0.9641	0.7150	0.8157	0.5561	0.5277	0.5340	0.4762	0.5235	0.9789	0.5594	0.7382	0.8166	0.7733
PN-Y-S	0.7284	0.5057	0.8108	0.8486	0.7234	0.7668	0.8111	0.9641	0.6997	0.8104	0.5612	0.5277	0.5290	0.4728	0.5227	0.9859	0.5594	0.7382	0.8343	0.7795

Table 1. Domain Generalization Results: We use the source pretrained model to directly test the target domain to evaluate the domain generalization ability of the pretrained model. NUC-0.1 and NUC-0.01 stand for different regularization strength λ_{NUC} in Equation 7 ProjectionNet (PN) can achieve similar or better results than the baseline methods.

2.3. Isolating Content Features in Practice

The optimizations in equation 5 and equation 6 are intractable since searching through the function class and finding the optimal representation function is generally expensive. In this section, we use the following two methods to approximate them in practice.

2.3.1. NUCLEAR NORM REGULARIZATION

Source Pretraining: To learn a low-dimensional representation, we choose a model $\phi_{\theta_{\text{rep}}}(\cdot)$ with trainable weights θ_{rep} (such as ResNet) and control the complexity of its output instead of searching the whole function class for the optimal representation function. For $e \in [E]$, we learn the predictor $\mathbf{x} \mapsto \langle \phi_{\theta_{\text{rep}}}(\mathbf{x}), \boldsymbol{\theta} \rangle$ where $\boldsymbol{\theta}$ is the weight of the last layer shared by all source environments via

$$\min_{\theta_{\text{rep}}, \boldsymbol{\theta}} \frac{1}{E} \sum_{e=1}^E \mathcal{L}(\langle \phi_{\theta_{\text{rep}}}(X^e), \boldsymbol{\theta} \rangle, \mathbf{y}^e) + \lambda_{\text{NUC}} \cdot \|\phi_{\theta_{\text{rep}}}(X^e)\|_* \quad (7)$$

where $\mathcal{L}(\cdot, \cdot)$ is the standard Cross-Entropy (CE) loss. The nuclear norm regularization (Shi et al., 2023) helps us learn a low-rank representation that captures the **content features** from the source environments. The learned $\phi_{\theta_{\text{rep}}}$ will be utilized in the target environment for finetuning. We vary regularization strength $\lambda_{\text{NUC}} \in \{0.01, 0.1\}$ to control the complexity of the feature space, larger λ_{NUC} will lead to an more invariant feature space. However, tuning the λ requires prior over the feature space or training multiple times.

Target Finetuning: We use the source pretrained $\phi_{\theta_{\text{rep}}}$ and $\boldsymbol{\theta}$ as the initialization and use ERM in the finetuning stage.

2.3.2. PROJECTIONNET (OURS)

The nuclear norm regularization has a fundamental limitation: we need to tune the regularization strength λ_{NUC} to control the complexity of the feature space. However, in practice, we may have no prior and it is unrealistic to tune the regularizer multiple times for large datasets source pretraining. To address this issue, we propose **ProjectionNet**, a training method that naturally distinguishes **invariant features** ϕ_y , **approximately shared features** ϕ_s and **environment-specific features** ϕ_e .

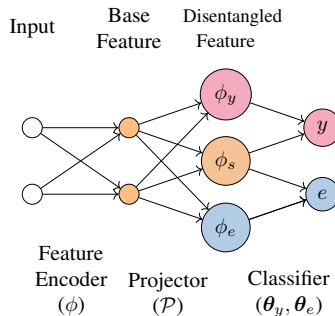


Figure 3. ProjectionNet: We disentangle the base representation ϕ into **target-specific feature** ϕ_y , **approximately shared feature** ϕ_s and **environment-specific feature** ϕ_e . (P_y, P_s, P_e) are the projection heads applied to the base feature. The $[\phi_y, \phi_s]$ are used in the target label prediction. $[\phi_s, \phi_e]$ are used in the environment label prediction.

Source Pretraining: For each training sample we consider the triplet (\mathbf{x}, y, e) where e is the environment (\mathbf{x}, y) belongs to. Let $\phi_{\theta_{\text{rep}}}$ with trainable weights θ_{rep} be some feature map. Besides the model weights, we would like to train 3 projections $\mathcal{P}_y, \mathcal{P}_s, \mathcal{P}_e$ such that $\phi_y = \phi_{\theta_{\text{rep}}}(\mathbf{x})\mathcal{P}_y$, $\phi_s = \phi_{\theta_{\text{rep}}}(\mathbf{x})\mathcal{P}_s$, $\phi_e = \phi_{\theta_{\text{rep}}}(\mathbf{x})\mathcal{P}_e$. The algorithm is summarized in equation 8.

$$\min_{\theta_{\text{rep}}, \theta_y, \theta_e, \mathcal{P}_e, \mathcal{P}_y, \mathcal{P}_s} \mathcal{L}_y + \mathcal{L}_e + \mathcal{L}_{\text{disentangle}} + \lambda \mathcal{L}_{\text{reg}} \quad (8)$$

where

$$\begin{aligned} \mathcal{L}_y &= \frac{1}{n_1} \sum_{i=1}^{n_1} \mathcal{L} \left(\begin{bmatrix} \phi_{\theta_{\text{rep}}}(\mathbf{x}_i) \mathcal{P}_y \\ \phi_{\theta_{\text{rep}}}(\mathbf{x}_i) \mathcal{P}_s \end{bmatrix} \theta_y, y_i \right), \\ \mathcal{L}_e &= \frac{1}{n_1} \sum_{i=1}^{n_1} \text{CE} \left(\begin{bmatrix} \phi_{\theta_{\text{rep}}}(\mathbf{x}_i) \mathcal{P}_s \\ \phi_{\theta_{\text{rep}}}(\mathbf{x}_i) \mathcal{P}_e \end{bmatrix} \theta_e, e_i \right), \\ \mathcal{L}_{\text{disentangle}} &= \|\mathcal{P}_y^\top \mathcal{P}_e\|_F^2 + \|\mathcal{P}_y^\top \mathcal{P}_s\|_F^2 + \|\mathcal{P}_e^\top \mathcal{P}_s\|_F^2, \\ \mathcal{L}_{\text{reg}} &= \|\mathcal{P}_e^\top \mathcal{P}_e - I\|_F^2 + \|\mathcal{P}_y^\top \mathcal{P}_y - I\|_F^2 + \|\mathcal{P}_s^\top \mathcal{P}_s - I\|_F^2. \end{aligned}$$

This method is based on the assumption that the approximately shared features are correlated to both y and the environment. We jointly minimize the 4 loss functions above. \mathcal{L}_y is the standard empirical minimization, it extracts the features that are correlated to the response y , *i.e.*, **invariant features** and **approximately shared features**. \mathcal{L}_e extracts the features that determine the environment of a training sample (\mathbf{x}, y) , *i.e.*, **approximately shared features** and **environmental features**. $\mathcal{L}_{\text{disentangle}}$ ensures that the learned learned \mathcal{P} 's are almost orthogonal to each other and \mathcal{L}_{reg} ensures the columns of the learned \mathcal{P} 's are almost orthogonal. The method is visualized in Figure 3.

Target Finetuning: We can flexibly choose to utilize ϕ_y or $[\phi_y, \phi_s]$ as the initialization for the target finetuning phase, which depends on whether we want to use invariant features or content features.

3. Theoretical Analysis

In this section, we will present the statistical analysis of the learning framework in Section 2.2. Before stating the main theorem, we make the following assumptions.

Assumption 3.1 (Homogeneous input distribution). We assume that all the tasks follow the same input distribution, *i.e.*, for $e \in [E + 1]$, $p_1 = \dots = p_{E+1} = p$.

This assumption is for the simplicity of theoretical analysis since otherwise we may need stronger assumptions on the representation function class. When the representation function is linear, we show that this assumption can be relaxed to moment boundedness conditions (see Section B).

We will use the covariance between two representations to measure the distance between representation functions. Our notion of representation covariance is generalized from Du et al. (2021) to measure the distance from different function classes. We defer the detailed properties of representation covariance to Section A.

Definition 3.2 (Covariance between representations). Let p be a distribution over \mathbb{R}^d and Φ_D be some function class with Φ_k / Φ_{D-k} defined in equation 1. For two representation functions $\phi \in \Phi_{d_1}$, $\phi' \in \Phi_{d_2}$, $d_1, d_2 \in \{D, k, D - k\}$, we define the covariance between ϕ and ϕ' with respect to p as $\Sigma_p(\phi, \phi') = \mathbb{E}_{\mathbf{x} \sim p} [\phi(\mathbf{x})\phi'(\mathbf{x})^\top] \in \mathbb{R}^{d_1 \times d_2}$, where d_1 and d_2 are the output dimension of ϕ and ϕ' . We also define the symmetric covariance as

$$S_p(\phi, \phi') = \begin{bmatrix} \Sigma_p(\phi, \phi) & \Sigma_p(\phi, \phi') \\ \Sigma_p(\phi', \phi) & \Sigma_p(\phi', \phi') \end{bmatrix} \in \mathbb{R}^{(d_1+d_2) \times (d_1+d_2)}.$$

If $\phi := \phi'$, we abbreviate $\Sigma_p(\phi, \phi) := \Sigma_p(\phi)$, $S_p(\phi, \phi) = S_p(\phi)$.

We make Assumption A.1 and A.2 on the ground-truth representation function class Φ_D and the input distribution p , which ensure the point-wise and uniform concentration of empirical covariance $S_{\hat{p}}$ to their population counterpart S_p . In our main theorem, we assume n_1 is large enough to guarantee uniform concentration and n_2 is large enough to guarantee point-wise concentration (this implies $n_1 \gtrsim n_2$).

The following assumption guarantees $\langle \phi_{D[1:k]}^*(\mathbf{x}), \theta_{[1:k]}^{*e} \rangle$ dominants in equation 4, that is, the contribution of content features to y is stronger than that of environmental features.

Assumption 3.3 (Dominance of content features).

$$\frac{\left\| \Sigma_p(\phi_{D[1:k]}^*) \right\|}{\left\| \Sigma_p(\phi_{D[k+1:D]}^*) \right\|} \gtrsim \frac{\text{Tr}(\Lambda_{22})}{\|\boldsymbol{\theta}^*\|^2 + \text{Tr}(\Lambda_{11})}$$

Assumption 3.4 (Diverse source tasks). Let $\Theta^* = [\boldsymbol{\theta}^{*1}, \dots, \boldsymbol{\theta}^{*E}]$. The smallest singular value of Θ^* satisfies $\sigma_{\min}^2(\Theta^*) \gtrsim \frac{E}{\|\boldsymbol{\theta}^*\|^2 + \text{Tr}(\Lambda_{11})}$.

This assumption requires source tasks to utilize all directions of the representation function, or otherwise the weakest direction will be hard to learn.

Our main results are the following theorems.

Theorem 3.5 (Source environment guarantee, informal version of Theorem A.3). *Under Assumption 3.1, A.2, 3.3, and 3.4, if n_1 is large enough, the average excess risk across the source environments with probability $1 - o(1)$ satisfies*

$$\begin{aligned} \overline{\text{ER}}(\widehat{\phi}_k^E, \widehat{\boldsymbol{\theta}}^1, \dots, \widehat{\boldsymbol{\theta}}^E) &:= \frac{1}{E} \sum_{e=1}^E \text{ER}_e(\widehat{\phi}_k^E, \widehat{\boldsymbol{\theta}}^e) \\ &\lesssim \underbrace{\sigma \sqrt{\frac{\mathcal{C}_{\text{cont}}}{n_1 E}} + \mathcal{C}_{\text{env}}}_{:=RE} \end{aligned}$$

where $\mathcal{C}_{\text{cont}} \asymp O(k)$ measures the complexity of content features and $\mathcal{C}_{\text{env}} \asymp O(D - k)$ measures the complexity of environmental features.

In this result, the first term indicates we are able to learn the (approximately) shared representation with all $n_1 E$ samples and the second term is the non-vanishing error caused by environmental features since we only learn content features. This result is vacuous but will be useful for the target environment.

Theorem 3.6 (Target environment guarantee, informal version of Theorem A.4). *Under Assumption 3.1, A.1, A.2, 3.3, and 3.4, we further assume that n_1 and n_2 are large enough but still $n_1 \lesssim n_2$. Under proper choice of λ_1 and λ_2 , the excess risk of the learned predictor $\mathbf{x} \mapsto \langle \widehat{\phi}_D^{E+1}(\mathbf{x}), \widehat{\boldsymbol{\theta}}^{E+1} \rangle$ in equation 6 on the target domain with probability $1 - o(1)$ satisfies*

$$\begin{aligned} &\mathbb{E}_{\boldsymbol{\theta}^{*E+1}} \left[\text{ER}(\widehat{\phi}_D^{E+1}, \widehat{\boldsymbol{\theta}}^{E+1}) \right] \\ &\lesssim \underbrace{\sigma \sqrt{\frac{\overline{\mathcal{C}}'_{\text{env}}}{n_2}} + \sigma \sqrt{\frac{k}{n_2}}}_{\text{adaptation error}} + \underbrace{\sigma \sqrt{\frac{RE}{n_2}}}_{\text{representation error}}, \end{aligned}$$

where $\overline{\mathcal{C}}'_{\text{env}} \asymp O(D - k)$ measures the complexity of the environmental representation function class.

In this excess risk, the first two terms are the adaptation error: it roughly is what the result will look like if we fine-tune the model with the perfect $\phi_{D[1:k]}^*$. The third term is the representation error caused by learning $\phi_{D[1:k]}^*$ with finite samples from the source tasks. It can be further reduced by target samples in the fine-tuning phase. Compared to previous work Chua et al. (2021); Du et al. (2021); Tripuraneni et al. (2020; 2021) that presents irreducible representation error (which does not go to zero as $n_2 \rightarrow \infty$) plus adaptation/estimation error, we no longer have the irreducible term from source tasks.

Remark 3.7 (Linear representation). When the ground-truth representation function class Φ_D is linear, we propose a spectral algorithm inspired by Tripuraneni et al. (2021) along with its statistical analysis in Section B. The idea is similar to the general case discussed above but is tractable in terms of optimization and our fine-tuning phase on the target environment removes the irreducible term from the risk bound in Tripuraneni et al. (2021).

4. Experiments

In Section 4.1, we verify our results with simulations under our exact theoretical framework in Section B, which is the case when the representation function is linear. In Section 4.2, we approximate the theoretical framework controlling the

feature space implicitly by using the **Nuclear Norm (NUC)** regularization and explicitly by learning the *Disentangled Representation* via **ProjectionNet**. We show that controlling the feature space to learn the approximately shared feature will benefit the downstream domain adaptation.

4.1. Synthetic Data

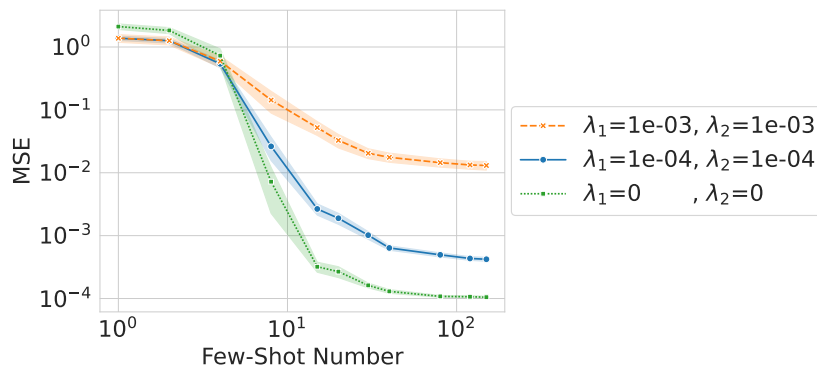


Figure 4. Target Loss v.s. few-shot number plot for linear synthetic data. Both Reg_1 and Reg_2 in Equation 22 help the domain adaptation performance.

We use synthetic data to validate the linear representation. The ground-truth representation R^* is a randomly generated orthogonal matrix², and for $e \in [E + 1]$, the environment-specific parameters θ^{*e} are sampled according to the meta distribution Equation 3. In **Few-shot domain adaptation**, we test the linear model via the close form solution of Equation 22. We present the loss v.s. few-shot number plot in Figure 4.

4.2. Real Data

We conducted an empirical evaluation of learning behaviors on VLCS (Fang et al., 2013), OfficeHome (Venkateswara et al., 2017), TerraIncognita (Beery et al., 2018) subset from DomainBed benchmark (Gulrajani & Lopez-Paz, 2020) for the real dataset experiment. We use the same training setting as DeepDG (Wang & Lu). We use three domains as source environments and one as the target environment. In the source domain training stage, we train the model 60 epochs with the source data in the source domain training stage. The model that performed best on the source data validation set was selected for further testing. This model was then applied to the target domain to assess its **domain generalization** capabilities. To test whether the representation is adaptive to the target domain, we do **linear probing** on the target domain with different sizes of target data; the tuning of the hyperparameter and selecting the best model are based on the target data validation set.

4.3. Training Details

In the target finetuning stage, we initialize the classifier from source pretrained θ over different feature parts: For example, PN-Y is the backbone with the classifier only using the target-specific feature.³

Domain Generalization We show the results of Domain Generalization in Table 1. The model is trained on the D_S and directly tested on the D_T . We show that ProjectionNet can achieve similar or better performance than DiWA with **20 times** less training time and without hyperparameter tuning headaches like NUC.

²Details in subsection E.1

³We have different training hyperparameters space with DomainBed. The absolute performance may differ from the DomainBed benchmark, but the relative rank is consistent. All the runs are averaged over 5 runs seeds. We show the figure with the shaded area representing the Standard Error. We describe the ablation study, full results and more detailed parameter settings in the appendix. Our code is available at <https://github.com/Xiang-Pan/ProjectionNet>.

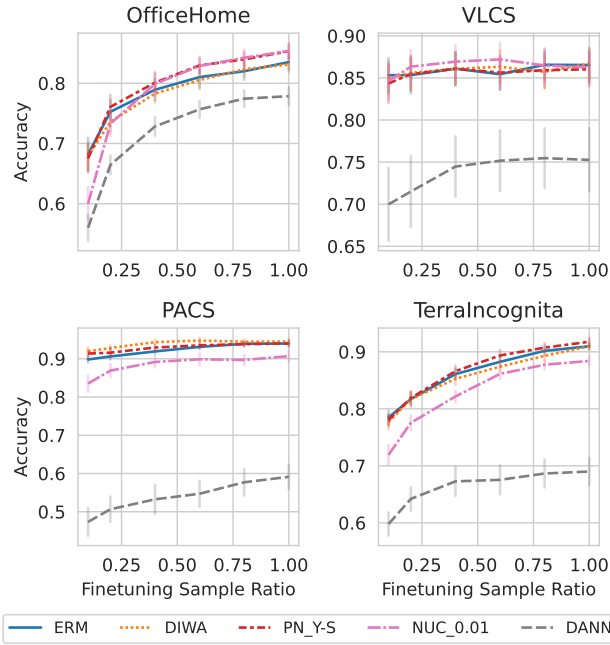


Figure 5. Linear Probing Results: We show the linear probing results, ProjectionNet share similar adaptive performance as DiWA

Linear Probing We show the linear probing results in Figure 5. With the target data, the linear probing performance increases, which suggests the feature from source pretraining is adaptive. However, there is a gap between the linear probing and target finetuning results. This suggests that we need to adjust the feature space to learn the target domain-specific feature.

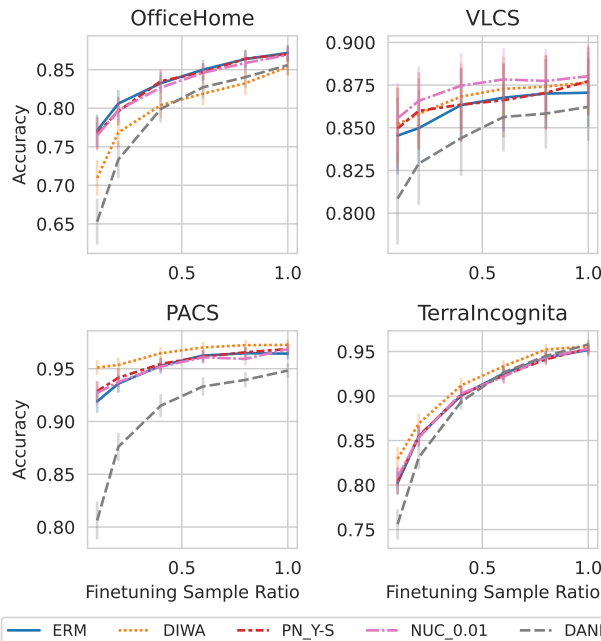


Figure 6. Target Finetuning Results: We show the target finetuning results with different feature parts. We can see that PN-YS and PN-YSE can achieve similar or better results than the traditional diverse feature learning method (DiWA) and strict invariant feature learning method (DANN).

Target Finetuning We tested the fixed backbone and feature encoder learning rate decay setting in domain adaptation; we show that for finetuning, we also need to adjust the feature encoder to learn the target domain-specific feature to achieve

good performance.

Feature Space Visualization To visualize the feature space and valid our hypothesis that the ProjectionNet learns approximately shared features helps, we visualize OfficeHome dataset alarm clock class using the GradCAM++ (Chattopadhyay et al., 2018) with source pretrained models feature space in Figure 2.

4.4. Empirical Takeaways

We found that in unsupervised domain generalization Table 1 or small target samples, methods with more invariant features (PN-Y, NUC-0.1) may achieve good performance; with large target fine-tuning samples, more diverse feature space will perform better. However, achieving invariant and diverse feature space is hard. ProjectionNet mitigates the paradox by disentangling the feature space into pieces with different invariance, which can be optionally used in downstream tasks.

Besides, we observe the following phenomena in our experiments. **Approximately Shared feature is not always helpful:** For datasets that domain generalization can achieve good performance (e.g., VLCS), invariant feature learning methods (DANN, PN-Y) will achieve good adaptation performance with finetuning. **Feature space adjustment is helpful with large target dataset size:** We see a clear gap between the target finetuning and the linear probing results, which suggests it is hard to learn a linear classifier as well as the target finetuning results. This process is comprehended as integrating the specific feature of the target domain into the representation. We show an ablation study that targets finetuning with feature learning rate decay, which decreases the performance most of the time (except for the VLCS dataset), which suggests that we need to adjust the feature space to learn the target domain-specific feature. **Disentangled Feature is more adaptive and semantical meaningful:** In the domain generalization setting, the PN-Y feature can achieve better performance than strict invariant feature learning (DANN, Large NUC Penalization) in most cases. In the target finetuning setting, we can see that PN-Y-S and PN-YSE can efficiently get similar or better results than the traditional diverse feature learning method (DiWA) and strict invariant feature learning method (DANN).

5. Conclusion

In this work, we present a theoretical framework for multi-source domain adaptation to incorporate different distributional shifts. Our theoretical framework naturally distinguishes content features from environmental features. We investigate the algorithms that can reduce the spurious correlation under our framework and derive generalization bound on the target distribution. We prove how adding regularization in both pre-training and fine-tuning phases reduces the impact of spurious features and quickly adapts to the target task with few samples. Our simulations and real-data experiments also support our findings.

References

- Ahuja, K., Shanmugam, K., Varshney, K., and Dhurandhar, A. Invariant risk minimization games. In *International Conference on Machine Learning*, pp. 145–155. PMLR, 2020.
- Ajakan, H., Germain, P., Larochelle, H., Laviolette, F., and Marchand, M. Domain-adversarial neural networks. *stat*, 1050: 15, 2014.
- Arjovsky, M., Bottou, L., Gulrajani, I., and Lopez-Paz, D. Invariant risk minimization. *arXiv preprint arXiv:1907.02893*, 2019.
- Beery, S., Van Horn, G., and Perona, P. Recognition in terra incognita. In *Proceedings of the European conference on computer vision (ECCV)*, pp. 456–473, 2018.
- Ben-David, S., Blitzer, J., Crammer, K., Kulesza, A., Pereira, F., and Vaughan, J. W. A theory of learning from different domains. *Machine learning*, 79:151–175, 2010.
- Berthelot, D., Roelofs, R., Sohn, K., Carlini, N., and Kurakin, A. Adamatch: A unified approach to semi-supervised learning and domain adaptation. In *International Conference on Learning Representations*, 2021.
- Cai, T., Gao, R., Lee, J., and Lei, Q. A theory of label propagation for subpopulation shift. In *International Conference on Machine Learning*, pp. 1170–1182. PMLR, 2021.
- Chattopadhyay, A., Sarkar, A., Howlader, P., and Balasubramanian, V. N. Grad-cam++: Generalized gradient-based visual explanations for deep convolutional networks. In *2018 IEEE winter conference on applications of computer vision (WACV)*, pp. 839–847. IEEE, 2018.
- Chen, Q. and Marchand, M. Algorithm-dependent bounds for representation learning of multi-source domain adaptation. In Ruiz, F., Dy, J., and van de Meent, J.-W. (eds.), *Proceedings of The 26th International Conference on Artificial Intelligence and Statistics*, volume 206 of *Proceedings of Machine Learning Research*, pp. 10368–10394. PMLR, 25–27 Apr 2023. URL <https://proceedings.mlr.press/v206/chen23h.html>.
- Chen, Y., Wei, C., Kumar, A., and Ma, T. Self-training avoids using spurious features under domain shift. *Advances in Neural Information Processing Systems*, 33:21061–21071, 2020.
- Chen, Y., Rosenfeld, E., Sellke, M., Ma, T., and Risteski, A. Iterative feature matching: Toward provable domain generalization with logarithmic environments. *Advances in Neural Information Processing Systems*, 35:1725–1736, 2022.
- Chua, K., Lei, Q., and Lee, J. D. How fine-tuning allows for effective meta-learning. In Beygelzimer, A., Dauphin, Y., Liang, P., and Vaughan, J. W. (eds.), *Advances in Neural Information Processing Systems*, 2021. URL <https://openreview.net/forum?id=-KGLlWv6kIc>.
- Cortes, C., Mansour, Y., and Mohri, M. Learning bounds for importance weighting. *Advances in neural information processing systems*, 23, 2010.
- Cortes, C., Mohri, M., and Muñoz Medina, A. Adaptation algorithm and theory based on generalized discrepancy. In *Proceedings of the 21th ACM SIGKDD International Conference on Knowledge Discovery and Data Mining*, pp. 169–178, 2015.
- Daumé III, H. Frustratingly easy domain adaptation. In *Proceedings of the 45th Annual Meeting of the Association of Computational Linguistics*, pp. 256–263, 2007.
- Davis, C. and Kahan, W. M. The rotation of eigenvectors by a perturbation III. *SIAM Journal on Numerical Analysis*, 7(1):1–46, 1970. ISSN 00361429. URL <http://www.jstor.org/stable/2949580>. Publisher: Society for Industrial and Applied Mathematics.
- Denevi, G., Ciliberto, C., Stamos, D., and Pontil, M. Learning to learn around a common mean. In Bengio, S., Wallach, H., Larochelle, H., Grauman, K., Cesa-Bianchi, N., and Garnett, R. (eds.), *Advances in Neural Information Processing Systems*, volume 31. Curran Associates, Inc., 2018. URL https://proceedings.neurips.cc/paper_files/paper/2018/file/b9a25e422ba96f7572089a00b838c3f8-Paper.pdf.

- Denevi, G., Pontil, M., and Ciliberto, C. The advantage of conditional meta-learning for biased regularization and fine tuning. In Larochelle, H., Ranzato, M., Hadsell, R., Balcan, M., and Lin, H. (eds.), *Advances in Neural Information Processing Systems*, volume 33, pp. 964–974. Curran Associates, Inc., 2020. URL https://proceedings.neurips.cc/paper_files/paper/2020/file/0a716fe8c7745e51a3185fc8be6ca23a-Paper.pdf.
- Deng, S., Ling, S., and Strohmer, T. Strong consistency, graph Laplacians, and the stochastic block model. *Journal of Machine Learning Research*, 22(117):1–44, 2021. URL <http://jmlr.org/papers/v22/20-391.html>.
- Du, S. S., Hu, W., Kakade, S. M., Lee, J. D., and Lei, Q. Few-shot learning via learning the representation, provably. In *International Conference on Learning Representations*, 2021. URL <https://openreview.net/forum?id=pW2Q2xLwIMD>.
- Fang, C., Xu, Y., and Rockmore, D. N. Unbiased metric learning: On the utilization of multiple datasets and web images for softening bias. In *Proceedings of the IEEE International Conference on Computer Vision*, pp. 1657–1664, 2013.
- Ganin, Y., Ustinova, E., Ajakan, H., Germain, P., Larochelle, H., Laviolette, F., Marchand, M., and Lempitsky, V. Domain-adversarial training of neural networks. *The journal of machine learning research*, 17(1):2096–2030, 2016.
- Gulrajani, I. and Lopez-Paz, D. In search of lost domain generalization. In *International Conference on Learning Representations*, 2020.
- HaoChen, J. Z., Wei, C., Kumar, A., and Ma, T. Beyond separability: Analyzing the linear transferability of contrastive representations to related subpopulations. *Advances in Neural Information Processing Systems*, 35:26889–26902, 2022.
- He, K., Zhang, X., Ren, S., and Sun, J. Deep residual learning for image recognition. In *Proceedings of the IEEE conference on computer vision and pattern recognition*, pp. 770–778, 2016.
- Heckman, J. J. Sample selection bias as a specification error. *Econometrica: Journal of the econometric society*, pp. 153–161, 1979.
- Koh, P. W., Sagawa, S., Marklund, H., Xie, S. M., Zhang, M., Balsubramani, A., Hu, W., Yasunaga, M., Phillips, R. L., Gao, I., et al. Wilds: A benchmark of in-the-wild distribution shifts. In *International Conference on Machine Learning*, pp. 5637–5664. PMLR, 2021.
- Kumar, A., Ma, T., and Liang, P. Understanding self-training for gradual domain adaptation. In *International Conference on Machine Learning*, pp. 5468–5479. PMLR, 2020.
- Kumar, A., Ma, T., Liang, P., and Raghunathan, A. Calibrated ensembles can mitigate accuracy tradeoffs under distribution shift. In *Uncertainty in Artificial Intelligence*, pp. 1041–1051. PMLR, 2022a.
- Kumar, A., Raghunathan, A., Jones, R., Ma, T., and Liang, P. Fine-tuning can distort pretrained features and underperform out-of-distribution. In *International Conference on Learning Representations*, 2022b.
- Lei, Q., Hu, W., and Lee, J. Near-optimal linear regression under distribution shift. In *International Conference on Machine Learning*, pp. 6164–6174. PMLR, 2021.
- Liu, E. Z., Haghgoo, B., Chen, A. S., Raghunathan, A., Koh, P. W., Sagawa, S., Liang, P., and Finn, C. Just train twice: Improving group robustness without training group information. In *International Conference on Machine Learning*, pp. 6781–6792. PMLR, 2021a.
- Liu, H., HaoChen, J. Z., Gaidon, A., and Ma, T. Self-supervised learning is more robust to dataset imbalance. In *International Conference on Learning Representations*, 2021b.
- Long, M., Cao, Z., Wang, J., and Jordan, M. I. Conditional adversarial domain adaptation. *Advances in neural information processing systems*, 31, 2018.
- Lu, C., Wu, Y., Hernández-Lobato, J. M., and Schölkopf, B. Nonlinear invariant risk minimization: A causal approach. *arXiv preprint arXiv:2102.12353*, 2021.
- Miyato, T., Maeda, S.-i., Koyama, M., and Ishii, S. Virtual adversarial training: a regularization method for supervised and semi-supervised learning. *IEEE transactions on pattern analysis and machine intelligence*, 41(8):1979–1993, 2018.

- Nam, J., Cha, H., Ahn, S., Lee, J., and Shin, J. Learning from failure: De-biasing classifier from biased classifier. *Advances in Neural Information Processing Systems*, 33:20673–20684, 2020.
- Park, G. Y. and Lee, S. W. Information-theoretic regularization for multi-source domain adaptation. In *Proceedings of the IEEE/CVF International Conference on Computer Vision (ICCV)*, pp. 9214–9223, October 2021.
- Pathak, R., Ma, C., and Wainwright, M. A new similarity measure for covariate shift with applications to nonparametric regression. In *International Conference on Machine Learning*, pp. 17517–17530. PMLR, 2022.
- Quinonero-Candela, J., Sugiyama, M., Schwaighofer, A., and Lawrence, N. D. *Dataset shift in machine learning*. Mit Press, 2008.
- Saenko, K., Kulis, B., Fritz, M., and Darrell, T. Adapting visual category models to new domains. In *Computer Vision—ECCV 2010: 11th European Conference on Computer Vision, Heraklion, Crete, Greece, September 5–11, 2010, Proceedings, Part IV 11*, pp. 213–226. Springer, 2010.
- Sagawa, S., Raghunathan, A., Koh, P. W., and Liang, P. An investigation of why overparameterization exacerbates spurious correlations. In *International Conference on Machine Learning*, pp. 8346–8356. PMLR, 2020.
- Shen, K., Jones, R. M., Kumar, A., Xie, S. M., HaoChen, J. Z., Ma, T., and Liang, P. Connect, not collapse: Explaining contrastive learning for unsupervised domain adaptation. In *International Conference on Machine Learning*, pp. 19847–19878. PMLR, 2022a.
- Shen, R., Bubeck, S., and Gunasekar, S. Data augmentation as feature manipulation. In *International conference on machine learning*, pp. 19773–19808. PMLR, 2022b.
- Shi, Z., Ming, Y., Fan, Y., Sala, F., and Liang, Y. Domain generalization via nuclear norm regularization. *arXiv preprint arXiv:2303.07527*, 2023.
- Shimodaira, H. Improving predictive inference under covariate shift by weighting the log-likelihood function. *Journal of statistical planning and inference*, 90(2):227–244, 2000.
- Srivastava, M., Hashimoto, T., and Liang, P. Robustness to spurious correlations via human annotations. In *International Conference on Machine Learning*, pp. 9109–9119. PMLR, 2020.
- Sun, Q., Chattopadhyay, R., Panchanathan, S., and Ye, J. A two-stage weighting framework for multi-source domain adaptation. In Shawe-Taylor, J., Zemel, R., Bartlett, P., Pereira, F., and Weinberger, K. (eds.), *Advances in Neural Information Processing Systems*, volume 24. Curran Associates, Inc., 2011. URL https://proceedings.neurips.cc/paper_files/paper/2011/file/d709f38ef758b5066ef31b18039b8ce5-Paper.pdf.
- Tripuraneni, N., Jordan, M., and Jin, C. On the theory of transfer learning: The importance of task diversity. *Advances in neural information processing systems*, 33:7852–7862, 2020.
- Tripuraneni, N., Jin, C., and Jordan, M. Provable meta-learning of linear representations. In *International Conference on Machine Learning*, pp. 10434–10443. PMLR, 2021.
- Tropp, J. A. User-friendly tail bounds for sums of random matrices. *Foundations of Computational Mathematics*, 12(4):389–434, August 2012. ISSN 1615-3375, 1615-3383. doi: 10.1007/s10208-011-9099-z. URL <http://link.springer.com/10.1007/s10208-011-9099-z>.
- Venkateswara, H., Eusebio, J., Chakraborty, S., and Panchanathan, S. Deep hashing network for unsupervised domain adaptation. In *Proceedings of the IEEE conference on computer vision and pattern recognition*, pp. 5018–5027, 2017.
- Wainwright, M. J. *High-Dimensional Statistics: A Non-Asymptotic Viewpoint*. Cambridge Series in Statistical and Probabilistic Mathematics. Cambridge University Press, 2019. doi: 10.1017/9781108627771.
- Wang, J. and Lu, W. Deepdg: Deep domain generalization toolkit. <https://github.com/jindongwang/transferlearning/tree/master/code/DeepDG>.
- Wang, M. and Deng, W. Deep visual domain adaptation: A survey. *Neurocomputing*, 312:135–153, 2018.

- Wei, C., Shen, K., Chen, Y., and Ma, T. Theoretical analysis of self-training with deep networks on unlabeled data. In *International Conference on Learning Representations*, 2020.
- Wortsman, M., Ilharco, G., Gadre, S. Y., Roelofs, R., Gontijo-Lopes, R., Morcos, A. S., Namkoong, H., Farhadi, A., Carmon, Y., Kornblith, S., et al. Model soups: averaging weights of multiple fine-tuned models improves accuracy without increasing inference time. In *International Conference on Machine Learning*, pp. 23965–23998. PMLR, 2022.
- Xie, Q., Dai, Z., Hovy, E., Luong, T., and Le, Q. Unsupervised data augmentation for consistency training. *Advances in neural information processing systems*, 33:6256–6268, 2020a.
- Xie, S. M., Kumar, A., Jones, R., Khani, F., Ma, T., and Liang, P. In-n-out: Pre-training and self-training using auxiliary information for out-of-distribution robustness. *arXiv preprint arXiv:2012.04550*, 2020b.
- Yang, S., Dong, Y., Ward, R., Dhillon, I. S., Sanghavi, S., and Lei, Q. Sample efficiency of data augmentation consistency regularization. In *International Conference on Artificial Intelligence and Statistics*, pp. 3825–3853. PMLR, 2023.
- Zadrozny, B. Learning and evaluating classifiers under sample selection bias. In *Proceedings of the twenty-first international conference on Machine learning*, pp. 114, 2004.
- Zhong, Z. S. and Ling, S. Improved theoretical guarantee for rank aggregation via spectral method. *arXiv preprint arXiv:2309.03808*, 2023.

A. General nonlinear representations

In this section, we will present the omitted details in Section 3 including Assumption A.1 and A.2, the complete version of Theorem 3.5 and 3.6, and the proof of them.

We make the following assumptions on the representation function class Φ_D and the input distribution p , which ensures the concentration properties of the representation covariances.

Assumption A.1 (Point-wise concentration). For some failure probability $\delta \in (0, 1)$, there exists a positive integer $N_{\text{point}}(\Phi_D, p, \delta)$ such that if $n \geq N_{\text{point}}(\Phi_D, p, \delta)$, then for any two given representation functions $\phi \in \Phi_{d_1}$, $\phi' \in \Phi_{d_2}$, $d_1, d_2 \in \{D, k, D - k\}$, n i.i.d. samples of p will with probability $1 - \delta$ satisfy

$$0.9S_p(\phi, \phi') \leq S_{\hat{p}}(\phi, \phi') \leq 1.1S_p(\phi, \phi')$$

where \hat{p} is the empirical distribution over the n samples.

Assumption A.2 (Uniform concentration). For some failure probability $\delta \in (0, 1)$, there exists a positive integer $N_{\text{unif}}(\Phi_D, q, \delta)$ such that if $n \geq N_{\text{unif}}(\Phi_D, q, \delta)$, then n i.i.d. samples of p will with probability $1 - \delta$ satisfy

$$0.9S_p(\phi, \phi') \leq S_{\hat{p}}(\phi, \phi') \leq 1.1S_p(\phi, \phi'), \\ \forall \phi \in \Phi_{d_1}, \phi' \in \Phi_{d_2},$$

where $d_1, d_2 \in \{D, k, D - k\}$ and \hat{p} is the empirical distribution over the n samples.

Assumption A.1 and A.2 are the conditions of the representation function class and the input distribution that ensure the concentration of empirical covariances to their population counterpart. Since Φ_k/Φ_{D-k} are function classes induced by some fixed Φ_D , the concentration of $S_{\hat{p}}$ in Φ_D automatically guarantees its concentration in Φ_k , Φ_{D-k} , and their union.

Since uniform concentration is stronger than point-wise concentration, we expect $N_{\text{unif}}(\Phi_D, q, \delta) \gtrsim N_{\text{point}}(\Phi_D, q, \delta)$. In particular, in the linear case discussed in Section B.2 where $\Phi_D = \{f : f(\mathbf{x}) = R^\top \mathbf{x}, R \in \mathcal{O}(d)\}$ and $\Phi_k = \{f : f(\mathbf{x}) = R^\top \mathbf{x}, R^\top R = I_k, R \in \mathbb{R}^{d \times k}\}$, we show that $N_{\text{unif}}(\Phi_D, q, \delta) = O(d)$ and $N_{\text{point}}(\Phi_D, q, \delta) = O(k)$ in Claim B.8 and B.9.

We present the complete version of Theorem 3.5 and 3.6 as follows.

Theorem A.3 (Full version of Theorem 3.5). *Under Assumption 3.1, A.2, 3.3, and 3.4, for some failure probability $\delta = o(1)$, we further assume $n_1 \gtrsim N_{\text{unif}}(\Phi_D, q, \delta)$, then the average excess risk across the source environments with probability $1 - o(1)$ satisfies*

$$\overline{\text{ER}}(\hat{\phi}_k^E, \hat{\theta}^1, \dots, \hat{\theta}^E) := \frac{1}{E} \sum_{e=1}^E \text{ER}_e(\hat{\phi}_k^E, \hat{\theta}^e) \lesssim \sigma \sqrt{\frac{C_{\text{cont}}}{n_1 E}} + C_{\text{env}}$$

where

$$C_{\text{cont}} := \left\| \Sigma_p(\phi_{D[1:k]}^*) \right\| \left(\|\theta^*\|^2 + \text{Tr}(\Lambda_{11}) \right), \quad C_{\text{env}} := \left\| \Sigma_p(\phi_{D[k+1:D]}^{*e}) \right\| \text{Tr}(\Lambda_{22}).$$

Theorem A.4 (Full version of Theorem 3.6). *Under Assumption 3.1, A.1, A.2, 3.3, and 3.4, for some failure probability $\delta = o(1)$, we further assume $n_1 \gtrsim N_{\text{unif}}(\Phi_D, q, \delta)$, $n_2 \gtrsim N_{\text{point}}(\Phi_D, q, \delta)$. Under the choice of λ_1 and λ_2 in 17, the excess risk of the learned predictor $\mathbf{x} \mapsto \langle \hat{\phi}_D^{E+1}(\mathbf{x}), \hat{\theta}^{E+1} \rangle$ in equation 6 on the target domain with probability $1 - o(1)$ satisfies*

$$\mathbb{E}_{\theta^{*E+1}} \left[\text{ER}_{E+1}(\hat{\phi}_D^{E+1}, \hat{\theta}^{E+1}) \right] \lesssim \sigma \sqrt{\frac{\overline{C}'_{\text{env}}}{n_2}} + \sigma \sqrt{\frac{k}{n_2}} + \sigma \sqrt{\frac{\text{RE}}{n_2}},$$

where

$$\overline{C}'_{\text{env}} := \left(\|\theta^*\|^2 + \text{Tr}(\Lambda_{11}) + \text{Tr}(\Lambda_{22}) \right) \max_{\phi \in \Phi_{D-k}} \text{Tr}(\Sigma_p(\phi)), \quad \text{RE} := \sigma \sqrt{\frac{C_{\text{cont}}}{n_1 E}} + C_{\text{env}}.$$

A.1. Representation divergence

First, we introduce the definition of representation divergence, which is helpful in the analysis of the excess risk. Note that it is a generalization of the representation divergence defined in (Du et al., 2021) where the authors only consider the divergence between representations in the same function class.

Definition A.5. Let q be a distribution over \mathbb{R}^d and Φ_D be some function class with Φ_k/Φ_{D-k} defined in equation 1. For two representation functions $\phi \in \Phi_{d_1}, \phi' \in \Phi_{d_2}, d_1, d_2 \in \{D, k, D-k\}$, we define the divergence between ϕ and ϕ' with respect to q as

$$D_q(\phi, \phi') = \Sigma_q(\phi', \phi') - \Sigma_q(\phi', \phi)(\Sigma_q(\phi, \phi))^\dagger \Sigma_q(\phi, \phi') \in \mathbb{R}^{d_2 \times d_2}.$$

It can be verified that $D_q(\phi, \phi') \succeq 0, D_q(\phi, \phi') = 0$ for any ϕ, ϕ' and q . The following lemma states the relation between covariance and divergence between representations. Note that in (Du et al., 2021), it holds for $\phi, \phi' \in \Phi$ for some function class Φ . It can be generalized to $\phi \in \Phi_{d_1}, \phi' \in \Phi_{d_2}, d_1, d_2 \in \{D, k, D-k\}$ using the same proof in (Du et al., 2021) due to the fact that Φ_k and Φ_{D-k} are induced by Φ_D .

Lemma A.6. Given two representation functions $\phi \in \Phi_{d_1}, \phi' \in \Phi_{d_2}, d_1, d_2 \in \{D, k, D-k\}$, and two distributions q, q' over \mathbb{R}^d . If

$$S_q(\phi, \phi') \succeq \alpha \cdot S_{q'}(\phi, \phi')$$

then

$$D_q(\phi, \phi') \succeq \alpha \cdot D_{q'}(\phi, \phi').$$

Proof. We will only show the case when $\phi \in \Phi_k$ and $\phi' \in \Phi_{D-k}$ since the technique is the same. For any $\mathbf{v} \in \mathbb{R}^{D-k}$, we will show that $\mathbf{v}^\top D_q(\phi, \phi') \mathbf{v} \geq \alpha \cdot \mathbf{v}^\top D_{q'}(\phi, \phi') \mathbf{v}$. We define the quadratic function $f(\mathbf{w}) := [\mathbf{w}^\top, -\mathbf{v}^\top] S_q(\phi, \phi') [\mathbf{w}^\top, -\mathbf{v}^\top]^\top$. Using the definition of $S_q(\phi, \phi')$, we get

$$\begin{aligned} f(\mathbf{w}) &= \mathbf{w}^\top \Sigma_q(\phi, \phi) \mathbf{w} - \mathbf{v}^\top \Sigma_q(\phi', \phi) \mathbf{w} - \mathbf{w}^\top \Sigma_q(\phi, \phi') \mathbf{v} + \mathbf{v}^\top \Sigma_q(\phi', \phi') \mathbf{v} \\ &= \mathbb{E}_{\mathbf{x} \sim q} [(\langle \phi(\mathbf{x}), \mathbf{w} \rangle - \langle \phi'(\mathbf{x}), \mathbf{v} \rangle)^2] \geq 0. \end{aligned}$$

Note that $f(\mathbf{w})$ has maximized at $\mathbf{w}^* = (\Sigma_q(\phi, \phi))^\dagger \Sigma_q(\phi, \phi') \mathbf{v}$

$$\min_{\mathbf{w} \in \mathbb{R}^k} f(\mathbf{w}) = f(\mathbf{w}^*) = \mathbf{v}^\top D_q(\phi, \phi') \mathbf{v}.$$

Similarly, let $g(\mathbf{w}) := [\mathbf{w}^\top, -\mathbf{v}^\top] S_{q'}(\phi, \phi') [\mathbf{w}^\top, -\mathbf{v}^\top]^\top$. We have

$$\min_{\mathbf{w} \in \mathbb{R}^k} g(\mathbf{w}) = \mathbf{v}^\top D_{q'}(\phi, \phi') \mathbf{v}.$$

Note that

$$S_q(\phi, \phi') \succeq \alpha \cdot S_{q'}(\phi, \phi')$$

implies $f(\mathbf{w}) \geq \alpha g(\mathbf{w})$ for any $\mathbf{w} \in \mathbb{R}^k$. Recall that $f(\mathbf{w})$ is minimized at \mathbf{w}^* , we have

$$\alpha \mathbf{v}^\top D_{q'}(\phi, \phi') \mathbf{v} = \alpha \min_{\mathbf{w} \in \mathbb{R}^k} g(\mathbf{w}) \leq \alpha g(\mathbf{w}^*) \leq f(\mathbf{w}^*) = \mathbf{v}^\top D_q(\phi, \phi') \mathbf{v},$$

which finishes the proof. \square

A.2. Proof of Theorem A.3

By the definition of average excess risk across source environment,

$$\overline{\text{ER}}(\widehat{\phi}_k^E, \widehat{\theta}^1, \dots, \widehat{\theta}^E) = \frac{1}{E} \sum_{e=1}^E \text{ER}_e(\widehat{\phi}_k^E, \widehat{\theta}^e). \quad (9)$$

For $e \in [E]$, we define the empirical excess risk on n_1 i.i.d. samples $(\mathbf{x}_1^e, y_1^e), \dots, (\mathbf{x}_{n_1}^e, y_{n_1}^e) \sim \mu^e$ as

$$\widehat{\text{ER}}(\widehat{\phi}_k^E, \widehat{\theta}^e) := \frac{1}{2n_1} \left\| \phi_D^*(X^e) \theta^{*e} - \widehat{\phi}_k^E(X^e) \widehat{\theta}^e \right\|^2. \quad (10)$$

Then each $\text{ER}_e(\widehat{\phi}_k^E, \widehat{\theta}^e)$ can be upper bounded by its empirical counterpart via

$$\begin{aligned} \text{ER}_e(\widehat{\phi}_k^E, \widehat{\theta}^e) &= \frac{1}{2} \mathbb{E}_{\mathbf{x} \sim p} [(\langle \phi_D^*(\mathbf{x}), \boldsymbol{\theta}^{*E+1} \rangle - \langle \widehat{\phi}_k^E(\mathbf{x}), \widehat{\theta}^e \rangle)^2] \\ &= \frac{1}{2} \begin{bmatrix} \widehat{\theta}^e \\ -\boldsymbol{\theta}^{*E+1} \end{bmatrix}^\top S_p(\widehat{\phi}_k^E, \phi_D^*) \begin{bmatrix} \widehat{\theta}^e \\ -\boldsymbol{\theta}^{*E+1} \end{bmatrix} \\ &\lesssim \begin{bmatrix} \widehat{\theta}^e \\ -\boldsymbol{\theta}^{*E+1} \end{bmatrix}^\top S_{\widehat{p}^e}(\widehat{\phi}_k^E, \phi_D^*) \begin{bmatrix} \widehat{\theta}^e \\ -\boldsymbol{\theta}^{*E+1} \end{bmatrix} \\ &= 2\widehat{\text{ER}}_e(\widehat{\phi}_k^E, \widehat{\theta}^e). \end{aligned}$$

Then to estimate equation 9, it suffices to upper bound the average empirical excess risk

$$\frac{1}{E} \sum_e \widehat{\text{ER}}_e(\widehat{\phi}_k^E, \widehat{\theta}^e) = \frac{1}{2n_1 E} \sum_{e=1}^E \left\| \phi_D^*(X^e) \boldsymbol{\theta}^{*e} - \widehat{\phi}_k^E(X^e) \widehat{\theta}^e \right\|^2. \quad (11)$$

By the optimality of $\widehat{\phi}_k, \widehat{\theta}_1, \dots, \widehat{\theta}_E$, the empirical risk of the source environments satisfies

$$\frac{1}{2n_1 E} \sum_{e=1}^E \left\| \mathbf{y}^e - \widehat{\phi}_k^E(X^e) \widehat{\theta}^e \right\|^2 \leq \frac{1}{2n_1 E} \sum_{e=1}^E \left\| \mathbf{y}^e - \phi_{D[1:k]}^*(X^e) \widehat{\theta}_{[1:k]}^e \right\|^2,$$

which implies that equation 11 can be decomposed into two terms

$$\begin{aligned} \frac{1}{2n_1 E} \sum_{e=1}^E \left\| \phi_D^*(X^e) \boldsymbol{\theta}^{*e} - \widehat{\phi}_k^E(X^e) \widehat{\theta}^e \right\|^2 &\leq \underbrace{\frac{1}{n_1 E} \sum_{e=1}^E \langle \widehat{\phi}_k^E(X^e) \widehat{\theta}^e - \phi_{D[1:k]}^*(X^e) \boldsymbol{\theta}_{[1:k]}^{*e}, \mathbf{z}^e \rangle}_{T_1} \\ &\quad + \underbrace{\frac{1}{2n_1 E} \sum_{e=1}^E \left\| \phi_{D[k+1:D]}^*(X^e) \boldsymbol{\theta}_{D[k+1:D]}^{*e} \right\|^2}_{T_2} \end{aligned} \quad (12)$$

where we use

$$\mathbf{y}^e = \phi_{D[1:k]}^*(X^e) \boldsymbol{\theta}_{[1:k]}^{*e} + \phi_{D[k+1:D]}^*(X^e) \boldsymbol{\theta}_{[k+1:D]}^{*e} + \mathbf{z}^e.$$

Estimation of T_1 . Using $\widehat{\phi}_k^E(X^e) \widehat{\theta}^e = \mathcal{P}_{\widehat{\phi}_k^E(X^e)} \mathbf{y}^e$, each summand of T_1 can be decomposed into

$$\begin{aligned} \langle \widehat{\phi}_k^E(X^e) \widehat{\theta}^e - \phi_{D[1:k]}^*(X^e) \boldsymbol{\theta}_{[1:k]}^{*e}, \mathbf{z}^e \rangle &= \underbrace{\langle -\mathcal{P}_{\widehat{\phi}_k^E(X^e)}^\perp \phi_{D[1:k]}^*(X^e) \boldsymbol{\theta}_{[1:k]}^{*e}, \mathbf{z}^e \rangle}_{T_{1,1,e}} \\ &\quad + \underbrace{\langle \mathcal{P}_{\widehat{\phi}_k^E(X^e)} \phi_{D[k+1:D]}^*(X^e) \boldsymbol{\theta}_{[k+1:D]}^{*e}, \mathbf{z}^e \rangle}_{T_{1,2,e}} \\ &\quad + \underbrace{\langle \mathcal{P}_{\widehat{\phi}_k^E(X^e)} \mathbf{z}^e, \mathbf{z}^e \rangle}_{T_{1,3,e}} \end{aligned}$$

Let $\mathbf{v}^e = n_1^{-1/2} \phi_{D[1:k]}^*(X^e) \boldsymbol{\theta}_{[1:k]}^{*e}$ which is independent of \mathbf{z}^e . Then

$$\begin{aligned} \frac{1}{n_1 E} \sum_{e=1}^E T_{1,1,e} &= \frac{1}{n_1 E} \sum_{e=1}^E \langle -\mathcal{P}_{\phi_k^E(X^e)}^\perp \phi_{D[1:k]}^*(X^e) \boldsymbol{\theta}_{[1:k]}^{*e}, \mathbf{z}^e \rangle \\ &\leq \frac{1}{\sqrt{n_1 E}} \sum_{e=1}^E \left\langle \frac{1}{\sqrt{n_1}} \phi_{D[1:k]}^*(X^e) \boldsymbol{\theta}_{[1:k]}^{*e}, \frac{1}{\sqrt{E}} \mathbf{z}^e \right\rangle \\ &= \frac{1}{\sqrt{n_1 E}} \sum_{e=1}^E \langle \mathbf{v}^e, \frac{1}{\sqrt{E}} \mathbf{z}^e \rangle \\ &\lesssim \frac{1}{\sqrt{n_1 E}} \sqrt{\frac{\sigma^2 \sum_{e=1}^E \|\mathbf{v}^e\|^2}{E}} \end{aligned}$$

where the last inequality is obtained via Bernstein's inequality. Note that we estimate $\|\mathbf{v}^e\|^2$ via

$$\begin{aligned} \|\mathbf{v}^e\|^2 &= \left\| n_1^{-1/2} \phi_{D[1:k]}^*(X^e) \boldsymbol{\theta}_{[1:k]}^{*e} \right\|^2 \\ &= \left\| \Sigma_{\hat{p}}^{1/2} (\phi_{D[1:k]}^*) \boldsymbol{\theta}_{[1:k]}^{*e} \right\|^2 \\ &\leq \left\| \Sigma_{\hat{p}} (\phi_{D[1:k]}^*) \right\| \left(\|\boldsymbol{\theta}^*\|^2 + \text{Tr}(\Lambda_{11}) \right) \\ &\lesssim \left\| \Sigma_p (\phi_{D[1:k]}^*) \right\| \left(\|\boldsymbol{\theta}^*\|^2 + \text{Tr}(\Lambda_{11}) \right) \end{aligned}$$

where we use $\boldsymbol{\theta}_{[1:k]}^{*e} \sim \mathcal{N}(\boldsymbol{\theta}^*, \Lambda_{11})$ and Assumption A.2. Thus,

$$\frac{1}{n_1 E} \sum_{e=1}^E T_{1,1,e} \lesssim \sigma \sqrt{\frac{\left\| \Sigma_p (\phi_{D[1:k]}^*) \right\| \left(\|\boldsymbol{\theta}^*\|^2 + \text{Tr}(\Lambda_{11}) \right)}{n_1 E}}.$$

Similarly,

$$\frac{1}{n_1 E} \sum_{e=1}^E T_{1,2,e} \lesssim \sigma \sqrt{\frac{\left\| \Sigma_p (\phi_{D[k+1:D]}^*) \right\| \sum_{j=D-k+1}^D (\Lambda_{22})_j}{n_1 E}}$$

where $\sum_{j=D-k+1}^D (\Lambda_{22})_j$ is the sum of top k entries in Λ_{22} , and

$$\frac{1}{n_1 E} \sum_{e=1}^E T_{1,3,e} \lesssim \frac{\sigma^2 k}{n_1}.$$

Then we obtain the estimation of T_1

$$\begin{aligned} T_1 &= \frac{1}{n_1 E} \sum_{e=1}^E (T_{1,1,e} + T_{1,2,e} + T_{1,3,e}) \\ &\lesssim \sigma \sqrt{\frac{\left\| \Sigma_p (\phi_{D[1:k]}^*) \right\| \left(\|\boldsymbol{\theta}^*\|^2 + \text{Tr}(\Lambda_{11}) \right)}{n_1 E}} + \sigma \sqrt{\frac{\left\| \Sigma_p (\phi_{D[k+1:D]}^*) \right\| \sum_{j=D-k+1}^D (\Lambda_{22})_j}{n_1 E}} + \frac{\sigma^2 k}{n_1} \\ &\lesssim \sigma \sqrt{\frac{\left\| \Sigma_p (\phi_{D[1:k]}^*) \right\| \left(\|\boldsymbol{\theta}^*\|^2 + \text{Tr}(\Lambda_{11}) \right)}{n_1 E}} \\ &= \sigma \sqrt{\frac{\mathcal{C}_{\text{cont}}}{n_1 E}} \end{aligned} \tag{13}$$

where we use Assumption 3.3 and omit the third term which is of small order in the last inequality.

Estimation of T_2 . Note that T_2 is the non-vanishing term as $n_1, E \rightarrow \infty$ because we only learn the content features from source environments. This term is the approximation error due to the environmental features, thus it can be bounded by the complexity of the environmental features.

$$\begin{aligned}
 T_2 &= \frac{1}{2n_1 E} \sum_{e=1}^E \left\| \phi_{D[k+1:D]}^*(X^e)^{*e} \boldsymbol{\theta}_{[k+1:D]}^{*e} \right\|^2 \\
 &= \frac{1}{E} \sum_{e=1}^E \left\| \Sigma_{\hat{p}}^{1/2}(\phi_{D[k+1:D]}^{*e}) \boldsymbol{\theta}_{[k+1:D]}^{*e} \right\|^2 \\
 &\lesssim \left\| \Sigma_p(\phi_{D[k+1:D]}^{*e}) \right\| \text{Tr}(\Lambda_{22}) \\
 &= \mathcal{C}_{\text{env}}
 \end{aligned} \tag{14}$$

Thus, with probability $1 - o(1)$, the average excess risk across source environments satisfies

$$\overline{\text{ER}}(\hat{\phi}_k^E, \hat{\boldsymbol{\theta}}^1, \dots, \hat{\boldsymbol{\theta}}^E) = \frac{1}{E} \sum_{e=1}^E \text{ER}_e(\hat{\phi}_k^E, \hat{\boldsymbol{\theta}}^e) \lesssim T_1 + T_2 \lesssim \sigma \sqrt{\frac{\mathcal{C}_{\text{cont}}}{n_1 E}} + \mathcal{C}_{\text{env}}.$$

A.3. Proof of Theorem A.4

In this section, we abbreviate $\text{ER}_{E+1}(\hat{\phi}_D^{E+1}, \hat{\boldsymbol{\theta}}^{E+1})$ as $\text{ER}(\hat{\phi}_D^{E+1}, \hat{\boldsymbol{\theta}}^{E+1})$ and $\widehat{\text{ER}}_{E+1}(\hat{\phi}_D^{E+1}, \hat{\boldsymbol{\theta}}^{E+1})$ as $\widehat{\text{ER}}(\hat{\phi}_D^{E+1}, \hat{\boldsymbol{\theta}}^{E+1})$. We will first bound the empirical excess risk of $\mathbf{x} \mapsto \langle \hat{\phi}_D^{E+1}(\mathbf{x}), \hat{\boldsymbol{\theta}}^{E+1} \rangle$ and then prove that it is close to its population counterpart. By the optimality of $(\hat{\phi}_D^{E+1}, \hat{\boldsymbol{\theta}}^{E+1})$ for equation 6, the empirical risk satisfies

$$\begin{aligned}
 &\frac{1}{2n_2} \left\| \mathbf{y}^{E+1} - \hat{\phi}_D^{E+1}(X^{E+1}) \hat{\boldsymbol{\theta}}^{E+1} \right\|^2 \\
 &\leq \frac{1}{2n_2} \left\| \mathbf{y}^{E+1} - \hat{\phi}_D^{E+1}(X^{E+1}) \hat{\boldsymbol{\theta}}^{E+1} \right\|^2 + \frac{\lambda_1}{n_2} \left\| \mathcal{P}_{\hat{\phi}_k^E(X^{E+1})}^\perp \hat{\phi}_D^{E+1}(X^{E+1}) \hat{\boldsymbol{\theta}}^{E+1} \right\|^2 + \frac{\lambda_2}{2} \left\| \hat{\boldsymbol{\theta}}^{E+1} \right\|^2 \\
 &\leq \frac{1}{2n_2} \left\| \mathbf{y}^{E+1} - \phi_D^*(X^{E+1}) \boldsymbol{\theta}^{*E+1} \right\|^2 + \frac{\lambda_1}{n_2} \left\| \mathcal{P}_{\hat{\phi}_k^E(X^{E+1})}^\perp \phi_D^*(X^{E+1}) \boldsymbol{\theta}^{*E+1} \right\|^2 + \frac{\lambda_2}{2} \left\| \boldsymbol{\theta}^{*E+1} \right\|^2.
 \end{aligned} \tag{15}$$

Let $A = [\phi_{D[1:k]}^*(X^{E+1}), \widehat{\phi}_k^E(X^{E+1})]$. By plugging $\mathbf{y}^{E+1} = \phi_D^*(X^{E+1})\boldsymbol{\theta}^{*E+1} + \mathbf{z}^{E+1}$ in equation 15, the empirical excess risk on the target task satisfies

$$\begin{aligned}
 \widehat{\text{ER}}(\widehat{\phi}_D^{E+1}, \widehat{\boldsymbol{\theta}}^{E+1}) &= \frac{1}{2n_2} \left\| \phi_D^*(X^{E+1})\boldsymbol{\theta}^{*E+1} - \widehat{\phi}_D^{E+1}(X^{E+1})\widehat{\boldsymbol{\theta}}^{E+1} \right\|^2 \\
 &\leq -\frac{1}{n_2} \left\langle \mathbf{z}^{E+1}, \phi_D^*(X^{E+1})\boldsymbol{\theta}^{*E+1} - \widehat{\phi}_D^{E+1}(X^{E+1})\widehat{\boldsymbol{\theta}}^{E+1} \right\rangle \\
 &\quad + \frac{\lambda_1}{n_2} \left\| \mathcal{P}_{\widehat{\phi}_k^E(X^{E+1})}^\perp \phi_D^*(X^{E+1})\boldsymbol{\theta}^{*E+1} \right\|^2 + \frac{\lambda_2}{2} \|\boldsymbol{\theta}^{*E+1}\|^2 \\
 &= -\frac{1}{n_2} \left\langle \mathbf{z}^{E+1}, \mathcal{P}_A \left(\phi_D^*(X^{E+1})\boldsymbol{\theta}^{*E+1} - \widehat{\phi}_D^{E+1}(X^{E+1})\widehat{\boldsymbol{\theta}}^{E+1} \right) \right\rangle \\
 &\quad - \frac{1}{n_2} \left\langle \mathbf{z}^{E+1}, \mathcal{P}_A^\perp \left(\phi_D^*(X^{E+1})\boldsymbol{\theta}^{*E+1} - \widehat{\phi}_D^{E+1}(X^{E+1})\widehat{\boldsymbol{\theta}}^{E+1} \right) \right\rangle \\
 &\quad + \frac{\lambda_1}{n_2} \left\| \mathcal{P}_{\widehat{\phi}_k^E(X^{E+1})}^\perp \phi_D^*(X^{E+1})\boldsymbol{\theta}^{*E+1} \right\|^2 + \frac{\lambda_2}{2} \|\boldsymbol{\theta}^{*E+1}\|^2 \\
 &\leq \underbrace{\frac{1}{n_2} \|\mathcal{P}_A \mathbf{z}^{E+1}\| \left\| \phi_D^*(X^{E+1})\boldsymbol{\theta}^{*E+1} - \widehat{\phi}_D^{E+1}(X^{E+1})\widehat{\boldsymbol{\theta}}^{E+1} \right\|}_{T_1} \\
 &\quad + \underbrace{\frac{1}{n_2} \left\langle \mathbf{z}^{E+1}, \mathcal{P}_A^\perp \phi_D^*(X^{E+1})\boldsymbol{\theta}^{*E+1} \right\rangle}_{T_2} \\
 &\quad + \underbrace{\frac{1}{n_2} \left\langle \mathbf{z}^{E+1}, \mathcal{P}_A^\perp \widehat{\phi}_D^{E+1}(X^{E+1})\widehat{\boldsymbol{\theta}}^{E+1} \right\rangle}_{T_3} \\
 &\quad + \underbrace{\frac{\lambda_1}{n_2} \left\| \mathcal{P}_{\widehat{\phi}_k^E(X^{E+1})}^\perp \phi_D^*(X^{E+1})\boldsymbol{\theta}^{*E+1} \right\|^2 + \frac{\lambda_2}{2} \|\boldsymbol{\theta}^{*E+1}\|^2}_{T_4}
 \end{aligned} \tag{16}$$

We will bound the 4 terms one by one.

Estimation of T_1 . Note that

$$\|\mathcal{P}_A \mathbf{z}^{E+1}\| \lesssim \sigma \sqrt{k},$$

then

$$T_1 \lesssim \frac{\sigma \sqrt{k}}{n_2} \left\| \phi_D^*(X^{E+1})\boldsymbol{\theta}^{*E+1} - \widehat{\phi}_D^{E+1}(X^{E+1})\widehat{\boldsymbol{\theta}}^{E+1} \right\| = 2\sigma \sqrt{\frac{k \widehat{\text{ER}}(\widehat{\phi}_D^{E+1}, \widehat{\boldsymbol{\theta}}^{E+1})}{n_2}}.$$

Estimation of T_2 .

$$\begin{aligned}
 T_2 &= \frac{1}{n_2} \left\langle \mathbf{z}^{E+1}, \mathcal{P}_A^\perp \phi_D^*(X^{E+1})\boldsymbol{\theta}^{*E+1} \right\rangle = \frac{1}{n_2} \left\| \phi_D^*(X^{E+1})^\top \mathcal{P}_A^\perp \mathbf{z}^{E+1} \right\| \|\boldsymbol{\theta}^{*E+1}\| \\
 &= \frac{1}{n_2} \left\| \phi_{D[k+1:D]}^*(X^{E+1})^\top \mathcal{P}_A^\perp \mathbf{z}^{E+1} \right\| \|\boldsymbol{\theta}^{*E+1}\| \\
 &\lesssim \sigma \sqrt{\frac{\text{Tr}(\Sigma_p(\phi_{D[k+1:D]}^*)) \left(\|\boldsymbol{\theta}^*\|^2 + \text{Tr}(\Lambda_{11}) + \text{Tr}(\Lambda_{22}) \right)}{n_2}} \\
 &= \lesssim \sigma \sqrt{\frac{\mathcal{C}'_{\text{env}}}{n_2}}
 \end{aligned}$$

where we use Assumption 3.3 and the fact that $A \perp \phi_{D[1:k]}^*(X^{E+1})$ and define $\mathcal{C}'_{\text{env}} := \text{Tr}(\Sigma_p(\phi_{D[k+1:D]}^*)) \left(\|\boldsymbol{\theta}^*\|^2 + \text{Tr}(\Lambda_{11}) + \text{Tr}(\Lambda_{22}) \right)$.

Estimation of T_3 . Similarly to T_2 , T_3 is bounded via

$$\begin{aligned}
 T_3 &= \frac{1}{n_2} \left\langle \mathbf{z}^{E+1}, \mathcal{P}_A^\perp \widehat{\phi}_D^{E+1}(X^{E+1}) \widehat{\boldsymbol{\theta}}^{E+1} \right\rangle \\
 &\leq \frac{1}{n_2} \left\| \widehat{\phi}_D^{E+1}(X^{E+1})^\top \mathcal{P}_A^\perp \mathbf{z}^{E+1} \right\| \left\| \widehat{\boldsymbol{\theta}}^{E+1} \right\| \\
 &\lesssim \sigma \sqrt{\frac{\text{Tr}(\Sigma_p(\widehat{\phi}_D^{E+1})) \left(\|\boldsymbol{\theta}^*\|^2 + \text{Tr}(\Lambda_{11}) + \text{Tr}(\Lambda_{22}) \right)}{n_2}} \\
 &\leq \sigma \sqrt{\frac{\overline{\mathcal{C}}_{\text{env}}}{n_2}}
 \end{aligned}$$

where $\overline{\mathcal{C}}_{\text{env}}$ is the maximum complexity of the environment features defined as

$$\overline{\mathcal{C}}_{\text{env}} := \left(\|\boldsymbol{\theta}^*\|^2 + \text{Tr}(\Lambda_{11}) + \text{Tr}(\Lambda_{22}) \right) \max_{\phi \in \Phi_{D-k}} \text{Tr}(\Sigma_p(\phi)).$$

Thus $T_3 \gtrsim T_2$ by definition.

Estimation of T_4 . The following lemma estimates $n_2^{-1} \left\| \mathcal{P}_{\widehat{\phi}_k^E(X^{E+1})}^\perp \phi_D^*(X^{E+1}) \boldsymbol{\theta}^{*E+1} \right\|^2$.

Lemma A.7. *Under the conditions in Theorem A.4, it holds with probability $1 - o(1)$ that*

$$\frac{1}{n_2} \left\| \mathcal{P}_{\widehat{\phi}_k^E(X^{E+1})}^\perp \phi_D^*(X^{E+1}) \boldsymbol{\theta}^{*E+1} \right\|^2 \lesssim \underbrace{\sigma \sqrt{\frac{\mathcal{C}_{\text{cont}}}{n_1 E}} + \mathcal{C}_{\text{env}}}_{:= \text{RE}}.$$

Then T_4 is bounded via

$$\begin{aligned}
 T_4 &= \frac{\lambda_1}{n_2} \left\| \mathcal{P}_{\widehat{\phi}_k^E(X^{E+1})}^\perp \phi_D^*(X^{E+1}) \boldsymbol{\theta}^{*E+1} \right\|^2 + \frac{\lambda_2}{2} \|\boldsymbol{\theta}^{*E+1}\|^2 \\
 &\lesssim \lambda_1 \text{RE} + \lambda_2 (\|\boldsymbol{\theta}^*\|^2 + \text{Tr}(\Lambda_{11}) + \text{Tr}(\Lambda_{22})).
 \end{aligned}$$

Combining the above 4 terms, and under the choice

$$\lambda_1 = \sqrt{\frac{\sigma^2}{n_2 \text{RE}}}, \quad \lambda_2 = \frac{\sigma \sqrt{\text{RE}}}{\sqrt{n_2} (\|\boldsymbol{\theta}^*\|^2 + \text{Tr}(\Lambda_{11}) + \text{Tr}(\Lambda_{22}))}, \quad (17)$$

we have the following quadratic inequality

$$\begin{aligned}
 \widehat{\text{ER}}(\widehat{\phi}_D^{E+1}, \widehat{\boldsymbol{\theta}}^{E+1}) &\lesssim 2\sigma \sqrt{\frac{k \widehat{\text{ER}}(\widehat{\phi}_D^{E+1}, \widehat{\boldsymbol{\theta}}^{E+1})}{n_2}} + \sigma \sqrt{\frac{\overline{\mathcal{C}}_{\text{env}}}{n_2}} \\
 &\quad + \lambda_1 \text{RE} + \lambda_2 (\|\boldsymbol{\theta}^*\|^2 + \text{Tr}(\Lambda_{11}) + \text{Tr}(\Lambda_{22})) \\
 &\lesssim 2\sigma \sqrt{\frac{k \widehat{\text{ER}}(\widehat{\phi}_D^{E+1}, \widehat{\boldsymbol{\theta}}^{E+1})}{n_2}} + \sigma \sqrt{\frac{\overline{\mathcal{C}}_{\text{env}}}{n_2}} + \sigma \sqrt{\frac{\text{RE}}{n_2}},
 \end{aligned} \quad (18)$$

which gives the solution

$$\widehat{\text{ER}}(\widehat{\phi}_D^{E+1}, \widehat{\boldsymbol{\theta}}^{E+1}) \lesssim \sigma \sqrt{\frac{\overline{\mathcal{C}}_{\text{env}}}{n_2}} + \sigma \sqrt{\frac{k}{n_2}} + \sigma \sqrt{\frac{\text{RE}}{n_2}}.$$

Finally, we will prove that the empirical excess risk is close to its population counterpart

$$\begin{aligned}
 \text{ER}(\widehat{\phi}_D^{E+1}, \widehat{\theta}^{E+1}) &= \frac{1}{2} \mathbb{E}_{\mathbf{x} \sim p} [(\langle \phi_D^*(\mathbf{x}), \boldsymbol{\theta}^{*E+1} \rangle - \langle \widehat{\phi}_D^{E+1}(\mathbf{x}), \widehat{\theta}^{E+1} \rangle)^2] \\
 &= \frac{1}{2} \begin{bmatrix} \widehat{\theta}^{E+1} \\ -\boldsymbol{\theta}^{*E+1} \end{bmatrix}^\top S_p(\widehat{\phi}_D^{E+1}, \phi_D^*) \begin{bmatrix} \widehat{\theta}^{E+1} \\ -\boldsymbol{\theta}^{*E+1} \end{bmatrix} \\
 &\lesssim \begin{bmatrix} \widehat{\theta}^{E+1} \\ -\boldsymbol{\theta}^{*E+1} \end{bmatrix}^\top S_{\widehat{p}^{E+1}}(\widehat{\phi}_D^{E+1}, \phi_D^*) \begin{bmatrix} \widehat{\theta}^{E+1} \\ -\boldsymbol{\theta}^{*E+1} \end{bmatrix} \\
 &= 2\widehat{\text{ER}}(\widehat{\phi}_D^{E+1}, \widehat{\theta}^{E+1}) \\
 &\lesssim \sigma \sqrt{\frac{\mathcal{C}'_{\text{env}}}{n_2}} + \sigma \sqrt{\frac{k}{n_2}} + \sigma \sqrt{\frac{\text{RE}}{n_2}}.
 \end{aligned} \tag{19}$$

A.4. Proof of Lemma A.7

Note that we have

$$\frac{1}{n_2} \left\| \mathcal{P}_{\widehat{\phi}_k^E(X^{E+1})}^\perp \phi_D^*(X^{E+1}) \boldsymbol{\theta}^{*E+1} \right\|^2 \leq \frac{1}{n_2} \left\| \mathcal{P}_{\widehat{\phi}_k^E(X^{E+1})}^\perp \phi_D^*(X^{E+1}) \right\|_F^2 \|\boldsymbol{\theta}^{*E+1}\|^2.$$

Let $\Theta^* = [\boldsymbol{\theta}^{*1}, \dots, \boldsymbol{\theta}^{*E}]$ and $\sigma_1(\Theta^*)$ be its smallest singular value. We have the following chain of inequalities

$$\begin{aligned}
 &\frac{1}{n_2} \left\| \mathcal{P}_{\widehat{\phi}_k^E(X^{E+1})}^\perp \phi_D^*(X^{E+1}) \right\|_F^2 \frac{\sigma_1^2(\Theta^*)}{E} \\
 &\leq \frac{1}{E} \text{Tr} \left(D_{\widehat{p}^{E+1}}(\widehat{\phi}_k^E, \phi_D^*) \right) \sigma_1^2(\Theta^*) \\
 &\lesssim \frac{1}{E} \text{Tr} \left(D_p(\widehat{\phi}_k^E, \phi_D^*) \right) \sigma_1^2(\Theta^*) \\
 &\leq \frac{1}{E} \left\| \left(D_p(\widehat{\phi}_k^E, \phi_D^*) \right)^{1/2} \Theta^* \right\|_F^2 \\
 &= \frac{1}{E} \sum_{e=1}^E \boldsymbol{\theta}^{*e\top} D_p(\widehat{\phi}_k^E, \phi_D^*) \boldsymbol{\theta}^{*e} \\
 &\lesssim \frac{1}{E} \sum_{e=1}^E \boldsymbol{\theta}^{*e\top} D_{\widehat{p}^e}(\widehat{\phi}_k^E, \phi_D^*) \boldsymbol{\theta}^{*e} \\
 &= \frac{1}{n_1 E} \sum_{e=1}^E \boldsymbol{\theta}^{*e\top} (\phi_D^*(X^e))^\top \left(I_{n_1} - \widehat{\phi}_k^E(X^e) \left[(\widehat{\phi}_k^E(X^e))^\top \widehat{\phi}_k^E(X^e) \right]^\dagger \widehat{\phi}_k^E(X^e) \right) \phi_D^*(X^e) \boldsymbol{\theta}^{*e} \\
 &= \frac{1}{n_1 E} \sum_{e=1}^E \left\| \mathcal{P}_{\widehat{\phi}_k^E(X^e)}^\perp \phi_D^*(X^e) \boldsymbol{\theta}^{*e} \right\|^2 \\
 &\lesssim \frac{1}{2n_1 E} \sum_{e=1}^E \left\| \phi_D^*(X^e) \boldsymbol{\theta}^{*e} - \widehat{\phi}_k^E(X^e) \widehat{\theta}^e \right\|^2 \\
 &\lesssim \underbrace{\sigma \sqrt{\frac{\mathcal{C}_{\text{cont}}}{n_1 E}}}_{\text{RE}} + \mathcal{C}_{\text{env}}.
 \end{aligned}$$

where we apply Assumption A.1 and A.2 and equation 10. Then using the gaussianity of $\boldsymbol{\theta}^{*E+1}$, we get

$$\begin{aligned}
 \frac{1}{n_2} \left\| \mathcal{P}_{\widehat{\phi}_k^E(X^{E+1})}^\perp \phi_D^*(X^{E+1}) \boldsymbol{\theta}^{*E+1} \right\|^2 &\leq \frac{1}{n_2} \left\| \mathcal{P}_{\widehat{\phi}_k^E(X^{E+1})}^\perp \phi_D^*(X^{E+1}) \right\|_F^2 \|\boldsymbol{\theta}^{*E+1}\|^2 \\
 &\lesssim \frac{E(\|\boldsymbol{\theta}^*\|^2 \text{Tr}(\Lambda_{11}) + \text{Tr}(\Lambda_{22}))}{\sigma_1^2(\Theta^*)} \text{RE}.
 \end{aligned}$$

Finally, under Assumption 3.3 and 3.4,

$$\frac{1}{n_2} \left\| \mathcal{P}_{\hat{\phi}_k^E(X^{E+1})}^\perp \phi_D^*(X^{E+1}) \boldsymbol{\theta}^{*E+1} \right\|^2 \lesssim \frac{E(\|\boldsymbol{\theta}^*\|^2 \text{Tr}(\Lambda_{11}) + \text{Tr}(\Lambda_{22}))}{\sigma_1^2(\Theta^*)} \text{RE} \lesssim \text{RE}.$$

B. Linear representations

In the linear case, the ground-truth representation function class is

$$\Phi_d = \{f : f(\mathbf{x}) = R^\top \mathbf{x}, R \in \mathcal{O}(d)\}.$$

In particular, we let the ground-truth representation function be $\phi_d^*(\mathbf{x}) = R^{*\top} \mathbf{x}$ where $R^* \in \mathcal{O}(d)$. Then the data generation process $(\mathbf{x}, y) \sim \mu_e$ for $e \in [E+1]$ can be described as

$$y = \langle \mathbf{x}, R^* \boldsymbol{\theta}^{e*} \rangle + z.$$

Given the meta distribution in equation 3, $R^* \boldsymbol{\theta}^{e*}$'s are i.i.d. rotated multivariate Gaussian random variables

$$\begin{aligned} R^* \boldsymbol{\theta}^{e*} &\sim \mathcal{N}(R_1^* \boldsymbol{\theta}^*, \Sigma_{\text{RM}}), \\ \Sigma_{\text{RM}} &= R_1^* \Lambda_{11} R_1^{*\top} + R_2^* \Lambda_{22} R_2^{*\top}, \end{aligned}$$

where $R^* = [R_1^*, R_2^*]$, R_1^* is the first k columns of R^* and R_2^* is the rest $(d-k)$ columns. The ‘‘RM’’ here stands for ‘‘rotated meta distribution’’.

B.1. The Meta-Representation Learning Algorithm

Our goal is to learn a low-dimensional representation

$$\hat{\phi}_k^E \in \Phi_k = \{f : f(\mathbf{x}) = R^\top \mathbf{x}, R^\top R = I_k, R \in \mathbb{R}^{d \times k}\}$$

from the source environments that capture the content features. In the linear case, it is equivalent to finding a $d \times k$ matrix with orthogonal columns to approximate R_1^* . If E is large enough, *i.e.*, we have enough source environments, a natural way of estimating R_1^* is to use the least k eigenvectors of the sample covariance matrix of $\hat{\boldsymbol{\theta}}^e$'s. This motivates the following learning process.

For each source environment $e \in [E]$, we obtain $\hat{\boldsymbol{\theta}}^e$ via empirical risk minimization

$$\hat{\boldsymbol{\theta}}^e = \underset{\boldsymbol{\theta}^e \in \mathbb{R}^d}{\text{argmin}} \frac{1}{2n_1} \|\mathbf{y}^e - X^e \boldsymbol{\theta}^e\|^2. \quad (20)$$

Let $\bar{\boldsymbol{\theta}}^E = E^{-1} \sum_{e=1}^E \hat{\boldsymbol{\theta}}^e$ be the ‘‘sample mean’’ of these learned parameters and consider the ‘‘sample covariance’’ with its eigendecomposition

$$\begin{aligned} \Sigma_{\hat{\boldsymbol{\theta}}} &= \frac{1}{E} \sum_{e=1}^E (\hat{\boldsymbol{\theta}}^e - \bar{\boldsymbol{\theta}}^E) (\hat{\boldsymbol{\theta}}^e - \bar{\boldsymbol{\theta}}^E)^\top \\ &= \hat{R}_1 \hat{\Lambda}_{11} \hat{R}_1^\top + \hat{R}_2 \hat{\Lambda}_{22} \hat{R}_2^\top \end{aligned} \quad (21)$$

where $\hat{\Lambda}_{11} \in \mathbb{R}^{k \times k}$ and $\hat{\Lambda}_{22} \in \mathbb{R}^{(d-k) \times (d-k)}$ are diagonal matrices with ascending entries, $\hat{\Lambda}_{11}$ consists of the least k eigenvalues of $\Sigma_{\hat{\boldsymbol{\theta}}}$ with eigenvectors $\hat{R}_1 \in \mathbb{R}^{d \times k}$ and $\hat{\Lambda}_{22}$ consists of the remaining $d-k$ eigenvalues with eigenvectors $\hat{R}_2 \in \mathbb{R}^{d \times (d-k)}$.

The learned representation \hat{R}_1 and the average parameter $\bar{\boldsymbol{\theta}}^E$ will be applied to the fine-tuning phase on the target environment via

$$\begin{aligned} \hat{\boldsymbol{\theta}}^{E+1} &= \underset{\boldsymbol{\theta}^{E+1} \in \mathbb{R}^d}{\text{argmin}} \frac{1}{2n_2} \|\mathbf{y}^{E+1} - X^{E+1} \boldsymbol{\theta}^{E+1}\|^2 \\ &\quad + \underbrace{\frac{\lambda_1}{2} \left\| \mathcal{P}_{\hat{R}_1}(\boldsymbol{\theta}^{E+1} - \bar{\boldsymbol{\theta}}^E) \right\|^2}_{\text{Reg}_1} + \underbrace{\frac{\lambda_2}{2} \left\| \mathcal{P}_{\hat{R}_1}^\perp(\boldsymbol{\theta}^{E+1}) \right\|^2}_{\text{Reg}_2}. \end{aligned} \quad (22)$$

This optimization is the empirical risk minimization on the target domain with two regularizing terms. Reg_1 penalizes the difference between $\theta - \bar{\theta}^E$ on the subspace spanned by the column space of the learned representation \widehat{R}_1 . This regularization encourages the learning dynamics to capture more content features approximately shared through all the environments. On the other hand, Reg_2 penalizes the weight in the directions that are perpendicular to the column space of \widehat{R}_1 , which discourages the learning dynamics from capturing the environmental features. This regularization-based fine-tuning process is motivated by the biased regularization (Denevi et al., 2018; 2020) which has been widely applied to the theoretical analysis of transfer learning.

We are interested in the excess risk of the learned predictor $\mathbf{x} \mapsto \langle \mathbf{x}, \widehat{\theta}^{E+1} \rangle$ on the target environment, *i.e.*, how much our learned model performs worse than the optimal model on the target task:

$$\text{ER}(\widehat{\theta}^{E+1}) = \frac{1}{2} \mathbb{E}_{(\mathbf{x}, y) \sim \mu_{E+1}} [\langle \mathbf{x}, R^* \theta^{*E+1} - \widehat{\theta}^{E+1} \rangle^2]. \quad (23)$$

We often calculate the expected excess risk with respect to the meta distribution, *i.e.*, $\mathbb{E}_{\theta^{*E+1}} [\text{ER}(\widehat{\theta}^{E+1})]$.

B.2. Theoretical Analysis

Before stating the main theorem, we first make some statistical assumptions on the input data. For $e \in [E + 1]$, we assume $\mathbb{E}_{\mathbf{x} \sim p_e} [\mathbf{x}] = \mathbf{0}$ and let $\Sigma_{X^e} = \mathbb{E}_{\mathbf{x} \sim p_e} [\mathbf{x} \mathbf{x}^\top]$. Note that a sample $\mathbf{x} \sim p_e$ can be generated from $\mathbf{x} = \Sigma_{X^e}^{1/2} \bar{\mathbf{x}}$ where $\bar{\mathbf{x}} \sim \bar{p}_e$ where $\mathbb{E}_{\bar{\mathbf{x}} \sim \bar{p}_e} [\bar{\mathbf{x}}] = \mathbf{0}$ and $\mathbb{E}_{\bar{\mathbf{x}} \sim \bar{p}_e} [\bar{\mathbf{x}} \bar{\mathbf{x}}^\top] = I_d$ (p_e is called the whitening of p_e). We make the following assumptions on the input distribution p_1, \dots, p_{E+1} .

Assumption B.1 (Subgaussian input). There exists $\rho > 0$ such that for $e \in [E + 1]$, $\bar{\mathbf{x}} \sim \bar{p}_e$ is ρ^2 -subgaussian.

Assumption B.2 (Covariance dominance). There exists $c > 0, c_2 > c_1 > 0$ and $\Sigma_X \succeq 0$ such that for $e \in [E]$, $c_1 \cdot \Sigma_X \preceq c \cdot \Sigma_{X^{E+1}} \preceq \Sigma_{X^e} \preceq c_2 \cdot \Sigma_X$.

Assumption B.1 is a standard assumption in statistical learning to obtain probabilistic tail bounds used in the proof. It might be replaced with other moment or boundedness conditions if we use different tail bounds in the analysis.

Assumption B.2 says that every direction spanned by Σ_{E+1} should be spanned by $\Sigma_e, e \in [E]$ and the parameter c quantifies how “easy” it is for Σ_e to cover Σ_{E+1} . We remark that instead of having $c \cdot \Sigma_{X^{E+1}} \preceq \Sigma_{X^e}$ for all $e \in [E]$, as long as this holds for a constant fraction of $[E]$, our result is valid. We also assume that Σ_{X^e} ’s are uniformly bounded by some PSD matrix Σ_X up to some constant, which facilitates our theoretical analysis.

Recall that we distinguish the content and environmental features based on the variation of their correlation with y . The following assumption guarantees the well-separation between these two features. Let $\Delta_\Lambda := \min(\Lambda_{22}) - \|\Lambda_{11}\|$ be the eigengap between environmental and content features.

Assumption B.3 (Well-separation).

$$\left\| \widehat{\Sigma}_\theta - \Sigma_{\text{RM}} \right\| \lesssim \Delta_\Lambda.$$

This assumption indicates the eigengap between the content feature space and environmental feature space in the covariance matrix Σ_{RM} is large enough so that the Davis-Kahan bound $\min_{O \in \mathcal{O}(k)} \left\| \widehat{R}_1 - R_1^* O \right\|$ is meaningful. One sufficient condition for the separation assumption is E and n_1 being sufficiently large: $\sqrt{\frac{d}{E}} \|\Lambda_{22}\| + \frac{\sigma^2}{n_1 \lambda_1(\Sigma_X)} \lesssim \Delta_\Lambda$.

Assumption B.4 (Content features dominance).

$$\frac{\text{Tr} \left(R_1^{*\top} \Sigma_X R_1^* \right)}{\text{Tr} \left(R_2^{*\top} \Sigma_X R_2^* \right)} \gtrsim \frac{\|\Lambda_{22}\|}{\|\Lambda_{11}\|}.$$

Remark B.5. In the liner case, equation 4 can be written as

$$y^e = \mathbf{x}^\top R_1^* \theta_{[1:k]}^{*e} + \mathbf{x}^\top R_2^* \theta_{[k+1:D]}^{*e} + z.$$

Assumption B.4 gaurentees

$$\mathbb{E}_{\theta^{*e}, (\mathbf{x}, y)} \left| \mathbf{x}^\top R_1^* \theta_{[1:k]}^{*e} \right| \gtrsim \mathbb{E}_{\theta^{*e}, (\mathbf{x}, y)} \left| \mathbf{x}^\top R_2^* \theta_{[k+1:D]}^{*e} \right|.$$

The following theorem gives a high probability bound of the excess risk for linear representations on the target domain.

Theorem B.6. *Under Assumption B.1, B.2, B.3 and B.4, we further assume that $k \leq d \leq E$ and the sample size in source and target environments satisfies $n_1 \gtrsim \rho^4 d$, $n_2 \gtrsim \rho^4 k$ and $n_1 \gtrsim n_2$. Under the choice of λ_1 and λ_2 in equation 27, with probability $1 - o(1)$, the excess risk of the learned predictor $\mathbf{x} \mapsto \langle \mathbf{x}, \hat{\boldsymbol{\theta}}^{E+1} \rangle$ in equation 22 is*

$$\begin{aligned} \mathbb{E}_{\boldsymbol{\theta}^{E+1}}[\text{ER}(\hat{\boldsymbol{\theta}}^{E+1})] &\lesssim \frac{\sigma^2 \|\Lambda_{11}\| \text{Tr}(R_1^{*\top} \Sigma_X R_1^*)}{n_2} + \frac{\sigma^2 \|\Lambda_{22}\| \text{Tr}(R_2^{*\top} \Sigma_X R_2^*)}{n_2} \\ &+ \frac{\sigma \|\Lambda_{22}\| \|\boldsymbol{\theta}^*\|}{n_2 (\min(\Lambda_{22}) - \|\Lambda_{11}\|)} \sqrt{\frac{d \text{Tr}(R_2^{*\top} \Sigma_X R_2^*)}{n_2 E}} + \xi(\sigma, n_1, n_2, d, k, E) \end{aligned}$$

where

$$\begin{aligned} \xi(\sigma, n_1, n_2, d, k, E) &= \frac{\sigma^2 \|\Sigma_X\| \text{Tr}(\Lambda_{11})}{n_2 E} + \frac{\sigma^4 \|\Sigma_X\| \text{Tr}(R_1^{*\top} \Sigma_X^{-1} R_1^*)}{n_1 n_2 E} + \frac{\sigma}{n_2} \sqrt{\frac{\text{Tr}(R_1^{*\top} \Sigma_X R_1^*) \text{Tr}(\Lambda_{11})}{n_2 E}} \\ &+ \frac{\sigma^2}{n_2} \sqrt{\frac{\text{Tr}(R_1^{*\top} \Sigma_X R_1^*) \text{Tr}(R_1^{*\top} \Sigma_X^{-1} R_1^*)}{n_1 n_2 E}} \end{aligned}$$

is the lower order terms.

Remark B.7. In our setting, traditional ridge regression will yield a $\sqrt{\frac{\sigma^2 \|\boldsymbol{\theta}^{*E+1}\|^2 \text{Tr}(\Sigma_X)}{n_2}}$ (and $\|\boldsymbol{\theta}^{*E+1}\|^2$ is bounded by $\|\boldsymbol{\theta}^*\|^2 + \|\Lambda_{11}\| + \|\Lambda_{22}\|$) rate. In comparison, our rate not only achieves a fast rate, but also manages to 1) quickly eliminate the error caused by the variation in utilizing content and environmental features (reflected by the Λ_{11} and Λ_{22} in the first two terms), and 2) fully utilize the shared part learned jointly from all E environments (reflected by the third term that involves $\|\boldsymbol{\theta}^*\|$ and is lower-order).

B.3. Proof of Theorem B.6

We first prove two claims on the covariance concentration for both source and target tasks.

Claim B.8 (covariance concentration of source tasks). Suppose $n_1 \gtrsim \rho^4 d$. Then it holds with probability $1 - o(1)$ that for $e \in [E]$,

$$0.9 \Sigma_{X^e} \preceq \frac{1}{n_1} X^{e\top} X^e \preceq 1.1 \Sigma_{X^e}.$$

Proof. For $e \in [E]$, we write $X^e = \bar{X}^e \Sigma_{X^e}^{1/2}$. Lemma C.2 gives

$$0.9 I_d \preceq \frac{1}{n_1} \bar{X}^{e\top} \bar{X}^e \preceq 1.1 I_d,$$

which implies that

$$0.9 \Sigma_{X^e} \preceq \frac{1}{n_2} \Sigma_{X^e}^{1/2} \bar{X}^{e\top} \bar{X}^e \Sigma_{X^e}^{1/2} \preceq 1.1 \Sigma_{X^e}.$$

Taking a union bound over all $e \in [E]$ finishes the proof. \square

Claim B.9 (covariance concentration of target tasks). Suppose $n_2 \gtrsim \rho^4 k$. Then for any $B \in \mathbb{R}^{d \times k}$, $k \leq d$, independent of X^{E+1} , it holds with probability $1 - o(1)$ that

$$0.9 B^\top \Sigma_{X^{E+1}} B \preceq \frac{1}{n_1} B^\top X^{E+1\top} X^{E+1} B \preceq 1.1 B^\top \Sigma_{X^{E+1}} B.$$

Proof. Let $X^{E+1} = \bar{X}^{E+1} \Sigma_{X^{E+1}}^{1/2}$. Let the SVD of $\Sigma_{X^{E+1}}^{1/2} B$ be UDV^\top where $U \in \mathbb{R}^{d \times k}$, $D, V \in \mathbb{R}^{k \times k}$. Then it can be verified that the rows of $X^{E+1} U$ are k -dimensional i.i.d. ρ^2 -subgaussian random vectors with zero mean and identity covariance. Then similarly to the proof of the source covariance concentration, Lemma C.2 together with some algebra operations finish the proof. \square

Then we will analyze the expected excess risk with respect to the meta distribution

$$\mathbb{E}_{\boldsymbol{\theta}^{*E+1}}[\text{ER}(\widehat{\boldsymbol{\theta}}^{E+1})] = \frac{1}{2} \mathbb{E}_{\boldsymbol{\theta}^{*E+1}} \mathbb{E}_{(\mathbf{x}, \mathbf{y}) \sim \mu_{E+1}} [(\langle \mathbf{x}, R^* \boldsymbol{\theta}^{*E+1} - \widehat{\boldsymbol{\theta}}^{E+1} \rangle)^2]. \quad (24)$$

The learned parameter of the target task from equation 22 has the closed form

$$\begin{aligned} \widehat{\boldsymbol{\theta}}^{E+1} &= \left(\frac{1}{n_2} X^{E+1\top} X^{E+1} + \lambda_1 \mathcal{P}_{\widehat{R}_1} + \lambda_2 \mathcal{P}_{\widehat{R}_1}^\perp \right)^{-1} \left(\frac{1}{n_2} X^{E+1\top} \mathbf{y}^{E+1} + \lambda_1 \mathcal{P}_{\widehat{R}_1} \bar{\boldsymbol{\theta}}^E \right) \\ &= C_{n_2, \lambda_1, \lambda_2}^{-1} \left(\frac{1}{n_2} X^{E+1\top} \mathbf{y}^{E+1} + \lambda_1 \mathcal{P}_{\widehat{R}_1} \bar{\boldsymbol{\theta}}^E \right). \end{aligned}$$

where

$$C_{n_2, \lambda_1, \lambda_2} = \left(\frac{1}{n_2} X^{E+1\top} X^{E+1} + \lambda_1 \mathcal{P}_{\widehat{R}_1} + \lambda_2 \mathcal{P}_{\widehat{R}_1}^\perp \right).$$

Recall that for $e \in [E + 1]$, the rotated meta distribution is

$$R^* \boldsymbol{\theta}^{*e} \stackrel{\text{i.i.d.}}{\sim} \mathcal{N}(R_1^* \boldsymbol{\theta}^*, \Sigma_{\text{RM}}), \quad \Sigma_{\text{RM}} = R_1^* \Lambda_{11} R_1^{*\top} + R_2^* \Lambda_{22} R_2^{*\top}.$$

Then it can be verified that

$$\begin{aligned} \widehat{\boldsymbol{\theta}}^{E+1} - R^* \boldsymbol{\theta}^{*E+1} &= C_{n_2, \lambda_1, \lambda_2}^{-1} \left(\frac{1}{n_2} X^{E+1\top} \mathbf{y}^{E+1} + \lambda_1 \mathcal{P}_{\widehat{R}_1} \bar{\boldsymbol{\theta}}^E \right) - R^* \boldsymbol{\theta}^{*E+1} \\ &= C_{n_2, \lambda_1, \lambda_2}^{-1} \left(\frac{1}{n_2} X^{E+1\top} (X^{E+1} R^* \boldsymbol{\theta}^{*E+1} + \mathbf{z}_{n_2}) + \lambda_1 \mathcal{P}_{\widehat{R}_1} \bar{\boldsymbol{\theta}}^E \right) - R^* \boldsymbol{\theta}^{*E+1} \\ &= \lambda_1 C_{n_2, \lambda_1, \lambda_2}^{-1} \mathcal{P}_{\widehat{R}_1} (\bar{\boldsymbol{\theta}}^E - R^* \boldsymbol{\theta}^{*E+1}) - \lambda_2 C_{n_2, \lambda_1, \lambda_2}^{-1} \mathcal{P}_{\widehat{R}_1}^\perp R^* \boldsymbol{\theta}^{*E+1} \\ &\quad + \frac{1}{n_2} C_{n_2, \lambda_1, \lambda_2}^{-1} X^{E+1\top} \mathbf{z}_{n_2} \end{aligned} \quad (25)$$

where in the second equality we use $\mathbf{y}^{E+1} = X^{E+1} R^* \boldsymbol{\theta}^{*E+1} + \mathbf{z}_{n_2}$. Plugging equation 25 into equation 24, the excess risk can be decomposed into 5 terms and we will bound each of them:

$$\begin{aligned} \mathbb{E}_{\boldsymbol{\theta}^{*E+1}}[\text{ER}(\widehat{\boldsymbol{\theta}}^{E+1})] &= \frac{1}{2} \mathbb{E}_{\boldsymbol{\theta}^{*E+1}} \left[\left(\widehat{\boldsymbol{\theta}}^{E+1} - R^* \boldsymbol{\theta}^{*E+1} \right)^\top \Sigma_{X^{E+1}} \left(\widehat{\boldsymbol{\theta}}^{E+1} - R^* \boldsymbol{\theta}^{*E+1} \right) \right] \\ &= \frac{1}{2} (T_1 + T_2 + T_3 + T_4 + T_5), \end{aligned} \quad (26)$$

where

$$\begin{aligned} T_1 &= \mathbb{E}_{\boldsymbol{\theta}^{*E+1}} \left[\lambda_1^2 (\bar{\boldsymbol{\theta}}^E - \boldsymbol{\theta}^{*E+1})^\top \mathcal{P}_{\widehat{R}_1} C_{n_2, \lambda_1, \lambda_2}^{-1} \Sigma_{X^{E+1}} C_{n_2, \lambda_1, \lambda_2}^{-1} \mathcal{P}_{\widehat{R}_1} (\bar{\boldsymbol{\theta}}^E - \boldsymbol{\theta}^{*E+1}) \right], \\ T_2 &= \mathbb{E}_{\boldsymbol{\theta}^{*E+1}} \left[\lambda_2^2 \boldsymbol{\theta}^{*E+1\top} \mathcal{P}_{\widehat{R}_1}^\perp C_{n_2, \lambda_1, \lambda_2}^{-1} \Sigma_{X^{E+1}} C_{n_2, \lambda_1, \lambda_2}^{-1} \mathcal{P}_{\widehat{R}_1}^\perp \boldsymbol{\theta}^{*E+1} \right], \\ T_3 &= \frac{1}{n_2^2} \mathbf{z}_{n_2}^\top X^{E+1} C_{n_2, \lambda_1, \lambda_2}^{-1} \Sigma_{X^{E+1}} C_{n_2, \lambda_1, \lambda_2}^{-1} X^{E+1\top} \mathbf{z}_{n_2}, \\ T_4 &= \mathbb{E}_{\boldsymbol{\theta}^{*E+1}} \left[\left\langle \lambda_1 C_{n_2, \lambda_1, \lambda_2}^{-1} \mathcal{P}_{\widehat{R}_1} (\bar{\boldsymbol{\theta}}^E - R^* \boldsymbol{\theta}^{*E+1}), \frac{1}{n_2} C_{n_2, \lambda_1, \lambda_2}^{-1} X^{E+1\top} \mathbf{z}_{n_2} \right\rangle \right], \\ T_5 &= \mathbb{E}_{\boldsymbol{\theta}^{*E+1}} \left[\left\langle -\lambda_2 C_{n_2, \lambda_1, \lambda_2}^{-1} \mathcal{P}_{\widehat{R}_1}^\perp R^* \boldsymbol{\theta}^{*E+1}, \frac{1}{n_2} C_{n_2, \lambda_1, \lambda_2}^{-1} X^{E+1\top} \mathbf{z}_{n_2} \right\rangle \right]. \end{aligned}$$

Estimation of T_1 . Let $\mathbf{v} = R^* \boldsymbol{\theta}^{*E+1} - R_1^* \boldsymbol{\theta}^*$. We have $\mathbb{E}_{\boldsymbol{\theta}^{*E+1}} [\mathbf{v}] = 0$ and $\mathbb{E}_{\boldsymbol{\theta}^{*E+1}} [\mathbf{v} \mathbf{v}^\top] = \Sigma_{\text{RM}}$. Then the first term T_1 can be written as

$$\begin{aligned}
 T_1 &= \mathbb{E}_{\boldsymbol{\theta}^{*E+1}} \left[\lambda_1^2 (\bar{\boldsymbol{\theta}}^E - R_1^* \boldsymbol{\theta}^* + \mathbf{v})^\top \mathcal{P}_{\widehat{R}_1} C_{n_2, \lambda_1, \lambda_2}^{-1} \Sigma_{X^{E+1}} C_{n_2, \lambda_1, \lambda_2}^{-1} \mathcal{P}_{\widehat{R}_1} (\bar{\boldsymbol{\theta}}^E - R_1^* \boldsymbol{\theta}^* + \mathbf{v}) \right] \\
 &= \lambda_1^2 (\bar{\boldsymbol{\theta}}^E - R_1^* \boldsymbol{\theta}^*)^\top \mathcal{P}_{\widehat{R}_1} C_{n_2, \lambda_1, \lambda_2}^{-1} \Sigma_{X^{E+1}} C_{n_2, \lambda_1, \lambda_2}^{-1} \mathcal{P}_{\widehat{R}_1} (\bar{\boldsymbol{\theta}}^E - R_1^* \boldsymbol{\theta}^*) \\
 &\quad + \lambda_1^2 \mathbb{E}_{\boldsymbol{\theta}^{*E+1}} \left[\mathbf{v}^\top \mathcal{P}_{\widehat{R}_1} C_{n_2, \lambda_1, \lambda_2}^{-1} \Sigma_{X^{E+1}} C_{n_2, \lambda_1, \lambda_2}^{-1} \mathcal{P}_{\widehat{R}_1} \mathbf{v} \right] \\
 &= \lambda_1^2 (\bar{\boldsymbol{\theta}}^E - R_1^* \boldsymbol{\theta}^*)^\top \mathcal{P}_{\widehat{R}_1} C_{n_2, \lambda_1, \lambda_2}^{-1} \Sigma_{X^{E+1}} C_{n_2, \lambda_1, \lambda_2}^{-1} \mathcal{P}_{\widehat{R}_1} (\bar{\boldsymbol{\theta}}^E - R_1^* \boldsymbol{\theta}^*) \\
 &\quad + \text{Tr} \left(\mathbb{E}_{\boldsymbol{\theta}^{*E+1}} \left[\widehat{R}_1^\top \mathbf{v} \mathbf{v}^\top \widehat{R}_1 \right] \lambda_1^2 \widehat{R}_1^\top C_{n_2, \lambda_1, \lambda_2}^{-1} \Sigma_{X^{E+1}} C_{n_2, \lambda_1, \lambda_2}^{-1} \widehat{R}_1 \right) \\
 &\leq \underbrace{\left\| \lambda_1 \Sigma_X^{1/2} C_{n_2, \lambda_1, \lambda_2}^{-1} \widehat{R}_1 \widehat{R}_1^\top (\bar{\boldsymbol{\theta}}^E - R_1^* \boldsymbol{\theta}^*) \right\|^2}_{T_{1,1}} + \underbrace{\lambda_1^2 \text{Tr} \left(\widehat{R}_1^\top C_{n_2, \lambda_1, \lambda_2}^{-1} \Sigma_X C_{n_2, \lambda_1, \lambda_2}^{-1} \widehat{R}_1 \right)}_{T_{1,2}} \left\| \mathbb{E}_{\boldsymbol{\theta}^{*E+1}} \left[\widehat{R}_1^\top \mathbf{v} \mathbf{v}^\top \widehat{R}_1 \right] \right\|.
 \end{aligned}$$

To bound $T_{1,1}$ we need the performance guarantee of $\bar{\boldsymbol{\theta}}^E$ on the direction of the content features, which is given by the following lemma.

Lemma B.10 (source task guarantee on the content feature space). *Under the conditions of Theorem B.6, with probability $1 - o(1)$,*

$$\left\| \mathcal{P}_{\widehat{R}_1} (\bar{\boldsymbol{\theta}}^E - R_1 \boldsymbol{\theta}^*) \right\| \lesssim \sqrt{\frac{1}{E} \text{Tr}(\Lambda_{11})} + \sqrt{\frac{\sigma^2 \text{Tr}(R_1^{*\top} \Sigma_X^{-1} R_1^*)}{n_1 E}} + \zeta(n_1, E, d)$$

and $\zeta(n_1, E, d)$ is the lower terms

$$\zeta(n_1, E, d) = (\min(\Lambda_{22}) - \|\Lambda_{11}\|)^{-1} \left(\sqrt{\frac{d}{E}} \|\Lambda_{22}\| + \frac{\sigma^2}{n_1 \lambda_1(\Sigma_X)} \right) \left(\sqrt{\frac{\text{Tr}(\Lambda_{11} + \Lambda_{22})}{E}} + \sqrt{\frac{\text{Tr}(\Sigma^{-1})}{n_1 E}} \right)$$

where $\lambda_i(\Sigma_X)$ denotes the i -th smallest eigenvalue of Σ_X .

Under the choice

$$\lambda_1 = \lambda_2 = \frac{\lambda_1(\Sigma_X) \sigma}{\sqrt{n_2} - \sigma}, \tag{27}$$

we have

$$\begin{aligned}
 T_{1,1} &\leq \lambda_1^2 \left\| \Sigma_X^{1/2} C_{n_2, \lambda_1, \lambda_2}^{-1} \widehat{R}_1 \right\|^2 \left\| \mathcal{P}_{\widehat{R}_1} (\bar{\boldsymbol{\theta}}^E - R_1 \boldsymbol{\theta}^*) \right\|^2 \\
 &\lesssim \lambda_1^2 \left\| \Sigma_X^{1/2} C_{n_2, \lambda_1, \lambda_2}^{-1} \widehat{R}_1 \right\|^2 \left(\frac{\text{Tr}(\Lambda_{11})}{E} + \frac{\sigma^2}{n_1 E} \text{Tr}(R_1^{*\top} \Sigma_X^{-1} R_1^*) \right) \\
 &\lesssim \frac{\sigma^2 \|\Sigma_X\|}{n_2} \left(\frac{\text{Tr}(\Lambda_{11})}{E} + \frac{\sigma^2}{n_1 E} \text{Tr}(R_1^{*\top} \Sigma_X^{-1} R_1^*) \right) \\
 &= \frac{\sigma^2 \|\Sigma_X\| \text{Tr}(\Lambda_{11})}{n_2 E} + \frac{\sigma^4 \|\Sigma_X\| \text{Tr}(R_1^{*\top} \Sigma_X^{-1} R_1^*)}{n_1 n_2 E}.
 \end{aligned}$$

Note that $T_{1,1}$ is of order $O(\sigma^2 k/n_2 E + \sigma^4 k/n_1 n_2 E)$ which will be omitted as a lower order term.

$$\begin{aligned}
 T_{1,2} &= \lambda_1^2 \text{Tr} \left(\widehat{R}_1^\top C_{n_2, \lambda_1, \lambda_2}^{-1} \Sigma_X C_{n_2, \lambda_1, \lambda_2}^{-1} \widehat{R}_1 \right) \left\| \mathbb{E}_{\boldsymbol{\theta}^{*E+1}} \left[\widehat{R}_1^\top \mathbf{v} \mathbf{v}^\top \widehat{R}_1 \right] \right\| \\
 &\leq \frac{\sigma^2 \text{Tr} \left(\widehat{R}_1^\top \Sigma_X \widehat{R}_1 \right)}{n_2} \left\| \widehat{R}_1^\top R_1^* \Lambda_{11} R_1^{*\top} \widehat{R}_1 + \widehat{R}_1^\top R_2^* \Lambda_{22} R_2^{*\top} \widehat{R}_1 \right\| \\
 &\lesssim \frac{\sigma^2 \text{Tr} \left(R_1^{*\top} \Sigma_X R_1^* \right)}{n_2} \left[\left(1 - \left\| R_2^{*\top} \widehat{R}_1 \right\|^2 \right) \|\Lambda_{11}\|^2 + \left\| R_2^{*\top} \widehat{R}_1 \right\|^2 \|\Lambda_{22}\| \right] \\
 &\lesssim \frac{\sigma^2 \|\Lambda_{11}\| \text{Tr} \left(R_1^{*\top} \Sigma_X R_1^* \right)}{n_2}
 \end{aligned}$$

where in the second equality we use $\Sigma_{\text{RM}} = R_1^* \Lambda_{11} R_1^{*\top} + R_2^* \Lambda_{22} R_2^{*\top}$, and in the third inequality we use Lemma B.11 that $\min_{O \in \mathcal{O}(k)} \|\widehat{R}_1 - R_1^* O\|^2 \asymp \|\widehat{R}_2^* \widehat{R}_1\|^2 = O(d/E + \sigma^2/n_1)$. $T_{1,2}$ is of order $O(\sigma^2 k/n_2)$ which is one of the dominant terms in the main theorem.

Estimation of T_2 . Similarly to the first term, the second term can be written as

$$\begin{aligned} T_2 &= \mathbb{E}_{\theta^{*E+1}} \left[\lambda_2^2 \theta^{*E+1\top} \mathcal{P}_{\widehat{R}_1}^\perp C_{n_2, \lambda_1, \lambda_2}^{-1} \Sigma_{X^{E+1}} C_{n_2, \lambda_1, \lambda_2}^{-1} \mathcal{P}_{\widehat{R}_1}^\perp \theta^{*E+1} \right] \\ &\lesssim \text{Tr} \left(\mathbb{E}_{\theta^{*E+1}} \left[\widehat{R}_2^\top \theta^{*E+1} \theta^{*E+1\top} \widehat{R}_2 \right] \lambda_2^2 \widehat{R}_2^\top C_{n_2, \lambda_1, \lambda_2}^{-1} \Sigma_X C_{n_2, \lambda_1, \lambda_2}^{-1} \widehat{R}_2 \right) \\ &\lesssim \lambda_2^2 \left(\left(1 - \|\widehat{R}_2^* \widehat{R}_1\|^2 \right) \|\Lambda_{22}\| + \|\widehat{R}_2^* \widehat{R}_1\|^2 \|\Lambda_{11}\| \right) \text{Tr} \left(\widehat{R}_2^\top C_{n_2, \lambda_1, \lambda_2}^{-1} \Sigma_X C_{n_2, \lambda_1, \lambda_2}^{-1} \widehat{R}_2 \right) \end{aligned}$$

Similarly to the second term of T_1 ,

$$T_2 \lesssim \frac{\sigma^2 \|\Lambda_{22}\| \text{Tr} (R_2^{*\top} \Sigma_X R_2^*)}{n_2}.$$

Under Assumption B.4, one can verify that $T_2 \lesssim T_{1,2}$.

Estimation of T_3 .

$$\begin{aligned} T_3 &= \frac{1}{n_2^2} \mathbf{z}_{n_2}^\top X^{E+1} C_{n_2, \lambda_1, \lambda_2}^{-1} \Sigma_{X^{E+1}} C_{n_2, \lambda_1, \lambda_2}^{-1} X^{E+1\top} \mathbf{z}_{n_2} \\ &= \frac{1}{n_2^2} \left\| \Sigma_{X^{E+1}}^{1/2} C_{n_2, \lambda_1, \lambda_2}^{-1} X^{E+1\top} \mathbf{z}_{n_2} \right\|^2 \\ &\lesssim \frac{1}{n_2^2} \left\| \mathcal{P}_{R_1^*} \Sigma_X^{1/2} C_{n_2, \lambda_1, \lambda_2}^{-1} X^{E+1\top} \mathbf{z}_{n_2} \right\|^2 + \frac{1}{n_2^2} \left\| \mathcal{P}_{R_2^*} \Sigma_X^{1/2} C_{n_2, \lambda_1, \lambda_2}^{-1} X^{E+1\top} \mathbf{z}_{n_2} \right\|^2 \\ &\lesssim \frac{\sigma^2 \text{Tr} (R_1^{*\top} \Sigma_X R_1^*)}{n_2} + \frac{\sigma^2 \text{Tr} (R_2^{*\top} \Sigma_X R_2^*)}{n_2} \\ &\lesssim \left(1 + \frac{\|\Lambda_{11}\|}{\|\Lambda_{22}\|} \right) \frac{\sigma^2 \text{Tr} (R_1^{*\top} \Sigma_X R_1^*)}{n_2} \end{aligned}$$

where we use Assumption B.4 in the last step.

Estimation of T_4 .

$$\begin{aligned} T_4 &= \mathbb{E}_{\theta^{*E+1}} \left[\langle \lambda_1 C_{n_2, \lambda_1, \lambda_2}^{-1} \mathcal{P}_{\widehat{R}_1} (\bar{\theta}^E - R_1^* \theta^{*E+1}), \frac{1}{n_2} C_{n_2, \lambda_1, \lambda_2}^{-1} X^{E+1\top} \mathbf{z}_{n_2} \rangle \right] \\ &= \langle \lambda_1 C_{n_2, \lambda_1, \lambda_2}^{-1} \mathcal{P}_{\widehat{R}_1} (\bar{\theta}^E - R_1^* \theta^*), \frac{1}{n_2} C_{n_2, \lambda_1, \lambda_2}^{-1} X^{E+1\top} \mathbf{z}_{n_2} \rangle \\ &= \frac{\lambda_1}{n_2} (\bar{\theta}^E - R_1^* \theta^*)^\top \mathcal{P}_{\widehat{R}_1} C_{n_2, \lambda_1, \lambda_2}^{-2} X^{E+1\top} \mathbf{z}_{n_2} \\ &\leq \left\| \mathcal{P}_{\widehat{R}_1} (\bar{\theta}^E - R_1^* \theta^*) \right\| \left\| \frac{\lambda_1}{n_2} \mathcal{P}_{\widehat{R}_1} C_{n_2, \lambda_1, \lambda_2}^{-2} X^{E+1\top} \mathbf{z}_{n_2} \right\| \\ &\lesssim \left(\sqrt{\frac{1}{E} \text{Tr}(\Lambda_{11})} + \sqrt{\frac{\sigma^2 \text{Tr} (R_1^{*\top} \Sigma_X^{-1} R_1^*)}{n_1 E}} \right) \left(\frac{\lambda_1 \sigma}{\sqrt{n_2}} \sqrt{\text{Tr} \left(\widehat{R}_1^\top C_{n_2, \lambda_1, \lambda_2}^{-2} \Sigma_X C_{n_2, \lambda_1, \lambda_2}^{-2} \widehat{R}_1 \right)} \right) \\ &\lesssim \frac{\sigma}{n_2} \sqrt{\frac{\text{Tr} (R_1^{*\top} \Sigma_X R_1^*)}{n_2}} \left(\sqrt{\frac{1}{E} \text{Tr}(\Lambda_{11})} + \sqrt{\frac{\sigma^2 \text{Tr} (R_1^{*\top} \Sigma_X^{-1} R_1^*)}{n_1 E}} \right) \\ &\lesssim \frac{\sigma}{n_2} \sqrt{\frac{\text{Tr} (R_1^{*\top} \Sigma_X R_1^*) \text{Tr}(\Lambda_{11})}{n_2 E}} + \frac{\sigma^2}{n_2} \sqrt{\frac{\text{Tr} (R_1^{*\top} \Sigma_X R_1^*) \text{Tr} (R_1^{*\top} \Sigma_X^{-1} R_1^*)}{n_1 n_2 E}} \end{aligned}$$

where in the second inequality we plug in our choice of λ_1 in equation 27.

Estimation of T_5 . The estimation of T_5 is almost the same as that of T_4 .

$$\begin{aligned}
 T_5 &= \mathbb{E}_{\boldsymbol{\theta}^{*E+1}} \left[\left\langle -\lambda_2 C_{n_2, \lambda_1, \lambda_2}^{-1} \mathcal{P}_{\widehat{R}_1}^\perp R^* \boldsymbol{\theta}^{*E+1}, \frac{1}{n_2} C_{n_2, \lambda_1, \lambda_2}^{-1} X^{E+1\top} \mathbf{z}_{n_2} \right\rangle \right] \\
 &= \left\langle -\lambda_2 C_{n_2, \lambda_1, \lambda_2}^{-1} \mathcal{P}_{\widehat{R}_1}^\perp R_1^* \boldsymbol{\theta}^*, \frac{1}{n_2} C_{n_2, \lambda_1, \lambda_2}^{-1} X^{E+1\top} \mathbf{z}_{n_2} \right\rangle \\
 &\lesssim \left\| \mathcal{P}_{\widehat{R}_1}^\perp R_1^* \boldsymbol{\theta}^* \right\| \left\| \frac{\lambda_2}{n_2} \mathcal{P}_{\widehat{R}_1}^\perp C_{n_2, \lambda_1, \lambda_2}^{-1} X^{E+1\top} \mathbf{z}_{n_2} \right\| \\
 &\lesssim \frac{\|\boldsymbol{\theta}^*\|}{(\min(\Lambda_{22}) - \|\Lambda_{11}\|)} \left(\sqrt{\frac{d}{E}} \|\Lambda_{22}\| + \frac{\sigma^2}{n_1 \lambda_1(\Sigma_X)} \right) \frac{\sigma}{n_2} \sqrt{\frac{\text{Tr}(R_2^{*\top} \Sigma_X R_2^*)}{n_2}} \\
 &\lesssim \frac{\|\boldsymbol{\theta}^*\|}{(\min(\Lambda_{22}) - \|\Lambda_{11}\|)} \left(\frac{\sigma \|\Lambda_{22}\|}{n_2} \sqrt{\frac{d \text{Tr}(R_2^{*\top} \Sigma_X R_2^*)}{n_2 E}} + \frac{\sigma^3 \lambda_1^{-1}(\Sigma_X)}{n_1 n_2} \sqrt{\frac{\text{Tr}(R_2^{*\top} \Sigma_X R_2^*)}{n_2}} \right) \\
 &\lesssim \frac{\sigma \|\Lambda_{22}\| \|\boldsymbol{\theta}^*\|}{n_2 (\min(\Lambda_{22}) - \|\Lambda_{11}\|)} \sqrt{\frac{d \text{Tr}(R_2^{*\top} \Sigma_X R_2^*)}{n_2 E}}.
 \end{aligned}$$

With $T_{1,2}, T_2, T_3, T_5$ being dominant terms and $T_{1,1}, T_4$ being the lower order terms, we obtain the final bound

$$\begin{aligned}
 \mathbb{E}_{\boldsymbol{\theta}^{*E+1}} [\text{ER}(\widehat{\boldsymbol{\theta}}^{E+1})] &= \frac{1}{2} (T_1 + T_2 + T_3 + T_4 + T_5) \\
 &\lesssim \frac{\sigma^2 \|\Lambda_{11}\| \text{Tr}(R_1^{*\top} \Sigma_X R_1^*)}{n_2} + \frac{\sigma^2 \|\Lambda_{22}\| \text{Tr}(R_2^{*\top} \Sigma_X R_2^*)}{n_2} \\
 &\quad + \frac{\sigma \|\Lambda_{22}\| \|\boldsymbol{\theta}^*\|}{n_2 (\min(\Lambda_{22}) - \|\Lambda_{11}\|)} \sqrt{\frac{d \text{Tr}(R_2^{*\top} \Sigma_X R_2^*)}{n_2 E}} + \xi(\sigma, n_1, n_2, d, k, E)
 \end{aligned}$$

where

$$\begin{aligned}
 \xi(\sigma, n_1, n_2, d, k, E) &= \frac{\sigma^2 \|\Sigma_X\| \text{Tr}(\Lambda_{11})}{n_2 E} + \frac{\sigma^4 \|\Sigma_X\| \text{Tr}(R_1^{*\top} \Sigma_X^{-1} R_1^*)}{n_1 n_2 E} + \frac{\sigma}{n_2} \sqrt{\frac{\text{Tr}(R_1^{*\top} \Sigma_X R_1^*) \text{Tr}(\Lambda_{11})}{n_2 E}} \\
 &\quad + \frac{\sigma^2}{n_2} \sqrt{\frac{\text{Tr}(R_1^{*\top} \Sigma_X R_1^*) \text{Tr}(R_1^{*\top} \Sigma_X^{-1} R_1^*)}{n_1 n_2 E}}.
 \end{aligned}$$

B.4. Proof of Lemma B.10

For $1 \leq e \leq E$, $\widehat{\boldsymbol{\theta}}^e$ is the OLS estimator:

$$\begin{aligned}
 \widehat{\boldsymbol{\theta}}^e &= (X^{e\top} X^e)^{-1} X^{e\top} \mathbf{y}^e \\
 &= (X^{e\top} X^e)^{-1} X^{e\top} (X^e \boldsymbol{\theta}^{*e} + \mathbf{z}^e) \\
 &= \boldsymbol{\theta}^{*e} + (X^{e\top} X^e)^{-1} X^{e\top} \mathbf{z}^e.
 \end{aligned}$$

Let $\widehat{O} \in \mathcal{O}(k)$ be such that

$$\widehat{O} = \underset{O \in \mathcal{O}(k)}{\text{argmin}} \left\| \widehat{R}_1 - R_1 O \right\|.$$

Then the ℓ_2 error can be decomposed as:

$$\begin{aligned} \left\| \widehat{R}_1^\top \left(\frac{1}{E} \sum_{e=1}^E \widehat{\theta}^e - R_1^* \theta^* \right) \right\| &\leq \left\| R_1^{*\top} \left(\frac{1}{E} \sum_{e=1}^E R^* \theta^{*e} - R_1 \theta^* \right) \right\| \\ &\quad + \left\| R_1^{*\top} \left(\frac{1}{E} \sum_{e=1}^E (X^{e\top} X^e)^{-1} X^{e\top} \mathbf{z}^e \right) \right\| \\ &\quad + \left\| \left(\widehat{R}_1^\top - \widehat{O}^\top R_1^{*\top} \right) \left(\frac{1}{E} \sum_{e=1}^E R^* \theta^{*e} - R_1 \theta^* \right) \right\| \\ &\quad + \left\| \left(\widehat{R}_1^\top - \widehat{O}^\top R_1^{*\top} \right) \left(\frac{1}{E} \sum_{e=1}^E (X^{e\top} X^e)^{-1} X^{e\top} \mathbf{z}^e \right) \right\|. \end{aligned}$$

where we use the fact that ℓ_2 norm is orthogonal invariant. Note that

$$R_1^{*\top} \left(\frac{1}{E} \sum_{e=1}^E R^* \theta^{*e} - R_1 \theta^* \right) \sim \mathcal{N} \left(\mathbf{0}, \frac{1}{E} \Lambda_{11} \right).$$

The Chernoff bound gives that with probability $1 - o(1)$,

$$\left\| R_1^{*\top} \left(\frac{1}{E} \sum_{e=1}^E R^* \theta^{*e} - R_1 \theta^* \right) \right\| \lesssim \sqrt{\frac{1}{E} \text{Tr}(\Lambda_{11})}.$$

Note that

$$R_1^{*\top} \left(\frac{1}{E} \sum_{e=1}^E (X^{e\top} X^e)^{-1} X^{e\top} \mathbf{z}^e \right) \sim \mathcal{N} \left(\mathbf{0}, \frac{\sigma^2}{n_1 E^2} \sum_{e=1}^E R_1^{*\top} \left(\frac{X^{e\top} X^e}{n_1} \right)^{-1} R_1^* \right).$$

The Chernoff bound gives that with probability $1 - o(1)$,

$$\left\| R_1^{*\top} \left(\frac{1}{E} \sum_{e=1}^E (X^{e\top} X^e)^{-1} X^{e\top} \mathbf{z}^e \right) \right\| \lesssim \frac{\sigma}{\sqrt{n_1 E}} \sqrt{\text{Tr}(R_1^{*\top} \Sigma_X^{-1} R_1^*)}$$

The following lemma provides the estimation of $\left\| \widehat{R}_1 - R_1^* \widehat{O} \right\|$.

Lemma B.11. *Under the conditions in Theorem B.6, with probability $1 - o(1)$,*

$$\left\| \widehat{R}_1 - R_1^* \widehat{O} \right\| \lesssim (\min(\Lambda_{22}) - \|\Lambda_{11}\|)^{-1} \left(\sqrt{\frac{d}{E}} \|\Lambda_{22}\| + \frac{\sigma^2}{n_1 \lambda_1(\Sigma_X)} \right).$$

Then the remaining two terms are of lower order.

$$\begin{aligned} &\left\| \left(\widehat{R}_1^\top - \widehat{O}^\top R_1^{*\top} \right) \left(\frac{1}{E} \sum_{e=1}^E \theta^{*e} - R_1 \theta^* \right) \right\| \lesssim \left\| \widehat{R}_1 - R_1 \widehat{O} \right\| \left\| \frac{1}{E} \sum_{e=1}^E \theta^{*e} - R_1 \theta^* \right\| \\ &\lesssim (\min(\Lambda_{22}) - \|\Lambda_{11}\|)^{-1} \left(\sqrt{\frac{d}{E}} \|\Lambda_{22}\| + \frac{\sigma^2}{n_1 \lambda_1(\Sigma_X)} \right) \sqrt{\frac{\text{Tr}(\Lambda_{11} + \Lambda_{22})}{E}}. \end{aligned}$$

Putting the terms together, we get

$$\begin{aligned} &\left\| \left(\widehat{R}_1^\top - \widehat{O}^\top R_1^{*\top} \right) \left(\frac{1}{E} \sum_{e=1}^E (X^{e\top} X^e)^{-1} X^{e\top} \mathbf{z}^e \right) \right\| \lesssim \left\| \widehat{R}_1 - R_1 \widehat{O} \right\| \left\| \frac{1}{E} \sum_{e=1}^E (X^{e\top} X^e)^{-1} X^{e\top} \mathbf{z}^e \right\| \\ &\lesssim (\min(\Lambda_{22}) - \|\Lambda_{11}\|)^{-1} \left(\sqrt{\frac{d}{E}} \|\Lambda_{22}\| + \frac{\sigma^2}{n_1 \lambda_1(\Sigma_X)} \right) \sqrt{\frac{\text{Tr}(\Sigma^{-1})}{n_1 E}}. \end{aligned}$$

B.5. Proof of Lemma B.11

Let $\widehat{O} \in \mathcal{O}(k)$ be such that

$$\widehat{O} = \operatorname{argmin}_{O \in \mathcal{O}(k)} \left\| \widehat{R}_1 - R_1 O \right\|.$$

It can be verified that $\widehat{O} = \bar{U} \bar{V}^\top$ given the SVD of $R_1^{*\top} \widehat{R}_1$ being $\bar{U} \bar{D} \bar{V}^\top$. Then Davis-Kahan Theorem (Theorem C.1) gives the bound

$$\begin{aligned} \left\| \widehat{R}_1 - R_1 \widehat{O} \right\| &= \left\| (I_d - R_1^* R_1^{*\top}) \widehat{R}_1 \right\| + \left\| R_1^{*\top} \widehat{R}_1 - \widehat{O} \right\| \\ &\leq 2 \left\| \sin \left(R_1, \widehat{R}_1 \right) \right\| \\ &\leq \frac{2 \left\| \widehat{\Sigma}_{\widehat{\theta}} - \Sigma_{\text{RM}} \right\|}{\min(\Lambda_{22}) - \|\Lambda_{11}\| - \left\| \widehat{\Sigma}_{\widehat{\theta}} - \Sigma_{\text{RM}} \right\|}. \end{aligned}$$

Under Assumption B.3,

$$\left\| \widehat{R}_1 - R_1 \widehat{O} \right\| \lesssim \frac{\left\| \widehat{\Sigma}_{\widehat{\theta}} - \Sigma_{\text{RM}} \right\|}{\min(\Lambda_{22}) - \|\Lambda_{11}\|}.$$

For readability of the proof, we define the auxiliary quantities as follows. Let

$$\begin{aligned} \Delta^e &= (X^{e\top} X^e)^{-1} X^{e\top} z^e \\ \bar{\theta}^{*E} &= \frac{1}{E} \sum_{e=1}^E \theta^{*e}, \\ \bar{\Delta}^E &= \frac{1}{E} \sum_{e=1}^E \Delta^e, \\ \widehat{\Sigma}_{\theta^*} &= \frac{1}{E} \sum_{e=1}^E (\theta^{*e} - \bar{\theta}^{*E}) (\theta^{*e} - \bar{\theta}^{*E})^\top, \\ \widehat{\Sigma}_{\theta^*}^0 &= \frac{1}{E} \sum_{e=1}^E (\theta^{*e} - R_1^* \theta^*) (\theta^{*e} - R_1^* \theta^*)^\top, \\ \widehat{\Sigma}_{\Delta} &= \frac{1}{E} \sum_{e=1}^E (\Delta^e - \bar{\Delta}^E) (\Delta^e - \bar{\Delta}^E)^\top, \\ \widehat{\Sigma}_{\Delta}^0 &= \frac{1}{E} \sum_{e=1}^E \Delta^e \Delta^{e\top}. \end{aligned}$$

Then $\left\| \widehat{\Sigma}_{\widehat{\theta}} - \Sigma_{\text{RM}} \right\|$ can be decomposed as:

$$\begin{aligned} \left\| \widehat{\Sigma}_{\widehat{\theta}} - \Sigma_{\text{RM}} \right\| &= \left\| \frac{1}{E} \sum_{e=1}^E (\widehat{\theta}^e - \bar{\theta}^E) (\widehat{\theta}^e - \bar{\theta}^E)^\top - \Sigma_{\text{RM}} \right\| \\ &= \left\| \frac{1}{E} \sum_{e=1}^E (\theta^{*e} - \bar{\theta}^{*E} + \Delta^e - \bar{\Delta}^E) (\theta^{*e} - \bar{\theta}^{*E} + \Delta^e - \bar{\Delta}^E)^\top - \Sigma_{\text{RM}} \right\| \\ &= \left\| \widehat{\Sigma}_{\theta^*} - \Sigma_{\text{RM}} \right\| + \left\| \widehat{\Sigma}_{\Delta} \right\| \\ &\quad + \left\| \frac{1}{E} \sum_{e=1}^E \theta^{*e} \Delta^{e\top} - \bar{\theta}^{*E} \bar{\Delta}^{E\top} + \frac{1}{E} \sum_{e=1}^E \Delta^e \theta^{*e\top} - \bar{\Delta}^E \bar{\theta}^{*E\top} \right\|. \end{aligned}$$

Estimation of $\left\| \widehat{\Sigma}_{\theta^*} - \Sigma_{\text{RM}} \right\|$. We have that

$$\left\| \widehat{\Sigma}_{\theta^*} - \Sigma_{\text{RM}} \right\| \leq \left\| \widehat{\Sigma}_{\theta^*}^0 - \Sigma_{\text{RM}} \right\| + \left\| (\bar{\theta}^{*E} - R_1^* \theta^*) (\bar{\theta}^{*E} - R_1^* \theta^*)^\top \right\|.$$

Since $\theta^e - R_1^* \theta^*$ is centered Gaussian with covariance Σ_{RM} , by the standard covariance estimation in (Wainwright, 2019), with probability $1 - o(1)$,

$$\left\| \widehat{\Sigma}_{\theta^*}^0 - \Sigma_{\text{RM}} \right\| \lesssim \sqrt{\frac{d}{E}} \|\Lambda_{22}\|.$$

The second term upper bounded by the squared norm of the Gaussian vector $\|\bar{\theta}^{*E} - R_1^* \theta^*\|$

$$\left\| (\bar{\theta}^{*E} - R_1^* \theta^*) (\bar{\theta}^{*E} - R_1^* \theta^*)^\top \right\| = \|\bar{\theta}^{*E} - R_1^* \theta^*\|^2 \lesssim \frac{\text{Tr}(\Lambda_{11} + \Lambda_{22})}{E}.$$

Estimation of $\left\| \widehat{\Sigma}_{\Delta} \right\|$. Similarly, Δ^e is a centered Gaussian with covariance $\sigma^2 \Sigma_X^{-1} / n_1$. Then

$$\begin{aligned} \left\| \widehat{\Sigma}_{\Delta} \right\| &\leq \|\Sigma_{\Delta}\| + \left\| \Sigma_{\Delta} - \widehat{\Sigma}_{\Delta}^0 \right\| + \|\bar{\Delta}^E \bar{\Delta}^{E\top}\| \\ &\lesssim \frac{\sigma^2}{n_1 \lambda_1(\Sigma)} \left(1 + \sqrt{\frac{d}{E}} \right) + \frac{\sigma^2 \text{Tr}(\Sigma_X^{-1})}{n_1 E} \end{aligned}$$

Estimation of $\left\| \frac{1}{E} \sum_{e=1}^E \theta^{*e} \Delta^{e\top} - \bar{\theta}^{*E} \bar{\Delta}^{E\top} + \frac{1}{E} \sum_{e=1}^E \Delta^e \theta^{*e\top} - \bar{\Delta}^E \bar{\theta}^{*E\top} \right\|$. Since the two parts of the sum are transpose of each other, it suffices to find the upper bound one of them only. Then we have that

$$\left\| \frac{1}{E} \sum_{e=1}^E \theta^{*e} \Delta^{e\top} - \bar{\theta}^{*E} \bar{\Delta}^{E\top} \right\| \leq \left\| \frac{1}{E} \sum_{e=1}^E (\theta^{*e} - R_1^* \theta^*) \Delta^{e\top} \right\| + \left\| (R_1^* \theta^* - \bar{\theta}^{*E}) \bar{\Delta}^{E\top} \right\|$$

Chernoff bound gives the upper bound of the second term. With probability $1 - o(1)$,

$$\begin{aligned} \left\| (R_1^* \theta^* - \bar{\theta}^{*E}) \bar{\Delta}^{E\top} \right\| &\leq \|R_1^* \theta^* - \bar{\theta}^{*E}\| \|\bar{\Delta}^E\| \\ &\lesssim \sqrt{\frac{\text{Tr}(\Lambda_{11} + \Lambda_{22})}{E} \frac{\sigma^2 \text{Tr}(\Sigma_X^{-1})}{n_1 E}} \end{aligned}$$

Then we will apply Matrix Bernstein (Theorem C.3) to find the upper bound of the first term. Note that each term is bounded by

$$\left\| \frac{1}{E} (\theta^{*e} - R_1^* \theta^*) \Delta^{e\top} \right\| \lesssim \frac{\sigma \sqrt{\text{Tr}(\Lambda_{11} + \Lambda_{22}) \text{Tr}(\Sigma_X^{-1})}}{\sqrt{n_1 E}}.$$

Then variance proxy is

$$\begin{aligned} \left\| \mathbb{E} \left[\sum_{e=1}^E \frac{1}{E^2} (\theta^{*e} - R_1^* \theta^*) \Delta^{e\top} \Delta^e (\theta^{*e} - R_1^* \theta^*)^\top \right] \right\| &\lesssim \frac{\mathbb{E}_{\theta^*} \|\theta^{*e} - R_1^* \theta^*\|^2 \|\Delta^e\|^2}{E} \\ &\lesssim \frac{\sigma^2 \text{Tr}(\Lambda_{11} + \Lambda_{22}) \text{Tr}(\Sigma_X^{-1})}{n_1 E}. \end{aligned}$$

Then, by Bernstein's inequality,

$$\begin{aligned} \left\| \frac{1}{E} \sum_{e=1}^E (\theta^{*e} - R_1^* \theta^*) \Delta^{e\top} \right\| &\lesssim \sqrt{\frac{\sigma^2 \text{Tr}(\Lambda_{11} + \Lambda_{22}) \text{Tr}(\Sigma_X^{-1}) \log(E)}{n_1 E}} + \frac{\sigma \sqrt{\text{Tr}(\Lambda_{11} + \Lambda_{22}) \text{Tr}(\Sigma_X^{-1}) \log(E)}}{\sqrt{n_1 E}} \\ &\lesssim \sqrt{\frac{\sigma^2 \text{Tr}(\Lambda_{11} + \Lambda_{22}) \text{Tr}(\Sigma_X^{-1}) \log(E)}{n_1 E}}. \end{aligned}$$

Thus, we combine the terms together and omit the lower order terms:

$$\left\| \widehat{\Sigma}_{\hat{\theta}} - \Sigma_{\text{RM}} \right\| \lesssim \sqrt{\frac{d}{E}} \|\Lambda_{22}\| + \frac{\sigma^2}{n_1 \lambda_1(\Sigma_X)}$$

and

$$\left\| \widehat{R}_1 - R_1^* \widehat{O} \right\| \lesssim \frac{\left\| \widehat{\Sigma}_{\hat{\theta}} - \Sigma_{\text{RM}} \right\|}{\min(\Lambda_{22}) - \|\Lambda_{11}\|} \lesssim (\min(\Lambda_{22}) - \|\Lambda_{11}\|)^{-1} \left(\sqrt{\frac{d}{E}} \|\Lambda_{22}\| + \frac{\sigma^2}{n_1 \lambda_1(\Sigma_X)} \right).$$

C. Technical ingredients

Theorem C.1 (Generalized Davis-Kahan theorem (Deng et al., 2021; Zhong & Ling, 2023)). *Consider the eigenvalue problem $N^{-1}M\mathbf{u} = \lambda\mathbf{u}$ where M and N are both Hermitian, and N is positive definite. Let X be the matrix that has the eigenvectors of $N^{-1}M$ as columns. Then $N^{-1}M$ is diagonalizable and can be written as*

$$N^{-1}M = X\Lambda X^H = X_1\Lambda_1 X_1^H + X_2\Lambda_2 X_2^H$$

where

$$X^{-1} = [X_1 \quad X_2]^{-1} = \begin{bmatrix} Y_1^H \\ Y_2^H \end{bmatrix}, \quad \Lambda = \begin{bmatrix} \Lambda_1 & \\ & \Lambda_2 \end{bmatrix}.$$

Suppose $\delta = \min_i |(\Lambda_2)_{ii} - \widehat{\lambda}|$ is the absolute separation of $\widehat{\lambda}$ from $(\Lambda_2)_{ii}$, then for any vector $\widehat{\mathbf{u}}$ we have

$$\|P\widehat{\mathbf{u}}\| \leq \frac{\sqrt{\kappa(N)} \left\| (N^{-1}M - \widehat{\lambda}I_n)\widehat{\mathbf{u}} \right\|}{\delta}.$$

where $P = (Y_2^\dagger)^H (Y_2)^H = I - (X_1^\dagger)^H (X_1)^H$ is the orthogonal projection matrix onto the orthogonal complement of the column space of X_1 , $\kappa(N) = \|N\| \|N^{-1}\|$ is the condition number of N and Y_2^\dagger is the Moore-Penrose inverse of Y_2 .

When $N = I$ and $(\widehat{\lambda}, \widehat{\mathbf{u}})$ be an eigen-pair of a matrix \widehat{M} , we have

$$\sin \theta \leq \frac{\left\| (M - \widehat{M})\widehat{\mathbf{u}} \right\|}{\delta}$$

where θ is the canonical angle between $\widehat{\mathbf{u}}$ and the column space of X_1 . In this case the theorem reduces to the classical Davis-Kahan theorem (Davis & Kahan, 1970).

Lemma C.2 ((Du et al., 2021), Lemma A.6). *Let $\mathbf{a}_1, \dots, \mathbf{a}_n$ be i.i.d. d -dimensional random vectors such that $\mathbb{E}[\mathbf{a}_i] = 0$, $\mathbb{E}[\mathbf{a}_i \mathbf{a}_i^\top] = I_d$, and \mathbf{a}_i is ρ^2 -subgaussian. If $n \gtrsim \rho^4 d$, then it holds with probability $1 - o(1)$ that*

$$0.9I_d \preceq \frac{1}{n} \sum_{i=1}^n \mathbf{a}_i \mathbf{a}_i^\top \preceq 1.1I_d.$$

Theorem C.3 (Matrix Bernstein (Tropp, 2012)). *Consider a finite sequence of independent random matrices $\{Z_k\}$. Assume that each random matrix satisfies*

$$\mathbb{E}Z_k = 0, \quad \|Z_k\| \leq R.$$

Then for all $t \geq 0$,

$$\mathbb{P} \left(\left\| \sum_k Z_k \right\| \geq t \right) \leq (d_1 + d_2) \cdot \exp \left(-\frac{t^2/2}{\sigma^2 + Rt/3} \right).$$

where

$$\sigma^2 = \max \left\{ \left\| \sum_k \mathbb{E}Z_k^\top Z_k \right\|, \left\| \sum_k \mathbb{E}Z_k Z_k^\top \right\| \right\}.$$

Then with probability at least $1 - n^{-\gamma+1}$,

$$\left\| \sum_k Z_k \right\| \leq \sqrt{2\gamma\sigma^2 \log(d_1 + d_2)} + \frac{2\gamma R \log(d_1 + d_2)}{3}.$$

D. Experimental Results

We show the full results in the following tables. B stands for base feature, Y stands for the target-specific feature, S stands for the shared feature, and E stands for the environment-specific feature. We use the Adam optimizer with $\text{lr} \in [1e-5, 5e-5, 1e-4]$, batch size $\in [32, 64, 128]$. We choose the best model based on the source validation accuracy.

D.1. Linear Probing Results

We fixed the source validation dataset based on random seed and use that validation dataset for hyperparameter tuning. We vary the hyperparameters of the logistic regression models: $C \in [1e-5, 1e-4, 1e-3, 1e-2, 1e-1]$, lbfgs solver, max iter = 1000. We report the results in the following Table 2, Table 3, Table 4, Table 5.

E_t	Method	0.10	0.20	0.40	0.60	0.80	1.00	mean
0	DANN	0.4527 ± 0.0107	0.5984 ± 0.0109	0.6527 ± 0.0090	0.7111 ± 0.0054	0.7193 ± 0.0092	0.7177 ± 0.0087	0.6420 ± 0.0090
	DIWA	0.5835 ± 0.0132	0.6675 ± 0.0097	0.7276 ± 0.0094	0.7358 ± 0.0082	0.7720 ± 0.0118	0.7909 ± 0.0048	0.7129 ± 0.0095
	ERM	0.5745 ± 0.0105	0.6848 ± 0.0046	0.7243 ± 0.0107	0.7539 ± 0.0108	0.7827 ± 0.0082	0.7926 ± 0.0085	0.7188 ± 0.0089
	NUC-0.01	0.4840 ± 0.0129	0.6543 ± 0.0043	0.7407 ± 0.0097	0.7934 ± 0.0136	0.8049 ± 0.0040	0.8165 ± 0.0062	0.7156 ± 0.0084
	NUC-0.1	0.4733 ± 0.0072	0.6782 ± 0.0111	0.7687 ± 0.0117	0.8049 ± 0.0038	0.8132 ± 0.0062	0.8099 ± 0.0077	0.7247 ± 0.0080
	PN-B	0.5852 ± 0.0051	0.6733 ± 0.0115	0.7449 ± 0.0068	0.7613 ± 0.0065	0.8165 ± 0.0025	0.8074 ± 0.0053	0.7314 ± 0.0063
	PN-B-Y	0.5770 ± 0.0076	0.6955 ± 0.0050	0.7490 ± 0.0068	0.7761 ± 0.0053	0.8074 ± 0.0094	0.8329 ± 0.0074	0.7396 ± 0.0069
	PN-B-Y-S-E	0.5844 ± 0.0057	0.7119 ± 0.0114	0.7366 ± 0.0077	0.7580 ± 0.0054	0.8041 ± 0.0110	0.8337 ± 0.0055	0.7381 ± 0.0078
	PN-Y	0.5877 ± 0.0080	0.7169 ± 0.0081	0.7481 ± 0.0102	0.7588 ± 0.0083	0.8066 ± 0.0075	0.8280 ± 0.0126	0.7410 ± 0.0091
	PN-Y-S	0.5745 ± 0.0070	0.7062 ± 0.0095	0.7432 ± 0.0135	0.7860 ± 0.0135	0.8041 ± 0.0127	0.8222 ± 0.0080	0.7394 ± 0.0107
	PN-Y-S-E	0.5901 ± 0.0098	0.7029 ± 0.0105	0.7498 ± 0.0068	0.7778 ± 0.0066	0.8082 ± 0.0028	0.8296 ± 0.0094	0.7431 ± 0.0077
1	DANN	0.4842 ± 0.0128	0.5986 ± 0.0077	0.6856 ± 0.0078	0.7011 ± 0.0090	0.7263 ± 0.0047	0.7318 ± 0.0072	0.6546 ± 0.0082
	DIWA	0.5716 ± 0.0082	0.6577 ± 0.0101	0.7121 ± 0.0077	0.7487 ± 0.0067	0.7808 ± 0.0050	0.7725 ± 0.0082	0.7072 ± 0.0077
	ERM	0.5538 ± 0.0071	0.6490 ± 0.0065	0.6989 ± 0.0054	0.7204 ± 0.0034	0.7432 ± 0.0038	0.7803 ± 0.0089	0.6909 ± 0.0058
	NUC-0.01	0.4838 ± 0.0070	0.6293 ± 0.0049	0.6879 ± 0.0055	0.7414 ± 0.0075	0.7730 ± 0.0063	0.7867 ± 0.0053	0.6837 ± 0.0061
	NUC-0.1	0.4824 ± 0.0101	0.6449 ± 0.0066	0.6728 ± 0.0095	0.7382 ± 0.0087	0.7744 ± 0.0061	0.7794 ± 0.0067	0.6820 ± 0.0080
	PN-B	0.5542 ± 0.0082	0.6568 ± 0.0028	0.7281 ± 0.0062	0.7684 ± 0.0059	0.7812 ± 0.0063	0.7973 ± 0.0026	0.7143 ± 0.0053
	PN-B-Y	0.5593 ± 0.0092	0.6545 ± 0.0035	0.7465 ± 0.0045	0.7808 ± 0.0092	0.7844 ± 0.0053	0.8009 ± 0.0064	0.7211 ± 0.0064
	PN-B-Y-S-E	0.5712 ± 0.0066	0.6526 ± 0.0076	0.7217 ± 0.0060	0.7698 ± 0.0060	0.7863 ± 0.0009	0.8064 ± 0.0044	0.7180 ± 0.0052
	PN-Y	0.5584 ± 0.0052	0.6563 ± 0.0068	0.7245 ± 0.0070	0.7817 ± 0.0058	0.7826 ± 0.0128	0.8018 ± 0.0056	0.7175 ± 0.0072
	PN-Y-S	0.5744 ± 0.0113	0.6517 ± 0.0025	0.7263 ± 0.0046	0.7744 ± 0.0070	0.7826 ± 0.0071	0.7899 ± 0.0092	0.7166 ± 0.0070
	PN-Y-S-E	0.5707 ± 0.0078	0.6613 ± 0.0035	0.7359 ± 0.0047	0.7661 ± 0.0034	0.7808 ± 0.0085	0.7995 ± 0.0030	0.7191 ± 0.0052
2	DANN	0.6649 ± 0.0056	0.7423 ± 0.0018	0.8230 ± 0.0062	0.8509 ± 0.0058	0.8667 ± 0.0036	0.8784 ± 0.0049	0.8044 ± 0.0046
	DIWA	0.7734 ± 0.0082	0.8189 ± 0.0059	0.8649 ± 0.0049	0.8959 ± 0.0036	0.9063 ± 0.0052	0.9045 ± 0.0055	0.8607 ± 0.0055
	ERM	0.7743 ± 0.0069	0.8401 ± 0.0019	0.8716 ± 0.0048	0.9113 ± 0.0038	0.8995 ± 0.0039	0.9122 ± 0.0033	0.8682 ± 0.0041
	NUC-0.01	0.7176 ± 0.0030	0.8320 ± 0.0049	0.9077 ± 0.0031	0.9126 ± 0.0046	0.9261 ± 0.0024	0.9302 ± 0.0028	0.8710 ± 0.0035
	NUC-0.1	0.7257 ± 0.0085	0.8279 ± 0.0052	0.8977 ± 0.0052	0.9198 ± 0.0032	0.9212 ± 0.0053	0.9248 ± 0.0023	0.8695 ± 0.0050
	PN-B	0.7689 ± 0.0024	0.8365 ± 0.0037	0.8689 ± 0.0053	0.8919 ± 0.0026	0.9140 ± 0.0034	0.9203 ± 0.0038	0.8667 ± 0.0035
	PN-B-Y	0.7721 ± 0.0083	0.8351 ± 0.0044	0.8613 ± 0.0039	0.8955 ± 0.0044	0.9144 ± 0.0034	0.9117 ± 0.0039	0.8650 ± 0.0047
	PN-B-Y-S-E	0.7797 ± 0.0038	0.8459 ± 0.0051	0.8730 ± 0.0039	0.8914 ± 0.0049	0.9162 ± 0.0008	0.9185 ± 0.0041	0.8708 ± 0.0038
	PN-Y	0.7527 ± 0.0071	0.8446 ± 0.0054	0.8770 ± 0.0042	0.8923 ± 0.0046	0.8991 ± 0.0060	0.9234 ± 0.0052	0.8649 ± 0.0054
	PN-Y-S	0.7703 ± 0.0074	0.8468 ± 0.0065	0.8671 ± 0.0033	0.8955 ± 0.0034	0.9027 ± 0.0039	0.9176 ± 0.0021	0.8667 ± 0.0044
	PN-Y-S-E	0.7770 ± 0.0069	0.8455 ± 0.0090	0.8829 ± 0.0074	0.8959 ± 0.0053	0.9023 ± 0.0054	0.9225 ± 0.0027	0.8710 ± 0.0061
3	DANN	0.6385 ± 0.0043	0.7183 ± 0.0051	0.7518 ± 0.0067	0.7638 ± 0.0044	0.7853 ± 0.0067	0.7862 ± 0.0058	0.7407 ± 0.0055
	DIWA	0.7867 ± 0.0085	0.8000 ± 0.0034	0.8271 ± 0.0040	0.8408 ± 0.0044	0.8344 ± 0.0037	0.8560 ± 0.0073	0.8242 ± 0.0052
	ERM	0.8248 ± 0.0050	0.8367 ± 0.0053	0.8619 ± 0.0044	0.8555 ± 0.0079	0.8546 ± 0.0084	0.8555 ± 0.0054	0.8482 ± 0.0061
	NUC-0.01	0.7156 ± 0.0052	0.8147 ± 0.0085	0.8596 ± 0.0033	0.8670 ± 0.0036	0.8656 ± 0.0049	0.8812 ± 0.0112	0.8339 ± 0.0061
	NUC-0.1	0.7165 ± 0.0111	0.8165 ± 0.0058	0.8587 ± 0.0017	0.8679 ± 0.0049	0.8624 ± 0.0030	0.8771 ± 0.0078	0.8332 ± 0.0057
	PN-B	0.7894 ± 0.0077	0.8312 ± 0.0036	0.8628 ± 0.0029	0.8651 ± 0.0031	0.8693 ± 0.0062	0.8633 ± 0.0066	0.8469 ± 0.0050
	PN-B-Y	0.7940 ± 0.0058	0.8252 ± 0.0023	0.8615 ± 0.0006	0.8656 ± 0.0034	0.8817 ± 0.0071	0.8647 ± 0.0039	0.8488 ± 0.0038
	PN-B-Y-S-E	0.7872 ± 0.0066	0.8353 ± 0.0099	0.8587 ± 0.0034	0.8633 ± 0.0039	0.8683 ± 0.0064	0.8665 ± 0.0060	0.8466 ± 0.0060
	PN-Y	0.7986 ± 0.0037	0.8422 ± 0.0074	0.8495 ± 0.0051	0.8615 ± 0.0046	0.8688 ± 0.0022	0.8720 ± 0.0028	0.8488 ± 0.0043
	PN-Y-S	0.7812 ± 0.0038	0.8381 ± 0.0030	0.8679 ± 0.0060	0.8628 ± 0.0039	0.8693 ± 0.0061	0.8835 ± 0.0028	0.8505 ± 0.0043
	PN-Y-S-E	0.7904 ± 0.0051	0.8454 ± 0.0051	0.8661 ± 0.0039	0.8706 ± 0.0048	0.8679 ± 0.0039	0.8697 ± 0.0059	0.8517 ± 0.0048

Table 2. Linear Probing results on OfficeHome dataset.

Bridging Domains with Approximately Shared Features

E_t	Method	0.10	0.20	0.40	0.60	0.80	1.00	mean
0	DANN	0.2956 ± 0.0118	0.3337 ± 0.0150	0.3171 ± 0.0079	0.3698 ± 0.0179	0.4059 ± 0.0192	0.4215 ± 0.0124	0.3572 ± 0.0140
	DIWA	0.9405 ± 0.0081	0.9346 ± 0.0033	0.9512 ± 0.0077	0.9551 ± 0.0036	0.9473 ± 0.0076	0.9444 ± 0.0065	0.9455 ± 0.0061
	ERM	0.8702 ± 0.0043	0.8673 ± 0.0042	0.8849 ± 0.0068	0.9044 ± 0.0059	0.9141 ± 0.0072	0.9190 ± 0.0037	0.8933 ± 0.0053
	NUC-0.01	0.8429 ± 0.0052	0.8780 ± 0.0056	0.8937 ± 0.0036	0.9015 ± 0.0066	0.8966 ± 0.0070	0.8966 ± 0.0054	0.8849 ± 0.0056
	NUC-0.1	0.8273 ± 0.0070	0.8702 ± 0.0099	0.8839 ± 0.0081	0.9024 ± 0.0044	0.8976 ± 0.0083	0.8937 ± 0.0099	0.8792 ± 0.0079
	PN-B	0.8810 ± 0.0077	0.8878 ± 0.0074	0.9239 ± 0.0065	0.9190 ± 0.0059	0.9307 ± 0.0071	0.9288 ± 0.0065	0.9119 ± 0.0068
	PN-B-Y	0.8849 ± 0.0072	0.8868 ± 0.0076	0.9190 ± 0.0037	0.9180 ± 0.0039	0.9337 ± 0.0045	0.9346 ± 0.0075	0.9128 ± 0.0057
	PN-B-Y-S-E	0.9024 ± 0.0044	0.9054 ± 0.0043	0.9220 ± 0.0046	0.9337 ± 0.0077	0.9434 ± 0.0061	0.9405 ± 0.0047	0.9246 ± 0.0053
	PN-Y	0.9054 ± 0.0048	0.9005 ± 0.0092	0.9268 ± 0.0034	0.9317 ± 0.0053	0.9337 ± 0.0048	0.9268 ± 0.0031	0.9208 ± 0.0051
	PN-Y-S	0.9122 ± 0.0084	0.8917 ± 0.0068	0.9220 ± 0.0074	0.9327 ± 0.0039	0.9337 ± 0.0037	0.9220 ± 0.0051	0.9190 ± 0.0059
PN-Y-S-E	0.9073 ± 0.0034	0.9024 ± 0.0067	0.9171 ± 0.0094	0.9239 ± 0.0067	0.9415 ± 0.0041	0.9210 ± 0.0086	0.9189 ± 0.0065	
1	DANN	0.3419 ± 0.0137	0.3983 ± 0.0048	0.4256 ± 0.0048	0.4359 ± 0.0102	0.4538 ± 0.0148	0.4906 ± 0.0068	0.4244 ± 0.0092
	DIWA	0.8906 ± 0.0098	0.9154 ± 0.0067	0.9231 ± 0.0072	0.9402 ± 0.0045	0.9402 ± 0.0038	0.9342 ± 0.0089	0.9239 ± 0.0068
	ERM	0.8752 ± 0.0114	0.9111 ± 0.0065	0.9231 ± 0.0062	0.9316 ± 0.0076	0.9470 ± 0.0037	0.9581 ± 0.0086	0.9244 ± 0.0074
	NUC-0.01	0.8436 ± 0.0083	0.8581 ± 0.0075	0.8897 ± 0.0044	0.8974 ± 0.0045	0.8906 ± 0.0042	0.9179 ± 0.0048	0.8829 ± 0.0056
	NUC-0.1	0.8308 ± 0.0046	0.8624 ± 0.0044	0.8923 ± 0.0076	0.8949 ± 0.0086	0.9034 ± 0.0068	0.9145 ± 0.0030	0.8830 ± 0.0058
	PN-B	0.9034 ± 0.0064	0.9205 ± 0.0064	0.9308 ± 0.0067	0.9256 ± 0.0026	0.9265 ± 0.0028	0.9436 ± 0.0046	0.9251 ± 0.0049
	PN-B-Y	0.9222 ± 0.0056	0.9162 ± 0.0064	0.9179 ± 0.0095	0.9171 ± 0.0032	0.9350 ± 0.0031	0.9359 ± 0.0076	0.9241 ± 0.0059
	PN-B-Y-S-E	0.9128 ± 0.0032	0.9248 ± 0.0072	0.9342 ± 0.0052	0.9359 ± 0.0041	0.9487 ± 0.0027	0.9487 ± 0.0043	0.9342 ± 0.0044
	PN-Y	0.9068 ± 0.0104	0.9282 ± 0.0048	0.9231 ± 0.0052	0.9359 ± 0.0019	0.9308 ± 0.0078	0.9487 ± 0.0014	0.9289 ± 0.0052
	PN-Y-S	0.9162 ± 0.0053	0.9342 ± 0.0017	0.9265 ± 0.0046	0.9427 ± 0.0048	0.9368 ± 0.0046	0.9556 ± 0.0052	0.9353 ± 0.0044
PN-Y-S-E	0.9077 ± 0.0074	0.9342 ± 0.0032	0.9291 ± 0.0040	0.9342 ± 0.0066	0.9479 ± 0.0039	0.9513 ± 0.0055	0.9340 ± 0.0051	
2	DANN	0.6431 ± 0.0062	0.6311 ± 0.0140	0.6862 ± 0.0122	0.6862 ± 0.0082	0.7186 ± 0.0143	0.7138 ± 0.0088	0.6798 ± 0.0106
	DIWA	0.9737 ± 0.0031	0.9737 ± 0.0015	0.9820 ± 0.0033	0.9880 ± 0.0000	0.9796 ± 0.0031	0.9844 ± 0.0031	0.9802 ± 0.0023
	ERM	0.9533 ± 0.0035	0.9569 ± 0.0035	0.9653 ± 0.0040	0.9677 ± 0.0056	0.9677 ± 0.0052	0.9593 ± 0.0035	0.9617 ± 0.0042
	NUC-0.01	0.9569 ± 0.0064	0.9737 ± 0.0045	0.9749 ± 0.0055	0.9916 ± 0.0031	0.9808 ± 0.0022	0.9880 ± 0.0019	0.9776 ± 0.0039
	NUC-0.1	0.9545 ± 0.0024	0.9760 ± 0.0019	0.9784 ± 0.0049	0.9868 ± 0.0022	0.9808 ± 0.0035	0.9904 ± 0.0024	0.9778 ± 0.0029
	PN-B	0.9701 ± 0.0060	0.9796 ± 0.0036	0.9796 ± 0.0041	0.9808 ± 0.0048	0.9737 ± 0.0031	0.9784 ± 0.0045	0.9770 ± 0.0043
	PN-B-Y	0.9784 ± 0.0059	0.9820 ± 0.0054	0.9856 ± 0.0031	0.9832 ± 0.0029	0.9772 ± 0.0048	0.9820 ± 0.0050	0.9814 ± 0.0045
	PN-B-Y-S-E	0.9796 ± 0.0041	0.9772 ± 0.0048	0.9808 ± 0.0029	0.9796 ± 0.0031	0.9784 ± 0.0052	0.9880 ± 0.0019	0.9806 ± 0.0037
	PN-Y	0.9749 ± 0.0029	0.9856 ± 0.0031	0.9832 ± 0.0040	0.9760 ± 0.0033	0.9892 ± 0.0012	0.9808 ± 0.0022	0.9816 ± 0.0028
	PN-Y-S	0.9725 ± 0.0024	0.9820 ± 0.0050	0.9784 ± 0.0062	0.9737 ± 0.0045	0.9784 ± 0.0024	0.9880 ± 0.0019	0.9788 ± 0.0037
PN-Y-S-E	0.9641 ± 0.0066	0.9760 ± 0.0063	0.9820 ± 0.0038	0.9904 ± 0.0024	0.9784 ± 0.0015	0.9832 ± 0.0040	0.9790 ± 0.0041	
3	DANN	0.6132 ± 0.0038	0.6626 ± 0.0069	0.7008 ± 0.0071	0.6962 ± 0.0120	0.7298 ± 0.0049	0.7394 ± 0.0091	0.6903 ± 0.0073
	DIWA	0.8718 ± 0.0055	0.8896 ± 0.0042	0.9170 ± 0.0032	0.9074 ± 0.0034	0.9115 ± 0.0053	0.9160 ± 0.0018	0.9022 ± 0.0039
	ERM	0.8936 ± 0.0039	0.8891 ± 0.0030	0.9033 ± 0.0052	0.9206 ± 0.0057	0.9277 ± 0.0046	0.9232 ± 0.0041	0.9096 ± 0.0044
	NUC-0.01	0.6972 ± 0.0055	0.7659 ± 0.0091	0.8081 ± 0.0034	0.8036 ± 0.0061	0.8193 ± 0.0023	0.8249 ± 0.0060	0.7865 ± 0.0054
	NUC-0.1	0.6987 ± 0.0042	0.7603 ± 0.0056	0.7969 ± 0.0103	0.8107 ± 0.0059	0.8249 ± 0.0064	0.8275 ± 0.0051	0.7865 ± 0.0063
	PN-B	0.8427 ± 0.0066	0.8718 ± 0.0097	0.8840 ± 0.0040	0.8967 ± 0.0039	0.9033 ± 0.0039	0.9013 ± 0.0061	0.8833 ± 0.0057
	PN-B-Y	0.8601 ± 0.0040	0.8636 ± 0.0026	0.8947 ± 0.0049	0.9018 ± 0.0013	0.8901 ± 0.0041	0.9069 ± 0.0061	0.8862 ± 0.0038
	PN-B-Y-S-E	0.8570 ± 0.0033	0.8616 ± 0.0057	0.8941 ± 0.0030	0.8987 ± 0.0035	0.9074 ± 0.0061	0.9018 ± 0.0055	0.8868 ± 0.0045
	PN-Y	0.8595 ± 0.0033	0.8585 ± 0.0035	0.8926 ± 0.0029	0.8997 ± 0.0030	0.9125 ± 0.0024	0.9120 ± 0.0039	0.8891 ± 0.0032
	PN-Y-S	0.8534 ± 0.0068	0.8555 ± 0.0026	0.8906 ± 0.0053	0.8911 ± 0.0027	0.9038 ± 0.0066	0.8947 ± 0.0057	0.8815 ± 0.0049
PN-Y-S-E	0.8631 ± 0.0047	0.8784 ± 0.0057	0.8835 ± 0.0049	0.8962 ± 0.0045	0.9013 ± 0.0025	0.8997 ± 0.0051	0.8870 ± 0.0046	

Table 3. Linear Probing results on PACS dataset.

Bridging Domains with Approximately Shared Features

E_t	Method	0.10	0.20	0.40	0.60	0.80	1.00	mean
0	DANN	0.9620 ± 0.0042	0.9761 ± 0.0065	0.9831 ± 0.0053	0.9859 ± 0.0039	0.9930 ± 0.0022	0.9930 ± 0.0031	0.9822 ± 0.0042
	DIWA	0.9873 ± 0.0052	0.9930 ± 0.0039	0.9972 ± 0.0028	1.0000 ± 0.0000	0.9887 ± 0.0053	1.0000 ± 0.0000	0.9944 ± 0.0029
	ERM	0.9901 ± 0.0036	0.9873 ± 0.0034	0.9873 ± 0.0056	0.9775 ± 0.0068	0.9831 ± 0.0036	0.9972 ± 0.0017	0.9871 ± 0.0041
	NUC-0.01	1.0000 ± 0.0000	1.0000 ± 0.0000	1.0000 ± 0.0000	1.0000 ± 0.0000	1.0000 ± 0.0000	0.9944 ± 0.0056	0.9991 ± 0.0009
	NUC-0.1	1.0000 ± 0.0000	1.0000 ± 0.0000	1.0000 ± 0.0000	1.0000 ± 0.0000	1.0000 ± 0.0000	1.0000 ± 0.0000	1.0000 ± 0.0000
	PN-B	0.9887 ± 0.0036	0.9930 ± 0.0022	0.9944 ± 0.0026	0.9972 ± 0.0017	0.9944 ± 0.0026	0.9986 ± 0.0014	0.9944 ± 0.0024
	PN-B-Y	0.9901 ± 0.0017	0.9944 ± 0.0014	0.9930 ± 0.0022	0.9972 ± 0.0017	0.9972 ± 0.0017	0.9958 ± 0.0017	0.9946 ± 0.0018
	PN-B-Y-S-E	0.9958 ± 0.0017	0.9944 ± 0.0026	0.9958 ± 0.0017	0.9944 ± 0.0014	0.9901 ± 0.0028	0.9972 ± 0.0017	0.9946 ± 0.0020
	PN-Y	0.9958 ± 0.0028	0.9915 ± 0.0041	0.9915 ± 0.0026	0.9901 ± 0.0017	0.9986 ± 0.0014	0.9972 ± 0.0017	0.9941 ± 0.0024
	PN-Y-S	0.9901 ± 0.0036	0.9845 ± 0.0041	0.9944 ± 0.0026	0.9930 ± 0.0000	0.9986 ± 0.0014	0.9915 ± 0.0026	0.9920 ± 0.0024
PN-Y-S-E	0.9944 ± 0.0026	0.9972 ± 0.0017	0.9972 ± 0.0017	0.9873 ± 0.0014	0.9915 ± 0.0026	0.9972 ± 0.0017	0.9941 ± 0.0020	
1	DANN	0.5429 ± 0.0039	0.5526 ± 0.0034	0.6293 ± 0.0076	0.6391 ± 0.0160	0.6429 ± 0.0081	0.6368 ± 0.0089	0.6073 ± 0.0080
	DIWA	0.7414 ± 0.0034	0.7504 ± 0.0102	0.7722 ± 0.0057	0.7729 ± 0.0070	0.7805 ± 0.0069	0.7992 ± 0.0096	0.7694 ± 0.0071
	ERM	0.7519 ± 0.0083	0.7263 ± 0.0088	0.7549 ± 0.0082	0.7586 ± 0.0101	0.7707 ± 0.0090	0.7609 ± 0.0096	0.7539 ± 0.0090
	NUC-0.01	0.7331 ± 0.0117	0.7677 ± 0.0088	0.7692 ± 0.0094	0.7722 ± 0.0070	0.7602 ± 0.0038	0.7654 ± 0.0104	0.7613 ± 0.0085
	NUC-0.1	0.7331 ± 0.0092	0.7451 ± 0.0150	0.7654 ± 0.0128	0.7609 ± 0.0054	0.7549 ± 0.0060	0.7737 ± 0.0102	0.7555 ± 0.0098
	PN-B	0.7113 ± 0.0066	0.7331 ± 0.0087	0.7669 ± 0.0110	0.7662 ± 0.0038	0.7421 ± 0.0044	0.7519 ± 0.0067	0.7452 ± 0.0069
	PN-B-Y	0.7083 ± 0.0066	0.7617 ± 0.0059	0.7699 ± 0.0084	0.7729 ± 0.0076	0.7571 ± 0.0104	0.7707 ± 0.0072	0.7568 ± 0.0077
	PN-B-Y-S-E	0.7248 ± 0.0069	0.7511 ± 0.0048	0.7767 ± 0.0035	0.7564 ± 0.0099	0.7481 ± 0.0128	0.7609 ± 0.0081	0.7530 ± 0.0077
	PN-Y	0.7346 ± 0.0050	0.7797 ± 0.0130	0.7992 ± 0.0116	0.7677 ± 0.0129	0.7519 ± 0.0059	0.7842 ± 0.0102	0.7695 ± 0.0098
	PN-Y-S	0.7203 ± 0.0059	0.7782 ± 0.0098	0.7714 ± 0.0077	0.7669 ± 0.0102	0.7466 ± 0.0112	0.7534 ± 0.0061	0.7561 ± 0.0085
PN-Y-S-E	0.7256 ± 0.0086	0.7774 ± 0.0129	0.7774 ± 0.0076	0.7571 ± 0.0137	0.7654 ± 0.0165	0.7511 ± 0.0069	0.7590 ± 0.0110	
2	DANN	0.7927 ± 0.0080	0.8012 ± 0.0114	0.7817 ± 0.0060	0.7976 ± 0.0056	0.7854 ± 0.0053	0.8091 ± 0.0126	0.7946 ± 0.0081
	DIWA	0.8201 ± 0.0075	0.8073 ± 0.0068	0.8189 ± 0.0039	0.8146 ± 0.0077	0.8049 ± 0.0066	0.8104 ± 0.0080	0.8127 ± 0.0067
	ERM	0.8104 ± 0.0077	0.8268 ± 0.0046	0.8293 ± 0.0048	0.8152 ± 0.0105	0.8299 ± 0.0078	0.8311 ± 0.0124	0.8238 ± 0.0080
	NUC-0.01	0.8067 ± 0.0100	0.8213 ± 0.0050	0.8262 ± 0.0043	0.8329 ± 0.0079	0.8140 ± 0.0027	0.8189 ± 0.0079	0.8200 ± 0.0063
	NUC-0.1	0.8006 ± 0.0072	0.8262 ± 0.0061	0.8354 ± 0.0042	0.8274 ± 0.0091	0.8220 ± 0.0058	0.8341 ± 0.0059	0.8243 ± 0.0064
	PN-B	0.7945 ± 0.0067	0.8030 ± 0.0055	0.8049 ± 0.0093	0.8152 ± 0.0033	0.8128 ± 0.0059	0.8073 ± 0.0047	0.8063 ± 0.0059
	PN-B-Y	0.7823 ± 0.0100	0.7848 ± 0.0101	0.7915 ± 0.0030	0.8171 ± 0.0057	0.8165 ± 0.0054	0.8104 ± 0.0095	0.8004 ± 0.0073
	PN-B-Y-S-E	0.8073 ± 0.0095	0.7970 ± 0.0051	0.7957 ± 0.0041	0.8067 ± 0.0058	0.7963 ± 0.0050	0.8165 ± 0.0113	0.8033 ± 0.0068
	PN-Y	0.7982 ± 0.0118	0.7933 ± 0.0049	0.8073 ± 0.0053	0.8183 ± 0.0053	0.8079 ± 0.0042	0.8055 ± 0.0089	0.8051 ± 0.0067
	PN-Y-S	0.7963 ± 0.0064	0.7866 ± 0.0059	0.8067 ± 0.0059	0.8030 ± 0.0062	0.8110 ± 0.0058	0.8293 ± 0.0042	0.8055 ± 0.0057
PN-Y-S-E	0.7957 ± 0.0062	0.7939 ± 0.0104	0.8024 ± 0.0090	0.8073 ± 0.0095	0.8213 ± 0.0074	0.8244 ± 0.0101	0.8075 ± 0.0088	
3	DANN	0.5018 ± 0.0121	0.5302 ± 0.0022	0.5846 ± 0.0061	0.5840 ± 0.0012	0.5976 ± 0.0075	0.5716 ± 0.0037	0.5616 ± 0.0055
	DIWA	0.8491 ± 0.0095	0.8728 ± 0.0047	0.8550 ± 0.0028	0.8651 ± 0.0039	0.8550 ± 0.0028	0.8580 ± 0.0048	0.8592 ± 0.0047
	ERM	0.8604 ± 0.0069	0.8728 ± 0.0129	0.8722 ± 0.0036	0.8663 ± 0.0077	0.8787 ± 0.0066	0.8722 ± 0.0049	0.8704 ± 0.0071
	NUC-0.01	0.8456 ± 0.0045	0.8645 ± 0.0042	0.8817 ± 0.0021	0.8828 ± 0.0093	0.8846 ± 0.0099	0.8716 ± 0.0074	0.8718 ± 0.0062
	NUC-0.1	0.8467 ± 0.0071	0.8686 ± 0.0050	0.8757 ± 0.0039	0.8864 ± 0.0064	0.8947 ± 0.0047	0.8751 ± 0.0068	0.8746 ± 0.0056
	PN-B	0.8609 ± 0.0047	0.8556 ± 0.0067	0.8740 ± 0.0050	0.8763 ± 0.0071	0.8657 ± 0.0061	0.8609 ± 0.0078	0.8656 ± 0.0062
	PN-B-Y	0.8621 ± 0.0052	0.8556 ± 0.0044	0.8722 ± 0.0065	0.8675 ± 0.0076	0.8651 ± 0.0123	0.8734 ± 0.0029	0.8660 ± 0.0065
	PN-B-Y-S-E	0.8728 ± 0.0039	0.8550 ± 0.0049	0.8574 ± 0.0055	0.8627 ± 0.0049	0.8680 ± 0.0058	0.8651 ± 0.0061	0.8635 ± 0.0052
	PN-Y	0.8521 ± 0.0064	0.8781 ± 0.0054	0.8911 ± 0.0025	0.8598 ± 0.0050	0.8722 ± 0.0044	0.8769 ± 0.0056	0.8717 ± 0.0049
	PN-Y-S	0.8669 ± 0.0085	0.8686 ± 0.0050	0.8710 ± 0.0091	0.8621 ± 0.0060	0.8805 ± 0.0070	0.8669 ± 0.0068	0.8693 ± 0.0071
PN-Y-S-E	0.8633 ± 0.0037	0.8692 ± 0.0041	0.8692 ± 0.0090	0.8615 ± 0.0059	0.8633 ± 0.0081	0.8746 ± 0.0030	0.8669 ± 0.0057	

Table 4. Linear Probing results on VLCS dataset.

Bridging Domains with Approximately Shared Features

E_t	Method	0.10	0.20	0.40	0.60	0.80	1.00	mean
0	DANN	0.6823 ± 0.0044	0.7198 ± 0.0051	0.7684 ± 0.0049	0.7827 ± 0.0032	0.7852 ± 0.0052	0.7886 ± 0.0087	0.7545 ± 0.0053
	DIWA	0.8249 ± 0.0058	0.8734 ± 0.0037	0.9055 ± 0.0062	0.9291 ± 0.0025	0.9422 ± 0.0076	0.9418 ± 0.0020	0.9028 ± 0.0046
	ERM	0.8346 ± 0.0055	0.8616 ± 0.0064	0.9084 ± 0.0028	0.9329 ± 0.0043	0.9367 ± 0.0032	0.9397 ± 0.0024	0.9023 ± 0.0041
	NUC-0.01	0.7928 ± 0.0052	0.8329 ± 0.0056	0.8730 ± 0.0059	0.9105 ± 0.0021	0.9219 ± 0.0020	0.9291 ± 0.0037	0.8767 ± 0.0041
	NUC-0.1	0.7975 ± 0.0110	0.8409 ± 0.0054	0.8624 ± 0.0039	0.9110 ± 0.0051	0.9139 ± 0.0036	0.9295 ± 0.0044	0.8759 ± 0.0055
	PN-B	0.8278 ± 0.0058	0.8844 ± 0.0045	0.9211 ± 0.0011	0.9405 ± 0.0018	0.9578 ± 0.0009	0.9603 ± 0.0044	0.9153 ± 0.0031
	PN-B-Y	0.8253 ± 0.0049	0.8700 ± 0.0049	0.9135 ± 0.0049	0.9473 ± 0.0033	0.9502 ± 0.0023	0.9603 ± 0.0035	0.9111 ± 0.0040
	PN-B-Y-S-E	0.8295 ± 0.0042	0.8819 ± 0.0024	0.9181 ± 0.0037	0.9405 ± 0.0020	0.9532 ± 0.0018	0.9553 ± 0.0017	0.9131 ± 0.0026
	PN-Y	0.8392 ± 0.0041	0.8819 ± 0.0035	0.9131 ± 0.0012	0.9540 ± 0.0026	0.9519 ± 0.0026	0.9608 ± 0.0032	0.9168 ± 0.0029
	PN-Y-S	0.8287 ± 0.0044	0.8747 ± 0.0051	0.9165 ± 0.0011	0.9502 ± 0.0029	0.9506 ± 0.0041	0.9578 ± 0.0019	0.9131 ± 0.0032
PN-Y-S-E	0.8300 ± 0.0032	0.8844 ± 0.0041	0.9190 ± 0.0061	0.9586 ± 0.0047	0.9515 ± 0.0012	0.9586 ± 0.0029	0.9170 ± 0.0037	
1	DANN	0.6875 ± 0.0026	0.7294 ± 0.0037	0.7760 ± 0.0028	0.7690 ± 0.0067	0.7727 ± 0.0052	0.7729 ± 0.0038	0.7512 ± 0.0041
	DIWA	0.8405 ± 0.0027	0.8692 ± 0.0027	0.8893 ± 0.0016	0.8955 ± 0.0047	0.9181 ± 0.0018	0.9281 ± 0.0026	0.8901 ± 0.0027
	ERM	0.8351 ± 0.0041	0.8643 ± 0.0016	0.8916 ± 0.0016	0.9064 ± 0.0022	0.9341 ± 0.0026	0.9300 ± 0.0022	0.8936 ± 0.0024
	NUC-0.01	0.7947 ± 0.0033	0.8246 ± 0.0038	0.8561 ± 0.0030	0.8836 ± 0.0021	0.8949 ± 0.0030	0.8998 ± 0.0016	0.8589 ± 0.0028
	NUC-0.1	0.7951 ± 0.0040	0.8366 ± 0.0059	0.8690 ± 0.0039	0.8852 ± 0.0045	0.8869 ± 0.0033	0.9008 ± 0.0024	0.8623 ± 0.0040
	PN-B	0.8310 ± 0.0061	0.8713 ± 0.0044	0.9074 ± 0.0013	0.9117 ± 0.0019	0.9220 ± 0.0021	0.9347 ± 0.0030	0.8963 ± 0.0031
	PN-B-Y	0.8302 ± 0.0066	0.8622 ± 0.0026	0.8996 ± 0.0037	0.9140 ± 0.0043	0.9300 ± 0.0016	0.9398 ± 0.0036	0.8960 ± 0.0037
	PN-B-Y-S-E	0.8267 ± 0.0050	0.8637 ± 0.0025	0.8922 ± 0.0029	0.9156 ± 0.0031	0.9296 ± 0.0047	0.9368 ± 0.0015	0.8941 ± 0.0033
	PN-Y	0.8248 ± 0.0036	0.8550 ± 0.0047	0.8895 ± 0.0021	0.9179 ± 0.0040	0.9290 ± 0.0011	0.9326 ± 0.0037	0.8915 ± 0.0032
	PN-Y-S	0.8197 ± 0.0053	0.8544 ± 0.0031	0.8926 ± 0.0015	0.9117 ± 0.0037	0.9257 ± 0.0023	0.9304 ± 0.0026	0.8891 ± 0.0031
PN-Y-S-E	0.8230 ± 0.0028	0.8706 ± 0.0021	0.8834 ± 0.0033	0.9166 ± 0.0055	0.9324 ± 0.0020	0.9347 ± 0.0011	0.8935 ± 0.0028	
2	DANN	0.5275 ± 0.0066	0.6045 ± 0.0061	0.6453 ± 0.0065	0.6403 ± 0.0081	0.6665 ± 0.0056	0.6690 ± 0.0043	0.6255 ± 0.0062
	DIWA	0.7264 ± 0.0102	0.7909 ± 0.0046	0.8040 ± 0.0039	0.8458 ± 0.0062	0.8499 ± 0.0091	0.8872 ± 0.0045	0.8174 ± 0.0064
	ERM	0.7330 ± 0.0112	0.7864 ± 0.0084	0.8317 ± 0.0043	0.8640 ± 0.0044	0.8831 ± 0.0055	0.8912 ± 0.0029	0.8316 ± 0.0061
	NUC-0.01	0.6448 ± 0.0048	0.7380 ± 0.0064	0.7889 ± 0.0045	0.8388 ± 0.0066	0.8589 ± 0.0071	0.8615 ± 0.0048	0.7885 ± 0.0057
	NUC-0.1	0.6534 ± 0.0067	0.7345 ± 0.0101	0.7950 ± 0.0103	0.8368 ± 0.0049	0.8615 ± 0.0063	0.8680 ± 0.0030	0.7915 ± 0.0069
	PN-B	0.7521 ± 0.0081	0.7945 ± 0.0082	0.8247 ± 0.0059	0.8443 ± 0.0048	0.8675 ± 0.0017	0.8811 ± 0.0036	0.8274 ± 0.0054
	PN-B-Y	0.7436 ± 0.0040	0.7884 ± 0.0069	0.8327 ± 0.0068	0.8630 ± 0.0083	0.8670 ± 0.0066	0.8922 ± 0.0054	0.8312 ± 0.0063
	PN-B-Y-S-E	0.7345 ± 0.0063	0.7904 ± 0.0058	0.8277 ± 0.0027	0.8670 ± 0.0063	0.8856 ± 0.0047	0.8992 ± 0.0047	0.8341 ± 0.0051
	PN-Y	0.7295 ± 0.0044	0.7748 ± 0.0089	0.8322 ± 0.0045	0.8620 ± 0.0059	0.8831 ± 0.0033	0.9103 ± 0.0029	0.8320 ± 0.0050
	PN-Y-S	0.7325 ± 0.0073	0.7904 ± 0.0079	0.8368 ± 0.0106	0.8660 ± 0.0037	0.8836 ± 0.0075	0.9008 ± 0.0023	0.8350 ± 0.0065
PN-Y-S-E	0.7451 ± 0.0070	0.7788 ± 0.0039	0.8287 ± 0.0046	0.8610 ± 0.0084	0.8932 ± 0.0060	0.8957 ± 0.0044	0.8338 ± 0.0057	
3	DANN	0.4942 ± 0.0087	0.5143 ± 0.0048	0.5014 ± 0.0034	0.5099 ± 0.0098	0.5218 ± 0.0020	0.5296 ± 0.0069	0.5118 ± 0.0059
	DIWA	0.7156 ± 0.0030	0.7340 ± 0.0052	0.8116 ± 0.0023	0.8255 ± 0.0030	0.8616 ± 0.0036	0.8810 ± 0.0030	0.8049 ± 0.0034
	ERM	0.7367 ± 0.0067	0.7554 ± 0.0093	0.8119 ± 0.0053	0.8265 ± 0.0045	0.8527 ± 0.0055	0.8779 ± 0.0010	0.8102 ± 0.0054
	NUC-0.01	0.6442 ± 0.0070	0.7061 ± 0.0072	0.7687 ± 0.0062	0.8122 ± 0.0052	0.8337 ± 0.0036	0.8456 ± 0.0033	0.7684 ± 0.0054
	NUC-0.1	0.6633 ± 0.0061	0.7139 ± 0.0055	0.7759 ± 0.0069	0.8027 ± 0.0046	0.8340 ± 0.0025	0.8442 ± 0.0053	0.7723 ± 0.0051
	PN-B	0.7310 ± 0.0068	0.7735 ± 0.0060	0.8221 ± 0.0049	0.8398 ± 0.0062	0.8660 ± 0.0029	0.8810 ± 0.0074	0.8189 ± 0.0057
	PN-B-Y	0.7241 ± 0.0069	0.7701 ± 0.0024	0.8265 ± 0.0038	0.8507 ± 0.0054	0.8724 ± 0.0058	0.8827 ± 0.0041	0.8211 ± 0.0047
	PN-B-Y-S-E	0.7446 ± 0.0054	0.7721 ± 0.0037	0.8173 ± 0.0032	0.8520 ± 0.0031	0.8861 ± 0.0061	0.8857 ± 0.0056	0.8263 ± 0.0045
	PN-Y	0.7357 ± 0.0037	0.7748 ± 0.0042	0.8126 ± 0.0065	0.8500 ± 0.0037	0.8680 ± 0.0046	0.8847 ± 0.0041	0.8210 ± 0.0045
	PN-Y-S	0.7391 ± 0.0058	0.7568 ± 0.0030	0.8184 ± 0.0070	0.8463 ± 0.0067	0.8694 ± 0.0082	0.8816 ± 0.0013	0.8186 ± 0.0053
PN-Y-S-E	0.7432 ± 0.0031	0.7823 ± 0.0065	0.7980 ± 0.0028	0.8432 ± 0.0010	0.8782 ± 0.0049	0.8898 ± 0.0032	0.8224 ± 0.0036	

Table 5. Linear Probing results on Terrain-Cognita dataset.

D.2. Target Finetuning Results

We use the source pretrained feature encoder and classifier as the initialization for the target finetuning. We use the same hyperparameter range as the source pretraining. The best model is chosen based on the target validation accuracy. We report the results in the following Table 6, Table 7, Table 8, Table 9.

E_t	Method	0.10	0.20	0.40	0.60	0.80	1.00	mean
0	DANN	0.6263 ± 0.0091	0.6650 ± 0.0098	0.7251 ± 0.0062	0.7588 ± 0.0051	0.7786 ± 0.0035	0.7984 ± 0.0045	0.7254 ± 0.0064
	DIWA	0.6329 ± 0.0423	0.6872 ± 0.0194	0.7366 ± 0.0069	0.7514 ± 0.0075	0.7630 ± 0.0119	0.8148 ± 0.0054	0.7310 ± 0.0156
	ERM	0.7407 ± 0.0079	0.7786 ± 0.0054	0.8000 ± 0.0042	0.8272 ± 0.0034	0.8362 ± 0.0040	0.8593 ± 0.0033	0.8070 ± 0.0047
	NUC-0.01	0.4535 ± 0.0069	0.6049 ± 0.0125	0.7103 ± 0.0065	0.7646 ± 0.0066	0.7770 ± 0.0067	0.8148 ± 0.0072	0.6875 ± 0.0077
	NUC-0.1	0.4461 ± 0.0051	0.6058 ± 0.0129	0.7029 ± 0.0073	0.7556 ± 0.0067	0.7852 ± 0.0067	0.8173 ± 0.0108	0.6855 ± 0.0083
	PN-Y	0.7588 ± 0.0100	0.7893 ± 0.0086	0.8082 ± 0.0059	0.8305 ± 0.0030	0.8519 ± 0.0037	0.8675 ± 0.0038	0.8177 ± 0.0058
	PN-Y-S	0.7621 ± 0.0035	0.7926 ± 0.0059	0.8239 ± 0.0049	0.8247 ± 0.0050	0.8502 ± 0.0046	0.8568 ± 0.0015	0.8184 ± 0.0043
	PN-Y-S-E	0.7605 ± 0.0082	0.7819 ± 0.0062	0.8140 ± 0.0072	0.8296 ± 0.0053	0.8510 ± 0.0044	0.8601 ± 0.0041	0.8162 ± 0.0059
1	DANN	0.4641 ± 0.0030	0.6105 ± 0.0124	0.7382 ± 0.0036	0.7922 ± 0.0048	0.8110 ± 0.0079	0.8352 ± 0.0049	0.7085 ± 0.0061
	DIWA	0.6229 ± 0.0045	0.7121 ± 0.0170	0.7510 ± 0.0160	0.8018 ± 0.0122	0.8110 ± 0.0114	0.8384 ± 0.0063	0.7562 ± 0.0113
	ERM	0.6526 ± 0.0100	0.7062 ± 0.0036	0.7629 ± 0.0072	0.7931 ± 0.0095	0.8220 ± 0.0073	0.8279 ± 0.0039	0.7608 ± 0.0069
	NUC-0.01	0.4288 ± 0.0057	0.5922 ± 0.0107	0.7231 ± 0.0064	0.7844 ± 0.0085	0.8165 ± 0.0018	0.8426 ± 0.0063	0.6979 ± 0.0066
	NUC-0.1	0.4279 ± 0.0051	0.5931 ± 0.0103	0.7199 ± 0.0067	0.7945 ± 0.0039	0.8151 ± 0.0081	0.8375 ± 0.0069	0.6980 ± 0.0068
	PN-Y	0.6526 ± 0.0028	0.7053 ± 0.0100	0.7616 ± 0.0041	0.8087 ± 0.0043	0.8247 ± 0.0006	0.8412 ± 0.0020	0.7657 ± 0.0040
	PN-Y-S	0.6293 ± 0.0051	0.6783 ± 0.0107	0.7442 ± 0.0033	0.7858 ± 0.0047	0.8014 ± 0.0051	0.8183 ± 0.0020	0.7429 ± 0.0052
	PN-Y-S-E	0.6302 ± 0.0062	0.6870 ± 0.0089	0.7368 ± 0.0067	0.7785 ± 0.0043	0.8046 ± 0.0028	0.8183 ± 0.0025	0.7426 ± 0.0052
2	DANN	0.7770 ± 0.0091	0.8450 ± 0.0053	0.8986 ± 0.0050	0.9099 ± 0.0043	0.9252 ± 0.0033	0.9365 ± 0.0024	0.8821 ± 0.0049
	DIWA	0.7856 ± 0.0131	0.8568 ± 0.0081	0.8878 ± 0.0066	0.9072 ± 0.0058	0.9207 ± 0.0086	0.9275 ± 0.0061	0.8809 ± 0.0080
	ERM	0.8572 ± 0.0201	0.8851 ± 0.0150	0.9068 ± 0.0082	0.9221 ± 0.0074	0.9342 ± 0.0011	0.9360 ± 0.0039	0.9069 ± 0.0093
	NUC-0.01	0.6923 ± 0.0082	0.8059 ± 0.0063	0.8820 ± 0.0031	0.9113 ± 0.0057	0.9324 ± 0.0042	0.9315 ± 0.0009	0.8592 ± 0.0047
	NUC-0.1	0.6995 ± 0.0058	0.8054 ± 0.0062	0.8838 ± 0.0036	0.9122 ± 0.0038	0.9342 ± 0.0037	0.9356 ± 0.0023	0.8618 ± 0.0042
	PN-Y	0.8266 ± 0.0124	0.8563 ± 0.0108	0.9023 ± 0.0049	0.9149 ± 0.0029	0.9324 ± 0.0031	0.9419 ± 0.0030	0.8957 ± 0.0062
	PN-Y-S	0.8176 ± 0.0117	0.8437 ± 0.0080	0.8919 ± 0.0064	0.8991 ± 0.0034	0.9207 ± 0.0028	0.9279 ± 0.0020	0.8835 ± 0.0057
	PN-Y-S-E	0.8288 ± 0.0205	0.8455 ± 0.0054	0.8842 ± 0.0031	0.9063 ± 0.0034	0.9185 ± 0.0039	0.9270 ± 0.0034	0.8851 ± 0.0066
3	DANN	0.7440 ± 0.0097	0.8128 ± 0.0080	0.8339 ± 0.0034	0.8477 ± 0.0039	0.8463 ± 0.0036	0.8537 ± 0.0017	0.8231 ± 0.0050
	DIWA	0.7972 ± 0.0120	0.8179 ± 0.0106	0.8399 ± 0.0090	0.8151 ± 0.0147	0.8349 ± 0.0143	0.8339 ± 0.0095	0.8232 ± 0.0117
	ERM	0.8335 ± 0.0067	0.8541 ± 0.0033	0.8596 ± 0.0020	0.8578 ± 0.0025	0.8624 ± 0.0065	0.8638 ± 0.0030	0.8552 ± 0.0040
	NUC-0.01	0.6445 ± 0.0087	0.7583 ± 0.0058	0.8266 ± 0.0037	0.8381 ± 0.0080	0.8495 ± 0.0064	0.8596 ± 0.0051	0.7961 ± 0.0063
	NUC-0.1	0.6450 ± 0.0098	0.7592 ± 0.0032	0.8174 ± 0.0041	0.8408 ± 0.0059	0.8431 ± 0.0084	0.8472 ± 0.0083	0.7921 ± 0.0066
	PN-Y	0.8564 ± 0.0065	0.8651 ± 0.0048	0.8780 ± 0.0045	0.8789 ± 0.0011	0.8798 ± 0.0021	0.8743 ± 0.0031	0.8721 ± 0.0037
	PN-Y-S	0.8596 ± 0.0038	0.8697 ± 0.0052	0.8803 ± 0.0032	0.8771 ± 0.0039	0.8849 ± 0.0028	0.8775 ± 0.0041	0.8748 ± 0.0038
	PN-Y-S-E	0.8537 ± 0.0071	0.8647 ± 0.0031	0.8771 ± 0.0037	0.8803 ± 0.0034	0.8826 ± 0.0029	0.8817 ± 0.0041	0.8733 ± 0.0041

Table 6. Target Finetuning results on OfficeHome dataset.

Bridging Domains with Approximately Shared Features

E_t	Method	0.10	0.20	0.40	0.60	0.80	1.00	mean
0	DANN	0.7132 ± 0.0216	0.8166 ± 0.0138	0.8644 ± 0.0079	0.8946 ± 0.0113	0.9063 ± 0.0036	0.9112 ± 0.0064	0.8511 ± 0.0108
	DIWA	0.9454 ± 0.0061	0.9463 ± 0.0067	0.9541 ± 0.0040	0.9580 ± 0.0057	0.9571 ± 0.0066	0.9649 ± 0.0056	0.9543 ± 0.0058
	ERM	0.9190 ± 0.0025	0.9356 ± 0.0036	0.9483 ± 0.0025	0.9620 ± 0.0028	0.9590 ± 0.0043	0.9512 ± 0.0034	0.9459 ± 0.0032
	NUC-0.01	0.8878 ± 0.0072	0.9102 ± 0.0045	0.9307 ± 0.0066	0.9483 ± 0.0025	0.9571 ± 0.0028	0.9541 ± 0.0037	0.9314 ± 0.0046
	NUC-0.1	0.8820 ± 0.0062	0.9141 ± 0.0045	0.9395 ± 0.0080	0.9502 ± 0.0024	0.9473 ± 0.0056	0.9551 ± 0.0036	0.9314 ± 0.0051
	PN-Y	0.9395 ± 0.0025	0.9463 ± 0.0038	0.9541 ± 0.0020	0.9600 ± 0.0032	0.9639 ± 0.0043	0.9698 ± 0.0028	0.9556 ± 0.0031
	PN-Y-S	0.9298 ± 0.0045	0.9415 ± 0.0034	0.9532 ± 0.0033	0.9639 ± 0.0029	0.9659 ± 0.0031	0.9707 ± 0.0027	0.9541 ± 0.0033
	PN-Y-S-E	0.9366 ± 0.0034	0.9346 ± 0.0072	0.9493 ± 0.0020	0.9590 ± 0.0040	0.9600 ± 0.0036	0.9620 ± 0.0024	0.9502 ± 0.0038
1	DANN	0.7812 ± 0.0120	0.8573 ± 0.0156	0.9043 ± 0.0118	0.9299 ± 0.0072	0.9419 ± 0.0074	0.9513 ± 0.0035	0.8943 ± 0.0096
	DIWA	0.9342 ± 0.0058	0.9453 ± 0.0053	0.9667 ± 0.0025	0.9701 ± 0.0030	0.9735 ± 0.0016	0.9726 ± 0.0022	0.9604 ± 0.0034
	ERM	0.8940 ± 0.0041	0.9051 ± 0.0031	0.9350 ± 0.0041	0.9453 ± 0.0034	0.9538 ± 0.0028	0.9538 ± 0.0021	0.9312 ± 0.0033
	NUC-0.01	0.8299 ± 0.0133	0.8846 ± 0.0081	0.9179 ± 0.0028	0.9274 ± 0.0056	0.9453 ± 0.0031	0.9538 ± 0.0055	0.9098 ± 0.0064
	NUC-0.1	0.8291 ± 0.0158	0.8829 ± 0.0068	0.9179 ± 0.0048	0.9376 ± 0.0064	0.9402 ± 0.0049	0.9547 ± 0.0052	0.9104 ± 0.0073
	PN-Y	0.9197 ± 0.0051	0.9325 ± 0.0096	0.9530 ± 0.0014	0.9590 ± 0.0010	0.9632 ± 0.0017	0.9658 ± 0.0019	0.9489 ± 0.0035
	PN-Y-S	0.9051 ± 0.0102	0.9214 ± 0.0100	0.9479 ± 0.0021	0.9496 ± 0.0016	0.9564 ± 0.0031	0.9607 ± 0.0034	0.9402 ± 0.0051
	PN-Y-S-E	0.9051 ± 0.0083	0.9256 ± 0.0067	0.9479 ± 0.0034	0.9521 ± 0.0021	0.9556 ± 0.0029	0.9581 ± 0.0025	0.9407 ± 0.0043
2	DANN	0.8970 ± 0.0179	0.9497 ± 0.0094	0.9760 ± 0.0042	0.9808 ± 0.0022	0.9796 ± 0.0031	0.9808 ± 0.0069	0.9607 ± 0.0073
	DIWA	0.9928 ± 0.0022	0.9928 ± 0.0035	0.9976 ± 0.0015	0.9988 ± 0.0012	0.9988 ± 0.0012	0.9976 ± 0.0015	0.9964 ± 0.0018
	ERM	0.9868 ± 0.0035	0.9892 ± 0.0035	0.9952 ± 0.0012	0.9940 ± 0.0033	0.9952 ± 0.0029	0.9964 ± 0.0015	0.9928 ± 0.0026
	NUC-0.01	0.9665 ± 0.0031	0.9760 ± 0.0054	0.9880 ± 0.0027	0.9856 ± 0.0041	0.9892 ± 0.0029	0.9868 ± 0.0029	0.9820 ± 0.0035
	NUC-0.1	0.9665 ± 0.0031	0.9784 ± 0.0041	0.9880 ± 0.0027	0.9856 ± 0.0015	0.9880 ± 0.0019	0.9868 ± 0.0044	0.9822 ± 0.0029
	PN-Y	0.9880 ± 0.0000	0.9880 ± 0.0000	0.9940 ± 0.0019	0.9916 ± 0.0015	0.9904 ± 0.0015	0.9916 ± 0.0015	0.9906 ± 0.0010
	PN-Y-S	0.9844 ± 0.0024	0.9928 ± 0.0022	0.9892 ± 0.0022	0.9940 ± 0.0019	0.9928 ± 0.0012	0.9964 ± 0.0024	0.9916 ± 0.0021
	PN-Y-S-E	0.9868 ± 0.0029	0.9916 ± 0.0024	0.9928 ± 0.0012	0.9952 ± 0.0022	0.9940 ± 0.0000	0.9928 ± 0.0012	0.9922 ± 0.0017
3	DANN	0.8336 ± 0.0041	0.8804 ± 0.0049	0.9150 ± 0.0061	0.9272 ± 0.0040	0.9298 ± 0.0029	0.9496 ± 0.0010	0.9059 ± 0.0038
	DIWA	0.9323 ± 0.0041	0.9298 ± 0.0048	0.9399 ± 0.0035	0.9537 ± 0.0023	0.9580 ± 0.0043	0.9552 ± 0.0033	0.9448 ± 0.0037
	ERM	0.8758 ± 0.0099	0.9135 ± 0.0029	0.9328 ± 0.0061	0.9486 ± 0.0055	0.9506 ± 0.0013	0.9557 ± 0.0013	0.9295 ± 0.0045
	NUC-0.01	0.7847 ± 0.0119	0.8687 ± 0.0076	0.9053 ± 0.0067	0.9170 ± 0.0037	0.9288 ± 0.0048	0.9338 ± 0.0065	0.8897 ± 0.0069
	NUC-0.1	0.7817 ± 0.0111	0.8687 ± 0.0021	0.8952 ± 0.0038	0.9150 ± 0.0046	0.9277 ± 0.0036	0.9450 ± 0.0034	0.8889 ± 0.0047
	PN-Y	0.9043 ± 0.0013	0.9216 ± 0.0028	0.9257 ± 0.0019	0.9389 ± 0.0055	0.9486 ± 0.0026	0.9476 ± 0.0037	0.9311 ± 0.0030
	PN-Y-S	0.8957 ± 0.0030	0.9099 ± 0.0022	0.9277 ± 0.0025	0.9384 ± 0.0062	0.9471 ± 0.0031	0.9466 ± 0.0031	0.9276 ± 0.0033
	PN-Y-S-E	0.8967 ± 0.0039	0.9104 ± 0.0046	0.9308 ± 0.0035	0.9379 ± 0.0047	0.9461 ± 0.0035	0.9496 ± 0.0052	0.9286 ± 0.0043

Table 7. Target Finetuning results on PACS dataset.

Bridging Domains with Approximately Shared Features

E_t	Method	0.10	0.20	0.40	0.60	0.80	1.00	mean
0	DANN	1.0000 ± 0.0000	1.0000 ± 0.0000	1.0000 ± 0.0000	1.0000 ± 0.0000	1.0000 ± 0.0000	1.0000 ± 0.0000	1.0000 ± 0.0000
	DIWA	1.0000 ± 0.0000	1.0000 ± 0.0000	1.0000 ± 0.0000	1.0000 ± 0.0000	1.0000 ± 0.0000	1.0000 ± 0.0000	1.0000 ± 0.0000
	ERM	0.9915 ± 0.0026	1.0000 ± 0.0000	1.0000 ± 0.0000	1.0000 ± 0.0000	1.0000 ± 0.0000	1.0000 ± 0.0000	0.9986 ± 0.0004
	NUC-0.01	0.9930 ± 0.0022	0.9915 ± 0.0026	0.9972 ± 0.0017	0.9986 ± 0.0014	0.9958 ± 0.0017	1.0000 ± 0.0000	0.9960 ± 0.0016
	NUC-0.1	0.9930 ± 0.0022	0.9930 ± 0.0022	0.9972 ± 0.0017	0.9986 ± 0.0014	0.9958 ± 0.0017	1.0000 ± 0.0000	0.9962 ± 0.0016
	PN-Y	0.9958 ± 0.0028	1.0000 ± 0.0000	1.0000 ± 0.0000	1.0000 ± 0.0000	1.0000 ± 0.0000	1.0000 ± 0.0000	0.9993 ± 0.0005
	PN-Y-S	0.9958 ± 0.0017	1.0000 ± 0.0000	1.0000 ± 0.0000	1.0000 ± 0.0000	1.0000 ± 0.0000	1.0000 ± 0.0000	0.9993 ± 0.0003
	PN-Y-S-E	0.9972 ± 0.0017	1.0000 ± 0.0000	1.0000 ± 0.0000	1.0000 ± 0.0000	1.0000 ± 0.0000	1.0000 ± 0.0000	0.9995 ± 0.0003
1	DANN	0.7053 ± 0.0080	0.7331 ± 0.0043	0.7586 ± 0.0111	0.7812 ± 0.0048	0.7699 ± 0.0070	0.7782 ± 0.0044	0.7544 ± 0.0066
	DIWA	0.7692 ± 0.0091	0.7617 ± 0.0061	0.7842 ± 0.0085	0.7872 ± 0.0061	0.7857 ± 0.0036	0.8000 ± 0.0036	0.7813 ± 0.0062
	ERM	0.7391 ± 0.0044	0.7474 ± 0.0087	0.7647 ± 0.0065	0.7850 ± 0.0018	0.7797 ± 0.0055	0.7699 ± 0.0069	0.7643 ± 0.0056
	NUC-0.01	0.7511 ± 0.0061	0.7504 ± 0.0079	0.7835 ± 0.0073	0.7729 ± 0.0082	0.7797 ± 0.0059	0.7977 ± 0.0048	0.7726 ± 0.0067
	NUC-0.1	0.7496 ± 0.0031	0.7436 ± 0.0036	0.7752 ± 0.0093	0.7850 ± 0.0084	0.7812 ± 0.0077	0.7782 ± 0.0043	0.7688 ± 0.0061
	PN-Y	0.7481 ± 0.0082	0.7541 ± 0.0057	0.7564 ± 0.0047	0.7805 ± 0.0035	0.7699 ± 0.0038	0.7759 ± 0.0081	0.7642 ± 0.0057
	PN-Y-S	0.7226 ± 0.0083	0.7421 ± 0.0149	0.7556 ± 0.0063	0.7489 ± 0.0090	0.7504 ± 0.0042	0.7692 ± 0.0068	0.7481 ± 0.0083
	PN-Y-S-E	0.7331 ± 0.0145	0.7083 ± 0.0051	0.7346 ± 0.0064	0.7534 ± 0.0059	0.7609 ± 0.0076	0.7647 ± 0.0107	0.7425 ± 0.0083
2	DANN	0.7476 ± 0.0078	0.7829 ± 0.0081	0.7994 ± 0.0066	0.8067 ± 0.0077	0.8238 ± 0.0059	0.8274 ± 0.0100	0.7980 ± 0.0077
	DIWA	0.7835 ± 0.0065	0.8110 ± 0.0050	0.8262 ± 0.0066	0.8335 ± 0.0048	0.8372 ± 0.0079	0.8378 ± 0.0054	0.8215 ± 0.0060
	ERM	0.7811 ± 0.0045	0.7933 ± 0.0054	0.8128 ± 0.0039	0.8110 ± 0.0062	0.8122 ± 0.0073	0.8323 ± 0.0067	0.8071 ± 0.0057
	NUC-0.01	0.7567 ± 0.0072	0.7884 ± 0.0080	0.8134 ± 0.0092	0.8262 ± 0.0039	0.8409 ± 0.0060	0.8256 ± 0.0066	0.8085 ± 0.0068
	NUC-0.1	0.7622 ± 0.0026	0.7841 ± 0.0077	0.8134 ± 0.0083	0.8244 ± 0.0080	0.8256 ± 0.0050	0.8171 ± 0.0064	0.8045 ± 0.0063
	PN-Y	0.8055 ± 0.0077	0.8226 ± 0.0039	0.8244 ± 0.0027	0.8396 ± 0.0071	0.8366 ± 0.0055	0.8329 ± 0.0024	0.8269 ± 0.0049
	PN-Y-S	0.8018 ± 0.0055	0.8165 ± 0.0046	0.8091 ± 0.0055	0.8250 ± 0.0028	0.8274 ± 0.0021	0.8433 ± 0.0052	0.8205 ± 0.0043
	PN-Y-S-E	0.7890 ± 0.0095	0.8061 ± 0.0061	0.8220 ± 0.0064	0.8293 ± 0.0054	0.8323 ± 0.0033	0.8366 ± 0.0053	0.8192 ± 0.0060
3	DANN	0.7811 ± 0.0070	0.8000 ± 0.0033	0.8178 ± 0.0072	0.8373 ± 0.0032	0.8396 ± 0.0049	0.8432 ± 0.0057	0.8198 ± 0.0052
	DIWA	0.8556 ± 0.0030	0.8598 ± 0.0035	0.8627 ± 0.0040	0.8704 ± 0.0046	0.8734 ± 0.0029	0.8686 ± 0.0062	0.8651 ± 0.0040
	ERM	0.8698 ± 0.0047	0.8586 ± 0.0068	0.8757 ± 0.0055	0.8746 ± 0.0054	0.8882 ± 0.0011	0.8799 ± 0.0057	0.8745 ± 0.0049
	NUC-0.01	0.8432 ± 0.0032	0.8598 ± 0.0042	0.8675 ± 0.0057	0.8704 ± 0.0052	0.8805 ± 0.0050	0.8846 ± 0.0034	0.8677 ± 0.0045
	NUC-0.1	0.8414 ± 0.0035	0.8592 ± 0.0035	0.8627 ± 0.0035	0.8669 ± 0.0026	0.8751 ± 0.0025	0.8746 ± 0.0080	0.8633 ± 0.0039
	PN-Y	0.8734 ± 0.0030	0.8793 ± 0.0060	0.8882 ± 0.0047	0.8953 ± 0.0038	0.8941 ± 0.0050	0.9012 ± 0.0043	0.8886 ± 0.0045
	PN-Y-S	0.8781 ± 0.0036	0.8811 ± 0.0024	0.8893 ± 0.0033	0.8905 ± 0.0026	0.9041 ± 0.0018	0.8964 ± 0.0036	0.8899 ± 0.0029
	PN-Y-S-E	0.8722 ± 0.0059	0.8899 ± 0.0047	0.8846 ± 0.0050	0.8893 ± 0.0020	0.8964 ± 0.0030	0.8935 ± 0.0028	0.8877 ± 0.0039

Table 8. Target Finetuning results on VLCS dataset.

Bridging Domains with Approximately Shared Features

E_t	Method	0.10	0.20	0.40	0.60	0.80	1.00	mean
0	DANN	0.8076 ± 0.0082	0.8650 ± 0.0055	0.9169 ± 0.0041	0.9549 ± 0.0023	0.9675 ± 0.0025	0.9764 ± 0.0012	0.9147 ± 0.0040
	DIWA	0.8793 ± 0.0043	0.8979 ± 0.0040	0.9401 ± 0.0045	0.9570 ± 0.0022	0.9726 ± 0.0013	0.9726 ± 0.0042	0.9366 ± 0.0034
	ERM	0.8696 ± 0.0055	0.8937 ± 0.0014	0.9409 ± 0.0043	0.9515 ± 0.0038	0.9671 ± 0.0035	0.9806 ± 0.0022	0.9339 ± 0.0035
	NUC-0.01	0.7793 ± 0.0040	0.8426 ± 0.0074	0.9143 ± 0.0020	0.9460 ± 0.0045	0.9591 ± 0.0032	0.9700 ± 0.0023	0.9019 ± 0.0039
	NUC-0.1	0.7772 ± 0.0031	0.8494 ± 0.0028	0.9177 ± 0.0030	0.9464 ± 0.0046	0.9553 ± 0.0031	0.9709 ± 0.0016	0.9028 ± 0.0030
	PN-Y	0.8835 ± 0.0046	0.9093 ± 0.0030	0.9414 ± 0.0049	0.9608 ± 0.0036	0.9679 ± 0.0026	0.9751 ± 0.0016	0.9397 ± 0.0034
	PN-Y-S	0.8772 ± 0.0045	0.9051 ± 0.0037	0.9376 ± 0.0017	0.9553 ± 0.0020	0.9658 ± 0.0017	0.9730 ± 0.0014	0.9357 ± 0.0025
	PN-Y-S-E	0.8787 ± 0.0020	0.9013 ± 0.0023	0.9430 ± 0.0024	0.9527 ± 0.0033	0.9679 ± 0.0039	0.9759 ± 0.0027	0.9366 ± 0.0028
1	DANN	0.8361 ± 0.0061	0.8949 ± 0.0032	0.9329 ± 0.0041	0.9556 ± 0.0020	0.9649 ± 0.0014	0.9747 ± 0.0008	0.9265 ± 0.0029
	DIWA	0.8797 ± 0.0051	0.9203 ± 0.0054	0.9446 ± 0.0031	0.9575 ± 0.0051	0.9731 ± 0.0010	0.9764 ± 0.0009	0.9419 ± 0.0034
	ERM	0.8333 ± 0.0071	0.8947 ± 0.0045	0.9331 ± 0.0035	0.9515 ± 0.0027	0.9653 ± 0.0028	0.9749 ± 0.0020	0.9255 ± 0.0038
	NUC-0.01	0.8070 ± 0.0062	0.8793 ± 0.0031	0.9265 ± 0.0042	0.9466 ± 0.0022	0.9620 ± 0.0020	0.9698 ± 0.0014	0.9152 ± 0.0032
	NUC-0.1	0.8154 ± 0.0032	0.8723 ± 0.0039	0.9331 ± 0.0036	0.9458 ± 0.0028	0.9624 ± 0.0015	0.9713 ± 0.0006	0.9167 ± 0.0026
	PN-Y	0.8591 ± 0.0037	0.9021 ± 0.0038	0.9312 ± 0.0023	0.9487 ± 0.0011	0.9620 ± 0.0012	0.9745 ± 0.0018	0.9296 ± 0.0023
	PN-Y-S	0.8472 ± 0.0050	0.8943 ± 0.0028	0.9370 ± 0.0025	0.9520 ± 0.0014	0.9651 ± 0.0020	0.9749 ± 0.0003	0.9284 ± 0.0023
	PN-Y-S-E	0.8509 ± 0.0030	0.9004 ± 0.0035	0.9312 ± 0.0027	0.9472 ± 0.0025	0.9645 ± 0.0012	0.9731 ± 0.0020	0.9279 ± 0.0025
2	DANN	0.6816 ± 0.0133	0.7673 ± 0.0072	0.8529 ± 0.0056	0.8922 ± 0.0072	0.9179 ± 0.0061	0.9441 ± 0.0042	0.8427 ± 0.0073
	DIWA	0.7778 ± 0.0104	0.8292 ± 0.0056	0.8826 ± 0.0065	0.9128 ± 0.0043	0.9370 ± 0.0052	0.9471 ± 0.0029	0.8811 ± 0.0058
	ERM	0.7526 ± 0.0056	0.8096 ± 0.0052	0.8579 ± 0.0062	0.8997 ± 0.0062	0.9179 ± 0.0045	0.9194 ± 0.0035	0.8595 ± 0.0052
	NUC-0.01	0.6222 ± 0.0102	0.7375 ± 0.0126	0.8489 ± 0.0054	0.8977 ± 0.0058	0.9224 ± 0.0033	0.9390 ± 0.0043	0.8280 ± 0.0069
	NUC-0.1	0.6121 ± 0.0090	0.7365 ± 0.0083	0.8489 ± 0.0065	0.8987 ± 0.0019	0.9249 ± 0.0037	0.9395 ± 0.0055	0.8268 ± 0.0058
	PN-Y	0.7647 ± 0.0045	0.8227 ± 0.0063	0.8665 ± 0.0052	0.8922 ± 0.0041	0.9123 ± 0.0043	0.9295 ± 0.0035	0.8647 ± 0.0047
	PN-Y-S	0.7446 ± 0.0049	0.8050 ± 0.0031	0.8584 ± 0.0074	0.8856 ± 0.0049	0.9098 ± 0.0041	0.9285 ± 0.0028	0.8553 ± 0.0046
	PN-Y-S-E	0.7446 ± 0.0031	0.7953 ± 0.0049	0.8559 ± 0.0042	0.8872 ± 0.0033	0.9159 ± 0.0048	0.9300 ± 0.0045	0.8548 ± 0.0041
3	DANN	0.6983 ± 0.0047	0.7969 ± 0.0062	0.8714 ± 0.0037	0.9034 ± 0.0022	0.9296 ± 0.0045	0.9364 ± 0.0019	0.8560 ± 0.0039
	DIWA	0.7806 ± 0.0067	0.8289 ± 0.0090	0.8806 ± 0.0041	0.9065 ± 0.0050	0.9259 ± 0.0039	0.9276 ± 0.0022	0.8750 ± 0.0052
	ERM	0.7534 ± 0.0062	0.8207 ± 0.0056	0.8704 ± 0.0047	0.8980 ± 0.0063	0.9231 ± 0.0027	0.9320 ± 0.0028	0.8663 ± 0.0047
	NUC-0.01	0.6476 ± 0.0060	0.7769 ± 0.0117	0.8571 ± 0.0085	0.8980 ± 0.0058	0.9184 ± 0.0042	0.9361 ± 0.0022	0.8390 ± 0.0064
	NUC-0.1	0.6374 ± 0.0029	0.7718 ± 0.0109	0.8585 ± 0.0083	0.8993 ± 0.0053	0.9214 ± 0.0029	0.9374 ± 0.0014	0.8376 ± 0.0053
	PN-Y	0.7673 ± 0.0037	0.8289 ± 0.0077	0.8721 ± 0.0088	0.8952 ± 0.0054	0.9252 ± 0.0032	0.9384 ± 0.0035	0.8712 ± 0.0054
	PN-Y-S	0.7486 ± 0.0041	0.8167 ± 0.0094	0.8714 ± 0.0057	0.8993 ± 0.0047	0.9241 ± 0.0020	0.9374 ± 0.0021	0.8663 ± 0.0047
	PN-Y-S-E	0.7524 ± 0.0066	0.8185 ± 0.0070	0.8673 ± 0.0059	0.8973 ± 0.0049	0.9238 ± 0.0012	0.9408 ± 0.0022	0.8667 ± 0.0046

Table 9. Target Finetuning results on TerrainCognita dataset.

D.3. Learning Rate Decay Results

We test the learning rate decay for the feature encoder, which is commonly used in domain adaptation methods. We use the same setting as the target finetuning experiment, but we decay the learning rate by 0.1. We report the results in Figure 7.

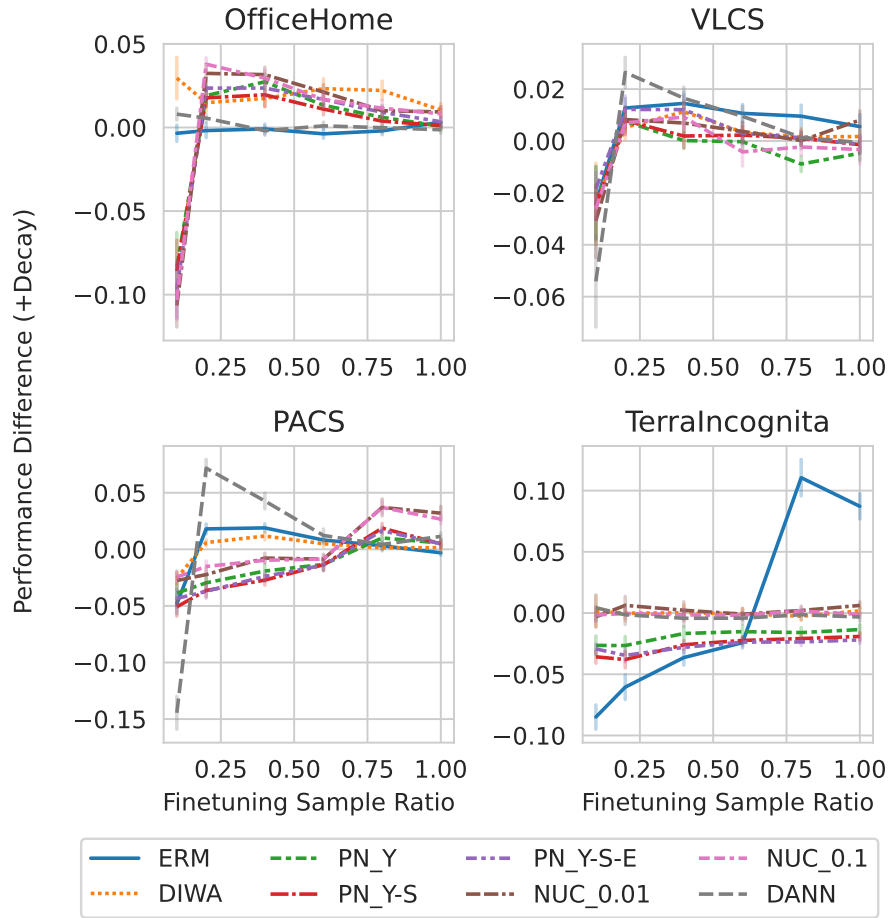


Figure 7. Feature Encoder Learning Rate Decay Results: We show that learning rate decay does not may improve the performance of the model on large FSL regimes but improves the performance on small FSL regimes.

E. Experiment Details

Our code is available <https://github.com/Xiang-Pan/ProjectionNet>.

E.1. Linear synthetic data

We have $E = 999$ source environments and a target environment indexed by 1000. The source and target sample sizes are $n_1 = 50, n_2 = 2000$ respectively, with the ambient input dimension $d = 10$, content feature dimension $k = 6$, and variance of noise $\sigma = 0.01$.

Generation of X^e For $e \in [E]$, $X^e \in \mathbb{R}^{n_1 \times d}$ and for $e = E + 1$, $X^{E+1} \in \mathbb{R}^{n_2 \times d}$. To guarantee Assumption B.4, we generate X^e via its SVD: $X^e = U^e S^e V^{e\top}$ where U^e and V^e are random orthogonal matrices, and the singular values S^e are sampled from the mixture of Gaussian distributions. Specifically, the top k singular values follow $\mathcal{N}(5, 1)$ and the rest $d - k$ follow $\mathcal{N}(0, 1)$.

Generation of θ^{*e} For $e \in [E + 1]$, θ^{*e} 's are i.i.d. samples of the meta distribution (equation 3) with the parameter choice $\theta^* = 6 \cdot \mathbf{1}_k, \Lambda_{11} = 0.1 \cdot I_k, \Lambda_{22} = 3 \cdot I_{d-k}$.

Generation of y^e For $e \in [E + 1]$, y^e 's are generated via

$$y^e = X^e R^* \theta^{*e} + z^e$$

where R^* is some random $d \times d$ orthogonal matrix and z^e 's are i.i.d. samples of $\mathcal{N}(0, \sigma^2 I_{n_1/n_2})$ independent of X^e 's.

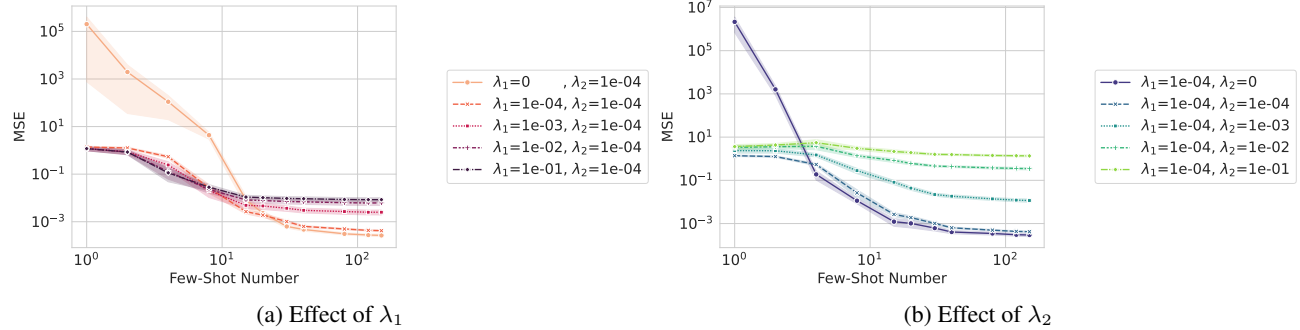


Figure 8. The effect of (λ_1, λ_2) and on the performance of the target task: No regularization leads to an unstable solution and overfitting when FSL is small, but large regularization prevent the full adaptation to the target task when FSL is large.

E.2. Real data

E.2.1. TRAINING CONFIGURATION

We use ResNet50 (He et al., 2016) as the backbone network and use the SGD optimizer to train the model, the training setting is the same as (Wang & Lu).

We use $\text{lr}_{\text{decay}} = 0.1, \text{lr}_{\text{Feature}} = \text{lr}_{\text{decay}} * \text{lr}_{\text{Classification}}$. We vary the learning rate decay from 0 (frozen) to 1 (not decayed) to control the $(\lambda_1$ and $\lambda_2)$ regularization strength. In the source training stage, we use the source validation set to select the best model; In the target training stage, we use the target validation set to select the best model.

Computation Resource: All the experiments can be done with A40, RTX 8000 GPU or A100 GPU, 32GB memory, and 16 CPU 2.9GHz cores (Intel Cascade Lake Platinum 8268 chips).